A priori Analysis of Global and Local Output Error Estimates for CG, DG and HDG Finite Element Discretizations

by

Hugh Alexander Carson

M.Eng. Aerospace and Aerothermal Engineering, Cambridge University (2014)

Submitted to the Department of Aeronautics and Astronautics in partial fulfillment of the requirements for the degree of

Master of Science in Aeronautics and Astronautics

at the

MASSACHUSETTS INSTITUTE OF TECHNOLOGY

June 2016

Signature redacted

Author ....
Department of Aeronautics and Astronautics
May 20, 2016

Certified by. Signature redacted ....
David L. Darmofal
Professor of Aeronautics and Astronautics
Thesis Supervisor

Accepted by.. Signature redacted ....
Paulo C. Lozano
Associate Professor of Aeronautics and Astronautics
Chair, Graduate Program Committee

A priori Analysis of Global and Local Output Error Estimates for CG, DG and HDG Finite Element Discretizations

by

Hugh Alexander Carson

Submitted to the Department of Aeronautics and Astronautics
on May 20, 2016, in partial fulfillment of the
requirements for the degree of
Master of Science in Aeronautics and Astronautics

Abstract

In this thesis, *a priori* convergence estimates are developed for outputs, output error estimates, and localizations of output error estimates for Galerkin finite element methods. Specifically, Continuous Galerkin (CG), Discontinuous Galerkin (DG), and Hybridized DG (HDG) methods are analyzed for the Poisson problem. A mixed formulation for DG output error estimation is proposed with improved convergence rates relative to the common approach utilizing statically condensed, p-dependent lifting operators. The HDG output error estimates are new and include the impact of stabilization. Comparisons to numerical results demonstrate (1) the sharpness of the estimates and (2) that the HDG estimates are approximately an order of magnitude more accurate than CG and DG.

Thesis Supervisor: David L. Darmofal
Title: Professor of Aeronautics and Astronautics

Acknowledgments

I would first like to thank my advisor, Professor David Darmofal, for bringing me to MIT and giving me the opportunity to join his research team and the ACDL, and for directing my journey into the wider world of CFD. Pushing me to be rigorous in my mathematics and nodding sagely as I waved my hands around with vague explanations then asking for more detail. I would also like to thank the voice at the end of the phone, Dr. Steven Allmaras, for all his enlightening discussions and for the fortunate decision to opt for a non-orthodox DG discretization that ultimately led to the work in this thesis on the statically condensed estimates. Dr. Marshall Galbraith deserves acknowledgement for teaching me essentially everything I know about c++, his patience as I learn the ways of templating, pushing for ever more unit testing, the discussions about the stranger points of BR2 and for creating the monolith that is SANS.

The other members of team SANS deserve my thanks, without whom the results section of this paper would never have happened, in particular Savithru and Arthur whose sections of the code were integral to my work. The work of the former members of the ProjectX team must be acknowledged, in particular Masa Yano who laid the groundwork for this thesis with his work on the DG estimates and helped with the explanation of the 1D results. Finally on the academic side of things, I would like to thank Professor Rob Miller for starting me off on the path towards a PhD all those years ago, giving me work in the summer at the Whittle Lab during my time at Cambridge and for expanding my academic horizons internationally.

On the social side of things, I'd like to thank my cube mates over the last two years, Carlee, Giulia, Philippe, Max and Cory for lightening my spirits in lab, even as the actual natural light in lab dwindles. In the ACDL Patrick did well to encourage everyone to socialize outside of the lab every once in a while and was always good for a chat when productivity was low. I'd also like to thank all of the other members of the ACDL who've been there when I was stuck on another frustrating problem and had to vent. My housemates this last year, Max, Greg, Grant and Andy, thank you for the persistent reminders that there are better places to be than in the Lab late on a friday and for all the fun nights.

My family has supported me over the years, without whom it would've been nigh impossible for me to be where I am, so I'd like to thank my sisters, Charley and Kate, and my parents, Sarah and Iain, for all of the support over the years. Being away from home for so long has only made me cherish my time there all the more, and all the skype chats have helped keep me sane through the winter months and frantic times.

All the members of Caius Boat Club, and particular all the M1s over the years, deserve thanks for getting me through my undergrad and helping me understand that not all hours spent working are created equal, and Bobby Thatcher and Josh Raymond for introducing me to the world of rowing and helping me develop the discipline without which I would likely have never reached here.

This research was supported through: a Research Agreement with Saudi Aramco, a Founding Member of the MIT Energy Initiative with technical monitors Dr. Ali Dogru and Dr. Nick Burgess; and a Research Agreement with The Boeing Company with technical monitor Dr. Mori Mani.

TABLE OF CONTENTS

List of Figures

List of Tables

CHAPTER 1

INTRODUCTION

A posteriori estimation aims to provide computable estimates of numerical error in the discrete approximate solutions of Partial Differential Equations (PDEs). The computed *a posteriori* estimate can then be used to correct the output and/or drive mesh adaptation. Energy-based *a posteriori* error estimates have been used for the Finite Element Method (FEM) since the 1980s [8, 9], particularly within the structural community given the physical relevance of the energy norm. Ainsworth and Oden provided a comprehensive summary of energy norm estimates (as well as other norms) wherein they draw attention to the use of duality arguments for analyzing the estimates in an *a posteriori* context[1]. Methods based upon localized residuals were developed for mesh adaptation by Babuška and Rheinboldt [7]. Estimates based on the solution of local Dirichlet problems and local Neumann problems were also developed by Bank and Weiser[9] and Babuška and Rheinboldt[6]. Verfürth analyzed these estimates for elliptic partial differential showing their equivalence[27].

In many applications, the convergence of the energy norm is less important the convergence of an output functional. A common output example would be the lift or drag in fluid dynamics. In a series of papers, Babuška and Miller showed with *a priori* analysis of *a posteriori* error that integrated output functionals from FEM could exhibit 'super convergence', converging faster than the solution error (e.g. the L^2 norm of the error). For instance, point values at critical locations, such as the stress at a joint in a structural FEM calculation, are often of interest. Babuška and Miller showed that the accuracy in these point quantities can be improved by restating them as weighted integrals, and demonstrated this improvement with numerous examples[3, 4, 5]. Barrett and Elliott analyzed the linear convection-diffusion equation and reached similar conclusions[10].

The relationship between error in the numerical approximation of the primal solution and the output functional is quantified by the adjoint PDE. The adjoint PDE measures the sensitivity of the output functional to errors in the numerical solution. Thus weighting a residual error by the adjoint at that location results in an estimate of the computed output functional's error. This Dual-Weighted Residual (DWR) method was developed for FEM by Becker and Rannacher[12, 13]. Adjoint based error estimation has also been developed for discretizations other than FEM, for example Finite Volume (FV) and Finite Difference (FD) methods, where it has largely been used for error correction to recover the 'super convergent' output functionals possible with FEM[25, 20, 22, 21].

For the purposes of adaptation, error estimates must be localized to facilitate decisions about where mesh refinement (and coarsening) should be performed. A typical residual localization for the Continuous Galerkin (CG) FEM uses a strong form residual, which introduces an element boundary contribution due to gradient jumps, to give an element-wise localization of the estimate[7, 12, 26]. An alternative localization proposed by Braack and Ern, for use with the DWR method, uses a patchwise reconstruction for the dual weighting[14]. This results in an estimate that avoids the need to evaluate the strong form of the residual, and also gives a node-wise localization of the estimate. Richter and Wick similarly produced a node-wise localization of the error that avoids the evaluation of the strong form through a partition of unity based approach[26]. For a more complete overview of output-based error estimation and earlier mesh adaptation schemes, for fluid dynamic applications in particular, the review papers of Hartmann and Houston[23], focused on DG methods, and Fidkowski and Darmofal[19], for general discretizations, provide a comprehensive literature review. The second DG method of Bassi and Rebay (BR2)[11], localized by elemental restriction of the test function, was analyzed by Yano in his PhD thesis [29].

The focus of this thesis is on *a priori* analysis of the convergence rates for localized DWR error estimates for the Continuous Galerkin (CG), Discontinuous Galerkin (DG) and Hybridizable Discontinuous Galerkin (HDG) schemes. The CG localization considered is the weighted strong form residual. For DG, an element-wise localization by restriction of the weight function is considered, and the effect of static condensation of the lifting operators in the BR2 scheme is also analyzed. The localization for HDG consists of an element-wise restriction of the scalar and gradient variables combined with a partition of unity of the error associated with the trace variables.

The outline of this thesis is as follows, in Chapter 2 the model Poisson primal and dual problems are outlined, alongside definitions that are necessary for the results in the following chapters. Then in Chapters 3 to 5 *a priori* asymptotic convergence rates for the error, and the error in the estimate, are derived for the CG, DG and HDG discretizations respectively. In Chapter 6 numerical results are presented for one and two dimensional test cases demonstrating the derived *a priori* asymptotic convergence rates for all of the discretizations and estimates considered. Finally, in Chapter 7, some concluding remarks are provided.

Chapter 2

Problem Definition and Notation

Consider the primal Poisson problem:

$$-\Delta u = f \text{ in } \Omega \tag{2.1a}$$

$$u = 0 \text{ on } \partial\Omega, \tag{2.1b}$$

where $\Omega \subset \mathbb{R}^d$ is a bounded domain of dimension d. To avoid additional technicalities in the *a priori* analysis, the solution u is assumed to be sufficiently smooth. This places restrictions on the domain shape and f (see for example Brenner and Scott [15, Theorem 1.4.6]). We denote the L^2 inner product by $(\cdot,\cdot)$ and the corresponding norm over Ω by $\|\cdot\|_{L^2(\Omega)}$, In addition inner products on a trace, such as $\int_{\partial\Omega} uv$, will be denoted by $\langle\cdot,\cdot\rangle$. Where additional clarity is useful, subscripts will be used in order to denote the domain of the integral. The problem is written in the variational form,

$$u \in \mathcal{V}: \; R(u,w) \equiv l(w) - a(u,w) = 0, \; \forall w \in \mathcal{V} \tag{2.2a}$$

$$a(v,w) = (\nabla v, \nabla w) \tag{2.2b}$$

$$l(w) = (f,w). \tag{2.2c}$$

The boundary conditions are enforced essentially by $\mathcal{V}$ where, for this problem, $\mathcal{V} \equiv H_0^1(\Omega)$. In approximating this problem discretely, we utilize a finite-dimensional space $\mathcal{V}_{h,p}$ and a modified problem statement

(2.3) $$u_{h,p} \in \mathcal{V}_{h,p} : \; R_h(u_{h,p}, w_{h,p}) \equiv l(w_{h,p}) - a_h(u_{h,p}, w_{h,p}) = 0, \; \forall w_{h,p} \in \mathcal{V}_{h,p}.$$

For the Galerkin methods considered here, $u_{h,p}$ and $w_{h,p}$ are taken from the same space defined on the quasi-uniform and shape regular triangulation $\mathcal{T}_h$. The subscript h is a notional measure of the local grid scale defined by the triangulation. For local interpolation errors, $h_\kappa \equiv \text{diam}(\kappa)$, however given the assumption of a quasi-uniform grid, all h_κ are within a constant factor of each other and thus will be replaced with h.

The h subscript when applied to $R_h(\cdot,\cdot)$ and $a_h(\cdot,\cdot)$ denote that the residual and bilinear term are discretization specific and therefore may differ from $R(\cdot,\cdot)$ and $a(\cdot,\cdot)$. Those residuals which display polynomial order dependence, for instance classical DG BR2, will be denoted $R_{h,p}(\cdot,\cdot)$ as seen in Chapter 4. $l(w)$ is not modified by the methods considered in this thesis, but it is possible with other methods.

For this thesis, the output is a volume integral given by $\mathcal{J}(u) \equiv (g, u)$. The corresponding dual problem is,

(2.4) $$\psi \in \mathcal{V} : \; R^\psi(w, \psi) \equiv \mathcal{J}(w) - a(w, \psi) = 0, \; \forall w \in \mathcal{V}.$$

For the Poisson problem and volume output functional, $\mathcal{J}(u)$, considered here, performing integration by parts gives the adjoint PDE

(2.5a) $$-\Delta\psi = g \text{ in } \Omega$$

(2.5b) $$\psi = 0 \text{ on } \partial\Omega.$$

As with the solution u, we assume that the adjoint solution, ψ, is assumed smooth, which places restrictions on g and the domain shape. As with the primal problem, the adjoint problem has a corresponding discrete weak form

(2.6) $$\psi_{h,p} \in \mathcal{V}_{h,p} : \; R_h^\psi(w_{h,p}, \psi_{h,p}) \equiv \mathcal{J}(w_{h,p}) - a_h(w_{h,p}, \psi_{h,p}) = 0, \; \forall w_{h,p} \in \mathcal{V}_{h,p}.$$

2.1 *A posteriori* output error estimation

In the DWR framework the output error, $\mathcal{E}$, can be expressed by the Functional Error Representation Formula

$$\mathcal{E} = \mathcal{J}(u) - \mathcal{J}(u_{h,p}) \tag{2.7a}$$

$$= R_h(u_{h,p}, \psi - v_{h,p}), \ \forall v_{h,p} \in \mathcal{V}_{h,p} \tag{2.7b}$$

when the discretized residuals satisfy an extended form of primal and adjoint consistency. These definitions are described within a DG context in Yano's thesis [29].

DEFINITION 1. Extended Primal Global Consistency

Given the exact primal solution $u \in \mathcal{V}$, the discretized primal residual satisfies

$$R_h(u, w) = 0, \ \forall w \in \oplus_\kappa \mathcal{V}(\kappa)$$

where $\mathcal{V}(\kappa)$ is the restriction of $\mathcal{V}$ to an element κ.

Extended consistency is stronger than normal consistency[2] which only requires $R_h(u, w) = 0, \forall w \in \mathcal{V}_{h,p}$. Normal consistency is automatically satisfied by Definition 1 if $\mathcal{V}_{h,p}(\kappa) \subset \mathcal{V}(\kappa)$.

DEFINITION 2. Extended Dual Global Consistency

Given the exact adjoint solution $\psi \in \mathcal{V}$, the discrete adjoint residual satisfies

$$R_h^{\psi}(w, \psi) = 0, \ \forall w \in \oplus_\kappa \mathcal{V}(\kappa).$$

The Functional Error Representation Formula is obtained using Definitions 1 and 2.

LEMMA 3. Functional Error Representation Formula

For a discretization that satisfies Extended Primal and Dual Global Consistency, the error in the output functional $\mathcal{E} \equiv \mathcal{J}(u) - \mathcal{J}(u_{h,p})$ is given by

$$\mathcal{E} = R_h(u_{h,p}, \psi - v_{h,p}), \ \forall v_{h,p} \in \mathcal{V}_{h,p}.$$

Proof.

$$\begin{aligned}
&(2.8a) \qquad \mathcal{E} \equiv \mathcal{J}(u) - \mathcal{J}(u_{h,p}) = \mathcal{J}(u - u_{h,p}) \\
&(2.8b) \qquad = a_h(u - u_{h,p}, \psi) \qquad \text{via Definition 2} \\
&(2.8c) \qquad = a_h(u - u_{h,p}, \psi - v_{h,p}) \qquad \text{via orthogonality} \\
&(2.8d) \qquad = l(\psi - v_{h,p}) - a_h(u_{h,p}, \psi - v_{h,p}) \qquad \text{via Definition 1} \\
&(2.8e) \qquad = R_h(u_{h,p}, \psi - v_{h,p}).
\end{aligned}$$

□

Another useful property of a discretization that satisfies Extended Primal and Dual Global Consistency is Global Residual Error Mapping.

LEMMA 4. Global Residual-Error Mapping

For all $p1, p2 \in \mathbb{N}$, *the global dual-weighted residuals are related by*

$$\begin{aligned}
R_h(v_{h,p1}, \psi - w_{h,p2}) &= a_h(u - v_{h,p1}, \psi - w_{h,p2}) \\
&= R_h^{\psi}(u - v_{h,p1}, w_{h,p2}), \ \forall (v_{h,p1}, w_{h,p2}) \in (\mathcal{V}_{h,p1} \times \mathcal{W}_{h,p2}),
\end{aligned}$$

where $u, \psi \in \mathcal{V}$ *are the exact solutions to the primal and adjoint respectively.*

Proof.

$$\begin{aligned}
&(2.9a) \qquad R_h(v_{h,p1}, \psi - w_{h,p2}) = l(\psi - w_{h,p2}) - a_h(v_{h,p1}, \psi - w_{h,p2}) \\
&(2.9b) \qquad = a_h(u, \psi - w_{h,p2}) - a_h(v_{h,p1}, \psi - w_{h,p2}) \qquad \text{via Definition 1} \\
&(2.9c) \qquad = a_h(u - v_{h,p1}, \psi - w_{h,p2}) \qquad \text{via bilinearity} \\
&(2.9d) \qquad = J(u - v_{h,p1}) - a_h(u - v_{h,p1}, w_{h,p2}) \qquad \text{via Definition 2} \\
&(2.9e) \qquad = R_h^{\psi}(u - v_{h,p1}, w_{h,p2}).
\end{aligned}$$

□

2.1.1 Localization

The localization, $r_\kappa(v, w)$, of the discrete primal residual is defined as

$$r_\kappa(v, w) = l_\kappa(w) - a_\kappa(v, w), \tag{2.10}$$

where $r_\kappa(v,w)$, $a_\kappa(v,w)$ and $l_\kappa(w) = (f,w)_\kappa$ are the discretization specific localized primal residual, primal bilinear and linear functional expressions respectively. Further $r_\kappa(v,w)$ is assumed to satisfy

$$R_h(v,w) = \sum_{\kappa \in \mathcal{T}_h} r_\kappa(v,w), \ \forall (v,w) \in (\oplus_\kappa \mathcal{V}(\kappa) \times \oplus_\kappa \mathcal{V}(\kappa)). \tag{2.11}$$

DEFINITION 5. Extended Primal Local Consistency

Given the exact solution $u \in \mathcal{V}$, the localized residual satisfies

$$r_\kappa(u,w) = 0, \ \forall w \in \mathcal{V}(\kappa),$$

where $\mathcal{V}(\kappa)$ enforces the boundary condition for those elements adjacent to the boundary.

The localization of the dual residual is defined as

$$r_\kappa^\psi(w,v) = \mathcal{J}_\kappa(w) - a_\kappa^\psi(w,v), \tag{2.12}$$

where $r_\kappa^\psi(w,v)$, $a_\kappa^\psi(w,v)$ and $\mathcal{J}_\kappa(w) = (g,w)_\kappa$ are the discretization specific localized adjoint residual, adjoint bilinear and output functional expressions respectively.

DEFINITION 6. Extended Dual Local Consistency

Given the exact adjoint solution $\psi \in \mathcal{V}$, the localized adjoint residual satisfies

$$r_\kappa^\psi(w,\psi) = 0, \ \forall w \in \mathcal{V}(\kappa).$$

Provided a localization of a residual satisfies Extended Primal Local Consistency it also satisfies Local Residual-Error Mapping.

LEMMA 7. Local Residual-Error Mapping

For all $p1, p2 \in \mathbb{N}$, given a localization that satisfies Extended Local Primal Consistency, the local dual-weighted primal residual can be represented by

$$r_\kappa(v_{h,p1}, \psi - w_{h,p2}) = a_\kappa(u - v_{h,p1}, \psi - w_{h,p2}) \ \forall (v_{h,p1}, w_{h,p2}) \in (\mathcal{V}_{h,p1} \times \mathcal{W}_{h,p2}),$$

where $u, \psi \in \mathcal{V}$ are the exact solutions.

Proof.

$$r_\kappa(v_{h,p1}, \psi - w_{h,p2}) = l_\kappa(\psi - w_{h,p2}) - a_\kappa(v_{h,p1}, \psi - w_{h,p2}) \tag{2.13a}$$

$$= a_\kappa(u, \psi - w_{h,p2}) - a_\kappa(v_{h,p1}, \psi - w_{h,p2}) \quad \text{via Definition 5} \tag{2.13b}$$

$$= a_\kappa(u - v_{h,p1}, \psi - w_{h,p2}) \; \forall (v_{h,p1}, w_{h,p2}) \in (\mathcal{V}_{h,p1} \times \mathcal{W}_{h,p2}). \tag{2.13c}$$

□

In addition to Local Residual Error Mapping, the proofs of Extended Primal and Dual Global Consistency follow from Extended Primal and Dual Local Consistency

COROLLARY 8. *Given a localization, $r_\kappa(v, w)$, of a residual, $R_h(v, w)$, that satisfies*

$$R_h(v, w) = \sum_{\kappa \in \mathcal{T}_h} r_\kappa(v, w) \tag{2.14}$$

and Definitions 5 and 6, $R_h(v, w)$ automatically satisfies Definitions 1 and 6 because $\mathcal{V} \subset (\oplus_\kappa \mathcal{V}(\kappa))$.

2.1.2 Error Estimates

Given $\psi \in \mathcal{V}$, where $\mathcal{V}$ is an infinite dimensional space, evaluating the true error via Equation (2.7b) is infeasible. The approach considered here is to instead approximate the adjoint in a higher p space than the primal. Though this method requires the solution of a linear system that is larger than that of the primal, it has been observed that for nonlinear primal problems the computational effort to solve the primal problem often dominates the total computational effort of the solution and error estimation process. For example, for a typical transonic Reynolds-Averaged Navier-Stokes (RANS) solution, the dual solve required approximately 10% of the computational time required for the primal solve[30]. As a result, in this work the following error estimate is considered,

$$\mathcal{E} \approx \tilde{\mathcal{E}} = R_h(u_{h,p}, \psi_{h,p'} - v_{h,p}), \; \forall v_{h,p} \in \mathcal{V}_{h,p}, \tag{2.15}$$

where $p' = p + p_{\text{inc}} : p_{\text{inc}} > 0$. The true error has a localization

$$\mathcal{E} = \sum_{\kappa \in \mathcal{T}_h} \eta_\kappa, \tag{2.16a}$$

$$\eta_\kappa = r_\kappa(u_{h,p}, \psi - \psi_{h,p}) \tag{2.16b}$$

which has a corresponding estimate

$$\eta_\kappa \approx \tilde{\eta}_\kappa = r_\kappa(u_{h,p}, \psi_{h,p'} - \psi_{h,p}). \tag{2.17}$$

The global estimate is defined by the primal residual solved for $u_{h,p}$, thus $R_h(u_{h,p}, v_{h,p}) = 0,\ \forall v_{h,p} \in \mathcal{V}_{h,p}$. However this orthonality does not always hold for the localized residual, i.e. $r_\kappa(u_{h,p}, v_{h,p}) \neq 0,\ \forall v_{h,p} \in \mathcal{V}_{h,p}$. When the orthogonality does hold locally, then the error estimate can be calculated as, $\tilde{\eta}_\kappa = r_\kappa(u_{h,p}, \psi_{h,p'})$, avoiding the need to calculate $\psi_{h,p}$.

2.2 Additional Notation

On interior traces of the triangulation, the jump operator, $[\![\cdot]\!]$, and average operator, $\{\cdot\}$, are defined for scalar, x, and vector, $\vec{y}$, quantities as

$$[\![x]\!] = (x\hat{n})^- + (x\hat{n})^+ \tag{2.18a}$$

$$[\![\vec{y}]\!] = (\vec{y} \cdot \hat{n})^- + (\vec{y} \cdot \hat{n})^+ \tag{2.18b}$$

$$\{x\} = \frac{1}{2}(x^- + x^+) \tag{2.18c}$$

$$\{\vec{y}\} = \frac{1}{2}(\vec{y}^{\,-} + \vec{y}^{\,+}). \tag{2.18d}$$

For boundary traces the jump and average operators take only the internal value, thus

$$\llbracket x \rrbracket = (x\hat{n})^+ \tag{2.19a}$$

$$\llbracket \vec{y} \rrbracket = (\vec{y} \cdot \hat{n})^+ \tag{2.19b}$$

$$\{x\} = x^+ \tag{2.19c}$$

$$\{\vec{y}\} = \vec{y}^{\,+}, \tag{2.19d}$$

where $\hat{n}^+$ is the outward facing normal on the trace of the element. Some additional notation for inner products are defined as

$$(v, w)_{\mathcal{T}_h} = \sum_{\kappa \in \mathcal{T}_h} (v, w)_\kappa, \tag{2.20a}$$

$$\langle v, w \rangle_{\partial \mathcal{T}_h} = \sum_{\kappa \in \mathcal{T}_h} \langle v, w \rangle_{\partial \kappa}, \tag{2.20b}$$

$$\langle v, w \rangle_{\mathcal{F}_h} = \sum_{f \in \mathcal{F}_h} \langle v, w \rangle_f. \tag{2.20c}$$

$\partial \mathcal{T}_h \equiv \{\partial \kappa : \kappa \in \mathcal{T}_h\}$ denotes the union of the boundaries of all $\kappa \in \mathcal{T}_h$. $\mathcal{F}_h^{\text{internal}} \equiv \{\partial \kappa^+ \cap \partial \kappa^-\} : \forall \kappa^+, \kappa^- \in \mathcal{T}_h$ denotes the set of internal traces associated with $\mathcal{T}_h$, $\mathcal{F}_h^{\text{boundary}} \equiv \{\partial \kappa \cap \partial \Omega\} : \kappa \in \mathcal{T}_h$ denotes the set of boundary traces associated with $\mathcal{T}_h$ and $\mathcal{F}_h \equiv \mathcal{F}_h^{\text{internal}} \cup \mathcal{F}_h^{\text{boundary}}$ denotes the set of all traces of $\mathcal{T}_h$. Equations (2.20b) and (2.20c) are different in that the first visits internal traces twice, once from either side, whereas the second visits each trace once which implies that

$$\frac{1}{2} \langle u, v \rangle_{\partial \mathcal{T}_h \setminus \partial \Omega} \equiv \langle u, v \rangle_{\mathcal{F}_h \setminus \partial \Omega}. \tag{2.21}$$

Finally, to simplify notation when taking limits, $A(h) \lesssim B(h)$ is defined as $A(h) \leq cB(h)$ in the limit of $h \to 0$ for $0 < c < \infty$.

CHAPTER 3

CONTINUOUS GALERKIN

The DWR framework was originally developed for the CG method[12] and combining DWR with classical theory for finite element methods[15] the asymptotic convergence rate of the output functional and its estimates can be bound as shown in this chapter.

3.1 Discretization

For the CG discretization, the approximation space $\mathcal{V}_{h,p}$ is made up of piecewise continuous polynomials of order p denoted $\mathbb{P}^p(\kappa)$,

$$\mathcal{V}_{h,p} \equiv \{v \in C^0(\Omega) \cap L^2(\Omega) : v|_\kappa \in \mathbb{P}^p(\kappa),\ \forall \kappa \in \mathcal{T}_h : v|_{\partial\Omega} = 0\}. \tag{3.1}$$

The bilinear form is

$$a_h(v, w) = (\nabla v, \nabla w)_{\mathcal{T}_h}. \tag{3.2}$$

3.2 Localization

The weighted strong form of the residual is used for the localization, following the method established by Babuška and Rheinboldt in their paper on residual based methods[7] and used by Becker and

Rannacher[12].

$$R_h(v,w) = (f,w)_{\mathcal{T}_h} - (\nabla v, \nabla w)_{\mathcal{T}_h} \tag{3.3a}$$

$$= (f,w)_{\mathcal{T}_h} + (\Delta v, w)_{\mathcal{T}_h} - \langle \nabla v \cdot \hat{n}, w\rangle_{\partial\mathcal{T}_h} \tag{3.3b}$$

$$= (f + \Delta v, w)_{\mathcal{T}_h} - \frac{1}{2}\langle [\![\nabla v]\!], w\rangle_{\partial\mathcal{T}_h}. \tag{3.3c}$$

From Equation (3.3c), $a_\kappa(v,w)$ and $l_\kappa(w)$, and thus $r_\kappa(v,w)$, are defined as

$$l_\kappa(w) = (f,w)_\kappa \tag{3.4a}$$

$$a_\kappa(v,w) = -(\Delta v, w)_\kappa + \frac{1}{2}\langle [\![\nabla v]\!], w\rangle_{\partial\kappa}. \tag{3.4b}$$

LEMMA 9. CG Extended Local Consistency

$$r_\kappa(u,w) = (f + \Delta u, w)_\kappa - \frac{1}{2}\langle [\![\nabla u]\!], w\rangle_{\partial\kappa} = 0, \ \forall w \in \mathcal{V}(\kappa)$$
$$r_\kappa^\psi(w,\psi) = (g + \Delta\psi, w)_\kappa - \frac{1}{2}\langle [\![\nabla \psi]\!], w\rangle_{\partial\kappa} = 0, \ \forall w \in \mathcal{V}(\kappa),$$

where $\mathcal{V}(\kappa)$ is the restriction of $\mathcal{V}$ to an element κ.

Proof. The volume integrals are zero since the strong form solutions satisfy Equations (2.1a) and (2.5a). The trace integrals are zero because of the assumption that u and ψ are in at least $C^1(\Omega)$.□

Given Extended Local Consistency is satisfied, Extended Global Consistency is also satisfied via 8.

3.3 Bilinear Error Bounds

For the following bounds, we assume shape regularity and also sufficient smoothness in u and ψ such that the following classical results[15, Theorem 4.4.4] hold

$$|u - u_{h,p}|_{H^m(\kappa)} \lesssim h_\kappa^{p+1-m} |u|_{H^{p+1}(\kappa)} \tag{3.5a}$$

$$|\psi - \psi_{h,p}|_{H^m(\kappa)} \lesssim h_\kappa^{p+1-m} |\psi|_{H^{p+1}(\kappa)}. \tag{3.5b}$$

Another useful result for the error analysis is $\|\Delta(u - u_{h,p})\|_{L^2(\kappa)} \lesssim h^{-1}|u - u_{h,p}|_{H^1(\kappa)}$[27].

For norms on the trace of an element, the standard trace theorem relationship may be used to bound the error in terms of the error in the adjacent element volumes[15, Theorem 1.6.6], which can then be bounded using the classical results above

$$\|[\![\nabla(u - u_{h,p})]\!]\|_{L^2(\partial\kappa)} \lesssim h^{-1/2}|u - u_{h,p}|_{H^1(\tilde{\kappa})} \lesssim h^{p-1/2}|u|_{H^{p+1}(\tilde{\kappa})} \tag{3.6a}$$

$$\|\psi - \psi_{h,p}\|_{L^2(\partial\kappa)} \lesssim h^{-1/2}\|\psi - \psi_{h,p}\|_{L^2(\tilde{\kappa})} \lesssim h^{p+1/2}|\psi|_{H^{p+1}(\tilde{\kappa})}. \tag{3.6b}$$

$\tilde{\kappa}$ denotes the set of elements that share a trace with κ. The next step to bounding the Error Representation Formula is to form a bound on the bilinear error.

LEMMA 10. CG Local Bilinear Error Bound

$$a_\kappa(u - u_{h,p1}, \psi - \psi_{h,p2}) \lesssim h^{p1+p2}|u|_{H^{p1+1}(\tilde{\kappa})}|\psi|_{H^{p2+1}(\kappa)},$$

where $(u_{h,p1}, \psi_{h,p2}) \in (\mathcal{V}_{h,p1} \times \mathcal{V}_{h,p2})$ *are finite element solutions of polynomial order* $p1, p2 \in \mathbb{N}$.

Proof.

$$a_\kappa(u - u_{h,p1}, \psi - \psi_{h,p2})$$

$$= -(\Delta(u - u_{h,p1}), \psi - \psi_{h,p2})_\kappa + \frac{1}{2}\langle [\![\nabla(u - u_{h,p1})]\!], \psi - \psi_{h,p2}\rangle_{\partial\kappa} \tag{3.7a}$$

$$\leq \|\Delta(u - u_{h,p1})\|_{L^2(\kappa)}\|\psi - \psi_{h,p2}\|_{L^2(\kappa)} + \frac{1}{2}\|[\![\nabla(u - u_{h,p1})]\!]\|_{L^2(\partial\kappa)}\|\psi - \psi_{h,p2}\|_{L^2(\partial\kappa)} \tag{3.7b}$$

$$\lesssim h^{p1-1}|u|_{H^{p1+1}(\kappa)}h^{p2+1}|\psi|_{H^{p2+1}(\kappa)} + h^{p1-\frac{1}{2}}|u|_{H^{p1+1}(\tilde{\kappa})}h^{p2+\frac{1}{2}}|\psi|_{H^{p2+1}(\kappa)} \tag{3.7c}$$

$$\lesssim h^{p1+p2}|u|_{H^{p1+1}(\tilde{\kappa})}|\psi|_{H^{p2+1}(\kappa)}. \tag{3.7d}$$

□

LEMMA 11. CG Global Bilinear Error Bound

$$a_h(u - u_{h,p1}, \psi - \psi_{h,p2}) \lesssim h^{p1+p2}|u|_{H^{p1+1}(\Omega)}|\psi|_{H^{p2+1}(\Omega)},$$

where $(u_{h,p1}, \psi_{h,p2}) \in (\mathcal{V}_{h,p1} \times \mathcal{V}_{h,p2})$ *are finite element solutions of polynomial order* $p1, p2 \in \mathbb{N}$.

Proof.

$$a_h(u - u_{h,p1}, \psi - \psi_{h,p2}) = \sum_{\kappa \in \mathcal{T}_h} a_\kappa(u - u_{h,p1}, \psi - \psi_{h,p2}) \tag{3.8a}$$

$$\lesssim \sum_{\kappa \in \mathcal{T}_h} h^{p1+p2}|u|_{H^{p1+1}(\tilde{\kappa})}|\psi|_{H^{p2+1}(\kappa)} \tag{3.8b}$$

$$\lesssim h^{p1+p2}|u|_{H^{p1+1}(\Omega)}|\psi|_{H^{p2+1}(\Omega)}. \tag{3.8c}$$

□

3.4 Global Error Bounds

In this section Lemma 11 is used to derive asymptotic convergence rates for $\mathcal{E}$ and $\mathcal{E} - \tilde{\mathcal{E}}$ for the CG discretization.

THEOREM 12. CG Global Error Bound
Let $u_{h,p} \in \mathcal{V}_{h,p}$ *be the finite element solution of order* p. *Then the global error satisfies*

$$|\mathcal{E}| \lesssim h^{2p}|u|_{H^{p+1}(\Omega)}|\psi|_{H^{p+1}(\Omega)}.$$

Proof.

$$|\mathcal{E}| = |R_h(u_{h,p}, \psi - v_{h,p})|, \ \forall v_{h,p} \in \mathcal{V}_{h,p} \tag{3.9a}$$

$$= |R_h(u_{h,p}, \psi - \psi_{h,p})| \tag{3.9b}$$

$$= |a_h(u - u_{h,p}, \psi - \psi_{h,p})| \quad \text{via Lemma 4} \tag{3.9c}$$

$$\lesssim h^{2p}|u|_{H^{p+1}(\Omega)}|\psi|_{H^{p+1}(\Omega)} \quad \text{via Lemma 11.} \tag{3.9d}$$

□

THEOREM 13. CG Global Estimate Error Bound
Let $u_{h,p}, \psi_{h,p'} \in (\mathcal{V}_{h,p} \times \mathcal{V}_{h,p'})$ *be the finite element solutions of order* p *and* p' *respectively. Then*

the error in the global estimate satisfies

$$|\mathcal{E} - \tilde{\mathcal{E}}| \lesssim h^{2p'} |u|_{H^{p'+1}(\Omega)} |\psi|_{H^{p'+1}(\Omega)}.$$

Proof.

$$\begin{aligned}
|\mathcal{E} - \tilde{\mathcal{E}}| &= |R_h(u_{h,p}, \psi - v_{h,p}) - R_h(u_{h,p}, \psi_{h,p'} - v_{h,p})|, \ \forall v_{h,p} \in \mathcal{V}_{h,p} && (3.10a)\\
&= |R_h(u_{h,p}, \psi - \psi_{h,p'})| && (3.10b)\\
&= |R_h^{\psi}(u - u_{h,p}, \psi_{h,p'})| \quad \text{via Lemma 4} && (3.10c)\\
&= |R_h^{\psi}(u - v_{h,p'}, \psi_{h,p'})|, \ \forall v_{h,p'} \in \mathcal{V}_{h,p'} \quad \text{via orthogonality} && (3.10d)\\
&= |a_h(u - v_{h,p'}, \psi - \psi_{h,p'})|, \ \forall v_{h,p'} \in \mathcal{V}_{h,p'} \quad \text{via Lemma 4} && (3.10e)\\
&\lesssim h^{2p'} |u|_{H^{p'+1}(\Omega)} |\psi|_{H^{p'+1}(\Omega)} \quad \text{via Lemma 11.} && (3.10f)
\end{aligned}$$

□

COROLLARY 14. CG Global Estimate Effectivity Bound

$$\frac{|\mathcal{E} - \tilde{\mathcal{E}}|}{|\mathcal{E}|} \lesssim h^{2p_{inc}}.$$

Proof.

$$\frac{|\mathcal{E} - \tilde{\mathcal{E}}|}{|\mathcal{E}|} \lesssim \frac{h^{2p'} |u|_{H^{p'+1}(\Omega)} |\psi|_{H^{p'+1}(\Omega)}}{h^{2p} |u|_{H^{p+1}(\Omega)} |\psi|_{H^{p+1}(\Omega)}} \lesssim h^{2p_{inc}}. \tag{3.11}$$

□

3.5 Local Error Bound

In this section Lemma 10 is used to derive asymptotic convergence rates for η_κ and $\eta_\kappa - \tilde{\eta}_\kappa$ for the CG discretization. In common with the global results, all that is necessary to bound the relevant formulae are Lemmas 7 and 10. The integration by parts of the global residual to arrive at the localized residual means that $r_\kappa(u_{h,p}, v_{h,p}) \neq 0, \ \forall v_{h,p} \in \mathcal{V}_{h,p}$ thus the adjoint solution in p must be explicitly subtracted to achieve the optimal convergence.

Theorems 15 and 16 contains semi-norms on the element κ, these semi norms converge to 0 with order $O(h^{\frac{d}{2}})$, thus when combined in a pair they give an additional $O(h^d)$ rate of convergence to the local estimate.

THEOREM 15. CG Local Error Bound

Let $(u_{h,p}, \psi_{h,p}) \in (\mathcal{V}_{h,p} \times \mathcal{V}_{h,p})$ *be the finite element solutions of order* p. *Then the local error satisfies*

$$|\eta_\kappa| \lesssim h^{2p} |u|_{H^{p+1}(\tilde{\kappa})} |\psi|_{H^{p+1}(\kappa)}.$$

Proof.

$$|\eta_\kappa| = |r_\kappa(u_{h,p}, \psi - \psi_{h,p})| \tag{3.12a}$$

$$= |a_\kappa(u - u_{h,p}, \psi - \psi_{h,p})| \quad \text{via Lemma 7} \tag{3.12b}$$

$$\lesssim h^{2p} |u|_{H^{p+1}(\tilde{\kappa})} |\psi|_{H^{p+1}(\kappa)} \quad \text{via Lemma 10} \tag{3.12c}$$

$$\lesssim h^{2p+d}. \tag{3.12d}$$

□

THEOREM 16. CG Local Estimate Error Bound

Let $u_{h,p}, \psi_{h,p'} \in (\mathcal{V}_{h,p} \times \mathcal{V}_{h,p'})$ *be the finite element solutions of order* p *and* p' *respectively. Then the error in the local estimate satisfies*

$$|\eta_\kappa - \tilde{\eta}_\kappa| \lesssim h^{p+p'} |u|_{H^{p+1}(\tilde{\kappa})} |\psi|_{H^{p+1}(\kappa)}.$$

Proof.

$$|\eta_\kappa - \tilde{\eta}_\kappa| = |r_\kappa(u_{h,p}, \psi - \psi_{h,p}) - r_\kappa(u_{h,p}, \psi_{h,p'} - \psi_{h,p})| \tag{3.13a}$$

$$= |r_\kappa(u_{h,p}, \psi - \psi_{h,p'})| \tag{3.13b}$$

$$= |a_\kappa(u - u_{h,p}, \psi - \psi_{h,p'})| \quad \text{via Lemma 7} \tag{3.13c}$$

$$\lesssim h^{p+p'} |u|_{H^{p+1}(\tilde{\kappa})} |\psi|_{H^{p'+1}(\kappa)} \quad \text{via Lemma 10} \tag{3.13d}$$

$$\lesssim h^{p+p'+d} \tag{3.13e}$$

□

COROLLARY 17. CG Local Estimate Effectivity Bound

$$\frac{|\eta_\kappa - \tilde{\eta}_\kappa|}{|\eta_\kappa|} \lesssim h^{p_{inc}}.$$

Proof.

$$\frac{|\eta_\kappa - \tilde{\eta}_\kappa|}{|\eta_\kappa|} \lesssim \frac{h^{p+p'} |u|_{H^{p+1}(\tilde{\kappa})} |\psi|_{H^{p'+1}(\kappa)}}{h^{2p} |u|_{H^{p+1}(\tilde{\kappa})} |\psi|_{H^{p+1}(\kappa)}} \lesssim h^{p_{inc}}. \tag{3.14}$$

□

3.6 One Dimensional Convergence

In one dimension, the local estimate for CG converges faster than the $p + p'$ rate determined in Theorem 16. In this section, we prove that the local estimate converges at $O(h^{2p'})$ in one dimension. To begin, we note that in one dimension, CG approximations are exact at the boundary of elements for Poisson problems[28]. As a result, terms such as $\psi - \psi_{h,p'}$ on $\partial\kappa$ will be zero. Thus the error in the error estimate $\eta_\kappa - \tilde{\eta}_\kappa$ can be written

$$\eta_\kappa - \tilde{\eta}_\kappa = r_\kappa(u_{h,p}, \psi - \psi_{h,p'}) = ((f + \Delta u_{h,p}), \psi - \psi_{h,p'})_\kappa. \tag{3.15}$$

Through Galerkin orthogonality of the adjoint equation

$$0 = (\nabla w, \nabla(\psi - \psi_{h,p'}))_{\mathcal{T}_h}, \ \forall w \in \mathcal{V}_{h,p'}, \tag{3.16}$$

integrating by parts and accounting for $\psi - \psi_{h,p'} = 0$ on $\partial\mathcal{T}_h$ gives

$$0 = (\Delta w, \psi - \psi_{h,p'})_{\mathcal{T}_h}, \ \forall w \in \mathcal{V}_{h,p'}. \tag{3.17}$$

For $w \in \mathcal{V}_{h,p'}$, then Δw is in a discontinuous polynomial space, specifically $q = \Delta w \in \oplus_\kappa \mathcal{V}_{h,p'-2}(\kappa)$. Thus, since this space is discontinuous, Equation (3.17) holds at the elemental level,

$$0 = -(q, (\psi - \psi_{h,p'})_\kappa, \ \forall q \in \mathcal{V}_{h,p'-2}(\kappa). \tag{3.18}$$

Using Equation (3.18), the error in the localized error estimate given in Equation (3.15) can be bounded,

$$((f+\Delta u_{h,p}),\psi-\psi_{h,p'})_\kappa = ((f+\Delta u_{h,p}+q),\psi-\psi_{h,p'})_\kappa,\ \forall q\in\mathcal{V}_{h,p'-2}(\kappa) \tag{3.19a}$$

$$\leq \|f+\Delta u_{h,p}+q\|_{L^2(\kappa)}\|\psi-\psi_{h,p'}\|_{L^2(\kappa)}. \tag{3.19b}$$

Since $u_{h,p}\in\mathcal{V}_{h,p}(\kappa)$, $\Delta u_{h,p}\in\mathcal{V}_{h,p-2}(\kappa)\subset\mathcal{V}_{h,p'-2}(\kappa)$

$$\|f+\Delta u_{h,p}+q\|_{L^2(\kappa)}\|\psi-\psi_{h,p'}\|_{L^2(\kappa)},\ \forall q\in\mathcal{V}_{h,p'-2}(\kappa) \tag{3.20a}$$

$$= \|f+\Delta u_{h,p'}\|_{L^2(\kappa)}\|\psi-\psi_{h,p'}\|_{L^2(\kappa)} \tag{3.20b}$$

$$= \|\Delta(u-u_{h,p'})\|_{L^2(\kappa)}\|\psi-\psi_{h,p'}\|_{L^2(\kappa)} \tag{3.20c}$$

$$\lesssim h^{p'-1}|u|_{H^{p'+1}(\kappa)}h^{p'+1}|\psi|_{H^{p'+1}(\kappa)} = h^{2p'}|u|_{H^{p'+1}(\kappa)}|\psi|_{H^{p'+1}(\kappa)} = h^{2p'+1}, \tag{3.20d}$$

which completes the proof.

CHAPTER 4

DISCONTINUOUS GALERKIN

The Discontinuous Galerkin (DG) scheme considered in this thesis is Bassi and Rebay's second version, BR2 [11]. The convergence of global and local DWR estimates for BR2 has already been analyzed by Yano[29] who showed that the p-dependency of the lifting operator can limit the convergence rate of the global error estimate. To resolve this a mixed formulation for the error estimate is proposed.

4.1 Discretization

For the DG discretization, the approximation space $\mathcal{V}_{h,p}$ is made up of piecewise discontinuous polynomials of order p,

$$\mathcal{V}_{h,p} \equiv \{v \in L^2(\Omega) : v|_\kappa \in \mathbb{P}^p(\kappa), \quad \forall \kappa \in \mathcal{T}_h\}, \tag{4.1}$$

and the bilinear term is given by

$$a_{h,p}(v,w) = (\nabla v, \nabla w)_{\mathcal{T}_h} \tag{4.2a}$$

$$- \langle \{\nabla v\}, [\![w]\!] \rangle_{\mathcal{F}_h} - \langle [\![v]\!], \{\nabla w\} \rangle_{\mathcal{F}_h} \tag{4.2b}$$

$$- \langle \xi \vec{r}^{\,f}_{h,p}([\![v]\!]), [\![w]\!] \rangle_{\mathcal{F}_h}. \tag{4.2c}$$

The p subscript denotes that the bilinear term is p dependent, this means the residual operator $R_{h,p}(v,w)$ is also p dependent. For stability ξ must be set to greater than the number of traces of the element where the residual is evaluated, i.e. 3 for 2D simplices[16]. The lifting operator is defined on trace $f \in \mathcal{F}_h$ by the expression[2],

$$\vec{r}^{f}_{h,p}(v) \in [\mathcal{V}_{h,p}]^d : (\vec{r}^{f}_{h,p}(v), g)_{\mathcal{T}_h} = -\langle v, \{g\}\rangle_f, \quad \forall g \in [\mathcal{V}_{h,p}]^d \tag{4.3}$$

where $v \in [L^1(f)]^d$. The p-dependence of the DG residual operator is contained in the expression for the lifting operator $\vec{r}^{f}_{h,p}(v)$[29], namely

$$\vec{r}^{f}_{h,q}(v_{h,q}) \neq \vec{r}^{f}_{h,p}(v_{h,q}), \quad v_{h,q} \in \mathcal{V}_{h,q}, \quad \forall q,p \in \mathbb{N} : q < p. \tag{4.4}$$

The p dependence suggests two similar estimates, one where the residual is evaluated in p, $\tilde{\mathcal{E}}^1$, and one where the residual is evaluated in p', $\tilde{\mathcal{E}}^2$[29].

$$\tilde{\mathcal{E}}^1 = R_{h,p}(u_{h,p}, \psi_{h,p'}) \tag{4.5a}$$

$$\tilde{\mathcal{E}}^2 = R_{h,p'}(u_{h,p}, \psi_{h,p'}) \tag{4.5b}$$

These estimates are analyzed in Section 4.6, placing them within a p independent framework, and their sub-optimal performance is explained.

An alternative strategy is to append the lifting operator definition in the weak form to the residual such that the bilinear term for the BR2 discretization is written as

$$a_h(v, \vec{r}^{F}; w, \vec{s}^{F}) = (\nabla v, \nabla w)_{\mathcal{T}_h} \tag{4.6a}$$

$$- \langle \{\nabla v\}, [\![w]\!]\rangle_{\mathcal{F}_h} - \langle [\![v]\!], \{\nabla w\}\rangle_{\mathcal{F}_h} - \langle \xi\{\vec{r}^{f}\}, [\![w]\!]\rangle_{\mathcal{F}_h} \tag{4.6b}$$

$$- \sum_{f \in \mathcal{F}_h} \Big((\vec{r}^{f}, \vec{s}^{f})_{\mathcal{T}_h} + \langle [\![v]\!], \{\vec{s}^{f}\}\rangle_f \Big), \tag{4.6c}$$

where $\vec{r}^{F}$ and $\vec{s}^{F} \in \mathcal{S}^{F}_{h,p}$ and $\mathcal{S}^{F}_{h,p} \equiv \prod_{f \in \mathcal{F}_h} [\mathcal{V}_{h,p}]^d$, and $\vec{r}^{f}$ is the element in $\vec{r}^{F}$ corresponding to face

f. The infinite dimensional equivalent is denoted $\mathcal{S}^F \equiv \prod_{f\in\mathcal{F}_h}[\mathcal{V}]^d$.

For succinctness $\mathbf{V} = (v, \vec{r}^F)$ and $\mathbf{W} = (w, \vec{s}^F)$ tuples are specified as arguments, thus $a_h(\mathbf{V}_{h,p}, \mathbf{W}) \equiv a_h(v_{h,p}, \vec{r}^F_{h,p}; w, \vec{s}^F)$. The discretization may be written as

$$(\mathbf{U}_{h,p}) \in (\mathcal{V}_{h,p} \times \mathcal{S}^F_{h,p}) : R_h(\mathbf{U}_{h,p}, \mathbf{W}_{h,p}) = 0, \quad \forall(\mathbf{W}_{h,p}) \in (\mathcal{V}_{h,p} \times \mathcal{S}^F_{h,p}). \tag{4.7}$$

The exact $\vec{r}^f$ is defined by substituting in the strong form solution $u \in C^1(\Omega)$, thus $[\![u]\!] = 0$. Then setting $w = 0$ shows that $\vec{r}^f = 0$ for the exact solution. The adjoint residual for the DG formulation can be written using the tuples as

$$R^\psi_h(\mathbf{W}, \mathbf{V}) = \mathcal{J}(w) - a_h(\mathbf{W}, \mathbf{V}). \tag{4.8}$$

Substituting in $\psi \in C^1(\Omega)$, $[\![\psi]\!] = 0$, then setting $w = 0$ shows that $\vec{\sigma}^f = 0$. The tuple of the adjoint variables is defined as $\mathbf{\Psi} = (\psi, \vec{\sigma}^F)$.

4.2 Localization

The DG residual is simply localized,

$$r_\kappa(\mathbf{V}, \mathbf{W}) = R_h(\mathbf{V}, \mathbf{W}|_\kappa), \tag{4.9}$$

because unlike CG, DG displays extended local consistency when the test functions are elementally restricted.

LEMMA 18. DG Extended Local Consistency

$$r_\kappa(\mathbf{U}, \mathbf{W}) = 0, \quad \forall \mathbf{W} \in (\mathcal{V}(\kappa) \times \mathcal{S}^F(\kappa))$$
$$r^\psi_\kappa(\mathbf{W}, \mathbf{\Psi}) = 0, \quad \forall \mathbf{W} \in (\mathcal{V}(\kappa) \times \mathcal{S}^F(\kappa)),$$

where $\mathcal{V}(\kappa)$ and $\mathcal{S}^F(\kappa)$ are the elemental restrictions of $\mathcal{V}$ and $\mathcal{S}^F$.

Proof. For the exact solution $\mathbf{U}$, $[\![u]\!] = 0$ and $\vec{r}^f = 0$ leaving

$$r_\kappa(\mathbf{U}, \mathbf{W}) = (f, w)_\kappa - (\nabla u, \nabla w)_\kappa + \langle \nabla u \cdot \hat{n}, w \rangle_{\partial\kappa} \tag{4.10a}$$

$$= (f + \Delta u, w)_\kappa = 0, \quad \forall w \in \mathcal{V}(\kappa). \tag{4.10b}$$

Similarly, for the dual localized residual

$$r_\kappa^\psi(\mathbf{W}, \mathbf{\Psi}) = (g, w)_\kappa - (\nabla \psi, \nabla w)_\kappa + \langle \nabla \psi \cdot \hat{n}, w \rangle_{\partial\kappa} \tag{4.11a}$$

$$= (g + \Delta \psi, w)_\kappa = 0, \quad \forall w \in \mathcal{V}(\kappa). \tag{4.11b}$$

□

LEMMA 19. DG Extended Global Consistency

$$R_h(\mathbf{U}, \mathbf{W}) = 0, \quad \forall \mathbf{W} \in \oplus_\kappa(\mathcal{V}(\kappa) \times \mathcal{S}^F(\kappa))$$
$$R_h^\psi(\mathbf{W}, \mathbf{\Psi}) = 0, \quad \forall \mathbf{W} \in \oplus_\kappa(\mathcal{V}(\kappa) \times \mathcal{S}^F(\kappa)).$$

Proof. Via Lemma 18, the proof follows naturally

$$R_h(\mathbf{U}, \mathbf{W}) = \sum_{\kappa \in \mathcal{T}_h} r_\kappa(\mathbf{U}, \mathbf{W}) = 0, \quad \forall \mathbf{W} \in \oplus_\kappa(\mathcal{V}(\kappa) \times \mathcal{S}^F(\kappa)) \tag{4.12a}$$

$$R_h^\psi(\mathbf{W}, \mathbf{\Psi}) = \sum_{\kappa \in \mathcal{T}_h} r_\kappa^\psi(\mathbf{W}, \mathbf{\Psi}) = 0, \quad \forall \mathbf{W} \in \oplus_\kappa(\mathcal{V}(\kappa) \times \mathcal{S}^F(\kappa)). \tag{4.12b}$$

□

4.3 Bilinear Error Bounds

Assuming sufficient smoothness of the solution, existing error bounds can be used[2],

$$|u - u_{h,p}|_{H^m(\kappa)} \lesssim h^{p+1-m} |u|_{H^{p+1}(\kappa)} \tag{4.13a}$$

$$|\psi - \psi_{h,p}|_{H^m(\kappa)} \lesssim h^{p+1-m} |\psi|_{H^{p+1}(\kappa)}. \tag{4.13b}$$

Given $u, \psi \in C^0$, bounds on interface jumps, $||[\![u_{h,p}]\!]||_{L^2(f)}$ and $||[\![\psi_{h,p}]\!]||_{L^2(f)}$ can be used[16]

$$||[\![u_{h,p}]\!]||_{L^2(f)} \lesssim h^{-\frac{1}{2}}||u - u_{h,p}||_{L^2(\kappa_f)} \tag{4.14a}$$

$$||[\![\psi_{h,p}]\!]||_{L^2(f)} \lesssim h^{-\frac{1}{2}}||\psi - \psi_{h,p}||_{L^2(\kappa_f)}. \tag{4.14b}$$

Trace scaling can also be applied to relate norms on the trace to the elements[15, Theorem 1.6.6],

$$|u - u_{h,p}|_{H^m(f)} \lesssim h^{-\frac{1}{2}}|u - u_{h,p}|_{H^m(\kappa_f)} \tag{4.15a}$$

$$|\psi - \psi_{h,p}|_{H^m(f)} \lesssim h^{-\frac{1}{2}}|\psi - \psi_{h,p}|_{H^m(\kappa_f)}. \tag{4.15b}$$

In addition, error bounds are required for $\vec{r}^{\,f}_{h,p}$ and $\vec{\sigma}^{\,f}_{h,p}$. The definitions of $\vec{r}^{\,f}_{h,p}$ and $\vec{\sigma}^{\,f}_{h,p}$ are unchanged, thus existing bounds for $\vec{r}^{\,f}_{h,p}$ and $\vec{\sigma}^{\,f}_{h,p}$ can be used[16], but the proof is repeated here for completeness.

LEMMA 20. DG Auxilliary Variable Bounds

$$||\vec{r}^{\,f}_{h,p}||_{L^2(\kappa_f)} \lesssim ||[\![u_{h,p}]\!]||_{L^2(f)}$$
$$||\vec{\sigma}^{\,f}_{h,p}||_{L^2(\kappa_f)} \lesssim ||[\![\psi_{h,p}]\!]||_{L^2(f)}.$$

Proof.

$$||\vec{r}^{\,f}_{h,p}||^2_{L^2(\kappa)} = (\vec{r}^{\,f}_{h,p}, \vec{r}^{\,f}_{h,p})_{\kappa_f} \tag{4.16a}$$

$$= -\langle \vec{r}^{\,f}_{h,p}, [\![u_{h,p}]\!]\rangle_f \tag{4.16b}$$

$$\leq ||\vec{r}^{\,f}_{h,p}||_{L^2(f)}||[\![u_{h,p}]\!]||_{L^2(f)} \tag{4.16c}$$

$$\lesssim h^{-\frac{1}{2}}||\vec{r}^{\,f}_{h,p}||_{L^2(\kappa_f)}||[\![u_{h,p}]\!]||_{L^2(f)} \tag{4.16d}$$

$$||\vec{r}^{\,f}_{h,p}||_{L^2(\kappa)} \lesssim h^{-\frac{1}{2}}||[\![u_{h,p}]\!]||_{L^2(f)}. \tag{4.16e}$$

$$\|\vec{\sigma}^f_{h,p}\|^2_{L^2(\kappa)} = (\vec{\sigma}^f_{h,p}, \vec{\sigma}^f_{h,p})_{\kappa_f} \tag{4.17a}$$

$$= -\xi\langle\vec{\sigma}^f_{h,p}, [\![\psi_{h,p}]\!]\rangle_f \tag{4.17b}$$

$$\lesssim \|\vec{\sigma}^f_{h,p}\|_{L^2(f)}\|[\![\psi_{h,p}]\!]\|_{L^2(f)} \tag{4.17c}$$

$$\lesssim h^{-\frac{1}{2}}\|\vec{\sigma}^f_{h,p}\|_{L^2(\kappa_f)}\|[\![\psi_{h,p}]\!]\|_{L^2(f)} \tag{4.17d}$$

$$\|\vec{\sigma}^f_{h,p}\|_{L^2(\kappa)} \lesssim h^{-\frac{1}{2}}\|[\![\psi_{h,p}]\!]\|_{L^2(f)}. \tag{4.17e}$$

□

LEMMA 21. DG Local Bilinear Error Bound

$$a_\kappa(\mathbf{U} - \mathbf{U}_{h,p1}, \mathbf{\Psi} - \mathbf{\Psi}_{h,p2}) \equiv a_h(\mathbf{U} - \mathbf{U}_{h,p1}, (\mathbf{\Psi} - \mathbf{\Psi}_{h,p2})|_\kappa) \lesssim h^{p1+p2}|u|_{H^{p1+1}(\tilde{\kappa})}|\psi|_{H^{p2+1}(\kappa)},$$

where $(\mathbf{U}_{h,p1}, \mathbf{\Psi}_{h,p2})$ *are finite element solutions of polynomial order* $p1, p2 \in \mathbb{N}$.

Proof.

$$a_\kappa(\mathbf{U} - \mathbf{U}_{h,p1}, \mathbf{\Psi} - \mathbf{\Psi}_{h,p2})$$

$$= \underbrace{(\nabla(u - u_{h,p1}), \nabla(\psi - \psi_{h,p2}))_\kappa}_{\mathbf{I}} + \underbrace{\langle\{\nabla(u - u_{h,p1})\}\cdot\hat{n}, \psi - \psi_{h,p2}\rangle_{\partial\kappa}}_{\mathbf{II}} \tag{4.18a}$$

$$+ \underbrace{\langle[\![u - u_{h,p1}]\!], \alpha\nabla(\psi - \psi_{h,p2})\rangle_{\partial\kappa}}_{\mathbf{III}} - \underbrace{\sum_{f\in\partial\kappa}\langle\xi\{\vec{r}^f_{h,p1}\}\cdot\hat{n}, \psi - \psi_{h,p2}\rangle_f}_{\mathbf{IV}} \tag{4.18b}$$

$$+ \underbrace{\sum_{f\in\partial\kappa}(\vec{r}^f_{h,p1}, \vec{\sigma}^f_{h,p2})_\kappa}_{\mathbf{V}} - \underbrace{\sum_{f\in\partial\kappa}\langle[\![u - u_{h,p1}]\!], \alpha\vec{\sigma}^f_{h,p2}\rangle_f}_{\mathbf{VI}}. \tag{4.18c}$$

Where $\alpha = \frac{1}{2},\ \forall f \in \mathcal{F}_h^{\text{internal}}$ and $\alpha = 1,\ \forall f \in \mathcal{F}_h^{\text{boundary}}$. In order to bound the whole, it suffices to bound the components individually

(I)

$$(\nabla(u - u_{h,p1}), \nabla(\psi - \psi_{h,p2}))_\kappa \tag{4.19a}$$

$$\leq \|\nabla(u - u_{h,p1})\|_{L^2(\kappa)}\|\nabla(\psi - \psi_{h,p2})\|_{L^2(\kappa)} \tag{4.19b}$$

$$\lesssim h^{p1+p2}|u|_{H^{p1+1}(\kappa)}|\psi|_{H^{p2+1}(\kappa)}. \tag{4.19c}$$

(II)

$$\langle\{\nabla(u-u_{h,p1})\},\psi-\psi_{h,p2}\rangle_{\partial\kappa} \tag{4.20a}$$

$$\leq \|\{\nabla(u-u_{h,p1})\}\cdot\hat{n}\|_{L^2(\partial\kappa)}\|\psi-\psi_{h,p2}\|_{L^2(\partial\kappa)} \tag{4.20b}$$

$$\lesssim h^{p1+p2}|u|_{H^{p1+1}(\tilde{\kappa})}|\psi|_{H^{p2+1}(\kappa)}. \tag{4.20c}$$

(III)

$$\langle[\![u-u_{h,p1}]\!],\alpha\nabla(\psi-\psi_{h,p2})\rangle_{\partial\kappa} \tag{4.21a}$$

$$\lesssim \|[\![u-u_{h,p1}]\!]\|_{L^2(\partial\kappa)}\|\nabla(\psi-\psi_{h,p2})\|_{L^2(\partial\kappa)} \tag{4.21b}$$

$$\lesssim h^{p1+p2}|u|_{H^{p1+1}(\tilde{\kappa})}|\psi|_{H^{p2+1}(\kappa)}. \tag{4.21c}$$

(IV)

$$\sum_{f\in\partial\kappa}\langle\xi\{\vec{r}^{\,f}_{h,p1}\}\cdot\hat{n},\psi-\psi_{h,p2}\rangle_f \tag{4.22a}$$

$$\lesssim \sum_{f\in\partial\kappa}\|\{\vec{r}^{\,f}_{h,p1}\}\|_{L^2(f)}\|\psi-\psi_{h,p2}\|_{L^2(f)} \tag{4.22b}$$

$$\lesssim \sum_{f\in\partial\kappa}h^{-1}\|\vec{r}^{\,f}_{h,p1}\|_{L^2(\kappa_f)}\|\psi-\psi_{h,p2}\|_{L^2(\kappa)} \tag{4.22c}$$

$$\lesssim h^{p1+p2}|u|_{H^{p1+1}(\tilde{\kappa})}|\psi|_{H^{p2+1}(\kappa)}. \tag{4.22d}$$

(V)

$$\sum_{f\in\partial\kappa}(\vec{r}^{\,f}_{h,p1},\vec{\sigma}^{\,f}_{h,p2})_\kappa \tag{4.23a}$$

$$\leq \sum_{f\in\partial\kappa}\|\vec{r}^{\,f}_{h,p1}\|_{L^2(\kappa)}\|\vec{\sigma}^{\,f}_{h,p2}\|_{L^2(\kappa)} \tag{4.23b}$$

$$\lesssim h^{p1+p2}|u|_{H^{p1+1}(\tilde{\kappa})}|\psi|_{H^{p2+1}(\tilde{\kappa})}. \tag{4.23c}$$

(VI)

$$\sum_{f\in\partial\kappa} \langle [\![u - u_{h,p1}]\!], \alpha\vec{\sigma}^f_{h,p2}\rangle_f \tag{4.24a}$$

$$\lesssim \sum_{f\in\partial\kappa} \|[\![u - u_{h,p1}]\!]\|_{L^2(f)}\|\vec{\sigma}^f_{h,p2}\|_{L^2(f)} \tag{4.24b}$$

$$\lesssim \sum_{f\in\partial\kappa} h^{-1}\|u - u_{h,p1}\|_{L^2(\tilde{\kappa})}\|\vec{\sigma}^f_{h,p2}\|_{L^2(\kappa)} \tag{4.24c}$$

$$\lesssim h^{p1+p2}|u|_{H^{p1+1}(\tilde{\kappa})}|\psi|_{H^{p2+1}(\tilde{\kappa})}. \tag{4.24d}$$

Thus,

$$a_\kappa(\mathbf{U} - \mathbf{U}_{h,p1}, \mathbf{\Psi} - \mathbf{\Psi}_{h,p2}) \lesssim h^{p1+p2}|u|_{H^{p1+1}(\tilde{\kappa})}|\psi|_{H^{p2+1}(\tilde{\kappa})}.$$

□

Using Corollary 8 the Global Bilinear Error Bound is given by

Lemma 22. DG Global Bilinear Form Error Bound

$$a_h(\mathbf{U} - \mathbf{U}_{h,p1}, \mathbf{\Psi} - \mathbf{\Psi}_{h,p2}) \lesssim h^{p1+p2}|u|_{H^{p1+1}(\Omega)}|\psi|_{H^{p2+1}(\Omega)}.$$

Proof.

$$a_h(\mathbf{U} - \mathbf{U}_{h,p1}, \mathbf{\Psi} - \mathbf{\Psi}_{h,p2}) = \sum_{\kappa\in\mathcal{T}_h} a_\kappa(\mathbf{U} - \mathbf{U}_{h,p1}, \mathbf{\Psi} - \mathbf{\Psi}_{h,p2}) \tag{4.25a}$$

$$\lesssim \sum_{\kappa\in\mathcal{T}_h} h^{p1+p2}|u|_{H^{p1+1}(\tilde{\kappa})}|\psi|_{H^{p2+1}(\tilde{\kappa})} \tag{4.25b}$$

$$\lesssim h^{p1+p2}|u|_{H^{p1+1}(\Omega)}|\psi|_{H^{p2+1}(\Omega)}. \tag{4.25c}$$

□

4.4 Global Error Bound

In this section Lemma 22 is used to derive asymptotic convergence rates for $\mathcal{E}$ and $\mathcal{E} - \tilde{\mathcal{E}}$ for the DG discretization.

THEOREM 23. DG Global Error Bound

$$|\mathcal{E}| \lesssim h^{2p}|u|_{H^{p+1}(\Omega)}|\psi|_{H^{p+1}(\Omega)}.$$

Proof.

$$|\mathcal{E}| = |R_h(\mathbf{U}_{h,p}, \mathbf{\Psi} - \mathbf{W}_{h,p})|, \ \forall \mathbf{W}_{h,p} \in (\mathcal{V}_{h,p} \times \mathcal{S}^F_{h,p}) \tag{4.26a}$$

$$= |R_h(\mathbf{U}_{h,p}, \mathbf{\Psi} - \mathbf{\Psi}_{h,p})| \tag{4.26b}$$

$$= |a_h(\mathbf{U} - \mathbf{U}_{h,p}, \mathbf{\Psi} - \mathbf{\Psi}_{h,p})| \quad \text{via Lemma 4} \tag{4.26c}$$

$$\lesssim h^{2p}|u|_{H^{p+1}(\Omega)}|\psi|_{H^{p+1}(\Omega)} \quad \text{via Lemma 22.} \tag{4.26d}$$

□

THEOREM 24. DG Global Estimate Error Bound

$$|\mathcal{E} - \tilde{\mathcal{E}}| \lesssim h^{2p'}|u|_{H^{p'+1}(\Omega)}|\psi|_{H^{p'+1}(\Omega)}.$$

Proof.

$$|\mathcal{E} - \tilde{\mathcal{E}}| = |R_h(\mathbf{U}_{h,p}, \mathbf{\Psi} - \mathbf{W}_{h,p}) - R_h(\mathbf{U}_{h,p}, \mathbf{\Psi}_{h,p'} - \mathbf{W}_{h,p})|, \ \forall \mathbf{W}_{h,p} \in (\mathcal{V}_{h,p} \times \mathcal{S}^F_{h,p}) \tag{4.27a}$$

$$= |R_h(\mathbf{U}_{h,p}, \mathbf{\Psi} - \mathbf{\Psi}_{h,p'})| \tag{4.27b}$$

$$= |R^{\psi}_h(\mathbf{U} - \mathbf{U}_{h,p}, \mathbf{\Psi}_{h,p'})| \quad \text{via Lemma 4} \tag{4.27c}$$

$$= |R^{\psi}_h(\mathbf{U} - \mathbf{W}_{h,p'}, \mathbf{\Psi}_{h,p'})|, \ \forall \mathbf{W}_{h,p'} \in (\mathcal{V}_{h,p'} \times \mathcal{S}^F_{h,p'}) \quad \text{via orthogonality} \tag{4.27d}$$

$$= |a_h(\mathbf{U} - \mathbf{W}_{h,p'}, \mathbf{\Psi} - \mathbf{\Psi}_{h,p'})|, \ \forall \mathbf{W}_{h,p'} \in (\mathcal{V}_{h,p'} \times \mathcal{S}^F_{h,p'}) \quad \text{via Lemma 4} \tag{4.27e}$$

$$\lesssim h^{2p'}|u|_{H^{p'+1}(\Omega)}|\psi|_{H^{p'+1}(\Omega)} \quad \text{via Lemma 22.} \tag{4.27f}$$

□

COROLLARY 25. DG Global Estimate Effectivity Bound

$$\frac{|\mathcal{E} - \tilde{\mathcal{E}}|}{|\mathcal{E}|} \lesssim h^{2p_{inc}}.$$

Proof.

$$\frac{|\mathcal{E} - \tilde{\mathcal{E}}|}{|\mathcal{E}|} \lesssim \frac{h^{2p'}|u|_{H^{p'+1}(\Omega)}|\psi|_{H^{p'+1}(\Omega)}}{h^{2p}|u|_{H^{p+1}(\Omega)}|\psi|_{H^{p+1}(\Omega)}} \lesssim h^{2p_{inc}}. \tag{4.28}$$

□

4.5 Local Error Bound

In this section Lemma 21 is used to derive asymptotic convergence rates for η_κ and $\eta_\kappa - \tilde{\eta}_\kappa$ for the DG discretization. In common with the global results, all that is necessary to bound the relevant formulae are Lemmas 7 and 21. Unlike for CG (see Theorem 15), the DG localized residual is the same as the global residual, aside from the local restriction of test functions, as such $r_\kappa(\mathbf{U}_{h,p}, \mathbf{W}_{h,p}) = 0,\ \forall \mathbf{W}_{h,p} \in \mathcal{V}_{h,p}$.

Theorems 26 and 27 contains semi-norms on the element κ, these semi norms also scale $h^{\frac{d}{2}}$, thus when combined in a pair they give an additional $O(h^d)$ convergence rate to the local estimates.

THEOREM 26. DG Local Error Bound

$$|\eta_\kappa| \lesssim h^{2p} |u|_{H^{p+1}(\tilde{\kappa})} |\psi|_{H^{p+1}(\tilde{\kappa})}.$$

Proof.

$$\begin{aligned}
&(4.29a) & |\eta_\kappa| &= |r_\kappa(\mathbf{U}_{h,p}, \mathbf{\Psi} - \mathbf{W}_{h,p})|,\ \forall \mathbf{W}_{h,p} \in (\mathcal{V}_{h,p}(\kappa) \times \mathcal{S}^F_{h,p}(\kappa)) \\
&(4.29b) & &= |r_\kappa(\mathbf{U}_{h,p}, \mathbf{\Psi} - \mathbf{\Psi}_{h,p})| \\
&(4.29c) & &= |a_\kappa(\mathbf{U} - \mathbf{U}_{h,p}, \mathbf{\Psi} - \mathbf{\Psi}_{h,p})| \quad \text{via Lemma 7} \\
&(4.29d) & &\lesssim h^{2p} |u|_{H^{p+1}(\tilde{\kappa})} |\psi|_{H^{p+1}(\tilde{\kappa})} \quad \text{via Lemma 21.}
\end{aligned}$$

□

THEOREM 27. DG Local Estimate Error Bound

$$|\eta_\kappa - \tilde{\eta}_\kappa| \lesssim h^{p+p'} |u|_{H^{p+1}(\tilde{\kappa})} |\psi_{h,p'}|_{H^{p+1}(\tilde{\kappa})}.$$

Proof.

$$\begin{aligned}
&(4.30a) & |\eta_\kappa - \tilde{\eta}_\kappa| &= |r_\kappa(\mathbf{U}_{h,p}, \mathbf{\Psi} - \mathbf{W}_{h,p}) - r_\kappa(\mathbf{U}_{h,p}, \mathbf{\Psi}_{h,p'} - \mathbf{W}_{h,p})|,\ \forall \mathbf{W}_{h,p} \in (\mathcal{V}_{h,p}(\kappa) \times \mathcal{S}^F_{h,p}(\kappa)) \\
&(4.30b) & &= |r_\kappa(\mathbf{U}_{h,p}, \mathbf{\Psi} - \mathbf{\Psi}_{h,p'})| \\
&(4.30c) & &= |a_\kappa(\mathbf{U} - \mathbf{U}_{h,p}, \mathbf{\Psi} - \mathbf{\Psi}_{h,p'})| \quad \text{via Lemma 7} \\
&(4.30d) & &\lesssim h^{p+p'} |u|_{H^{p+1}(\tilde{\kappa})} |\psi|_{H^{p'+1}(\tilde{\kappa})} \quad \text{via Lemma 21.}
\end{aligned}$$

□

COROLLARY 28. DG Local Estimate Effectivity Bound

$$\frac{|\eta_\kappa - \tilde{\eta}_\kappa|}{|\eta_\kappa|} \lesssim h^{p_{inc}}.$$

Proof.

$$\frac{|\eta_\kappa - \tilde{\eta}_\kappa|}{|\eta_\kappa|} \lesssim \frac{h^{p+p'}|u|_{H^{p+1}(\tilde{\kappa})}|\psi|_{H^{p'+1}(\kappa)}}{h^{2p}|u|_{H^{p+1}(\tilde{\kappa})}|\psi|_{H^{p+1}(\kappa)}} \lesssim h^{p_{inc}}. \tag{4.31}$$

□

4.6 Statically Condensed Estimation

The full estimate $\tilde{\mathcal{E}}$ can be separated into two components,

$$\tilde{\mathcal{E}} = \tilde{\mathcal{E}}^u + \tilde{\mathcal{E}}^{\vec{r}^F} \tag{4.32a}$$

$$\tilde{\mathcal{E}}^u = R_h^u(\mathbf{U}_{h,p}, \psi_{h,p'}) \tag{4.32b}$$

$$\tilde{\mathcal{E}}^{\vec{r}^F} = R_h^{\vec{r}^F}(\mathbf{U}_{h,p}, \vec{\sigma}_{h,p'}^F), \tag{4.32c}$$

where $R_h^u(\mathbf{V}, w)$ is the residual of the scalar equation, and $R_h^{\vec{r}^F}(\mathbf{V}, \vec{s}^f)$ is the residual of the auxilliary equation. There is a corresponding separation of the local estimate

$$\tilde{\eta}_\kappa = \tilde{\eta}_\kappa^u + \tilde{\eta}_\kappa^{\vec{r}^F} \tag{4.33a}$$

$$\tilde{\eta}_\kappa^u = R_h^u(\mathbf{U}_{h,p}, \psi_{h,p'}|_\kappa) \tag{4.33b}$$

$$\tilde{\eta}_\kappa^{\vec{r}^F} = R_h^{\vec{r}^F}(\mathbf{U}_{h,p}, \vec{\sigma}_{h,p'}^F|_\kappa). \tag{4.33c}$$

To compare the two estimates, $\tilde{\mathcal{E}}^1 = R_{h,p}(u_{h,p}, \psi_{h,p'})$ and $\tilde{\mathcal{E}}^2 = R_{h,p'}(u_{h,p}, \psi_{h,p'})$ against $\tilde{\mathcal{E}}$, they can be written in the p independent residual as

$$\tilde{\mathcal{E}}^1 = R_h^u(\mathbf{U}_{h,p}, \psi_{h,p'}) \tag{4.34a}$$

$$\tilde{\mathcal{E}}^2 = R_h^u((u_{h,p}, \vec{r}_{h,p'}^F), \psi_{h,p'}) \tag{4.34b}$$

$\tilde{\mathcal{E}}^1$ and $\tilde{\mathcal{E}}^2$ only evaluate the residual for the scalar calculation. However, $\tilde{\mathcal{E}}^2$ by resolving for $\vec{r}_{h,p'}^F$ means that $R_h^{\vec{r}^F}((u_{h,p}, \vec{r}_{hp'}^F), \phi_{h,p'}^F) = 0$, $\forall \phi_{h,p'}^F \in \mathcal{S}_{h,p'}^F$. Thus $\vec{\sigma}_{h,p'}^F$ can be introduced when calculating $\mathcal{E} - \tilde{\mathcal{E}}^2$, and Lemma 4 can be used. $\mathcal{E} - \tilde{\mathcal{E}}^1$ will not converge with $O(h^{2p'})$ because it is not the whole residual, thus Lemma 4 cannot be used. Thus $\tilde{\mathcal{E}}^2 \equiv \tilde{\mathcal{E}}$ and $\tilde{\mathcal{E}}^1 \equiv \tilde{\mathcal{E}}^u$.

$\tilde{\eta}^1_\kappa$ and $\tilde{\eta}^2_\kappa$ can also be written in the p independent residual,

$$\tilde{\eta}^1_\kappa = \tilde{\eta}^u_\kappa \tag{4.35a}$$

$$\tilde{\eta}^2_\kappa = R^u_h(u_{h,p}, \vec{r}^F_{h,p'}, \psi_{h,p'}|_\kappa). \tag{4.35b}$$

$\tilde{\eta}^1_\kappa \equiv \tilde{\eta}^u_\kappa$, thus from Lemma 21 $\eta_\kappa - \tilde{\eta}^1_\kappa$ will converge at $O(h^{p+p'})$ but will have a larger error than $\tilde{\eta}_\kappa$ because $\tilde{\eta}_\kappa - \tilde{\eta}^1_\kappa = \tilde{\eta}^{\vec{r}^F}_\kappa$ also converges with order $O(h^{p+p'})$, so the ratio remains $O(1)$ with mesh refinement.

$\tilde{\eta}^2_\kappa$ performs significantly worse than $\tilde{\eta}_\kappa$, because Lemma 7 does not map to the adjoint residual. Consequently orthogonality cannot remove the error associated with the inconsistent value of $\vec{r}^F_{h,p'}$. The convergence is thus reduced to purely that of the primal variables, giving $O(h^p)$ as predicted by Yano [29].

Given the ultimate goal of using the estimates to drive an adaptive algorithm, $\tilde{\mathcal{E}}^1$, $\tilde{\eta}^1_\kappa$ was chosen by Yano[29].

Chapter 5

Hybridizable Discontinuous Galerkin

The Hybridizable Discontinuous Galerkin, or HDG, method is a mixed method, in which the first derivative on the scalar variable is introduced as an auxilliary variable, $\vec{q}$,

$$\vec{q} - \nabla u = 0 \quad \text{in } \Omega \tag{5.1a}$$

$$-\nabla \cdot \vec{q} = f \quad \text{in } \Omega \tag{5.1b}$$

$$u = 0 \quad \text{on } \partial\Omega. \tag{5.1c}$$

The particular HDG method here is derived from the Local Discontinuous Galerkin (LDG) method and is sometimes referred to as the LDG-H method [17, 18].

5.1 Discretization

The HDG residual, in common with CG and DG, can be written with a linear functional and a bilinear functional. In addition to replacing the solution gradient with an additional variable HDG replaces the trace of the scalar on the element boundaries with an additional variable $\hat{u}$. Thus $\hat{u} = u$ and $\hat{\psi} = \psi$ on the element traces, for the exact solutions u and ψ. For ease of notation $\mathbf{U} \equiv (u, \vec{q}, \hat{u})$, $\mathbf{\Psi} \equiv (\psi, \vec{\varphi}, \hat{\psi})$ and $\mathbf{W} \equiv (w, \vec{s}, \hat{w})$, thus $R_h(\mathbf{U}_{h,p}, \mathbf{W}) \equiv R_h(u_{h,p}, \vec{q}_{h,p}, \hat{u}_{h,p}; w, \vec{s}, \hat{w})$.

The discretization is defined by

$$\mathcal{V}_{h,p} \equiv \{v \in L^2(\Omega) : v|_\kappa \in \mathbb{P}^p(\kappa), \quad \forall \kappa \in \mathcal{T}_h\} \tag{5.2a}$$

$$\mathcal{Q}_{h,p} \equiv \{\vec{q} \in [L^2(\Omega)]^d : \vec{q}|_\kappa \in [\mathbb{P}^p(\kappa)]^d, \quad \forall \kappa \in \mathcal{T}_h\} \tag{5.2b}$$

$$\mathcal{M}_{h,p} \equiv \{m \in [L^2(\mathcal{F}_h)]^{d-1} : m|_f \in [\mathbb{P}^p(f)]^{d-1}, \quad \forall f \in \mathcal{F}_h\}, \tag{5.2c}$$

with bilinear term

$$a_h(v, \vec{t}, \hat{v}; w, \vec{s}, \hat{w}) = (\vec{t}, \nabla w)_{\mathcal{T}_h} + \langle \vec{F}_v \cdot \hat{n}, w \rangle_{\partial \mathcal{T}_h} \tag{5.3a}$$

$$+ (\vec{t}, \vec{s})_{\mathcal{T}_h} + (v, \nabla \cdot \vec{s})_{\mathcal{T}_h} - \langle \hat{v}, \vec{s} \cdot \hat{n} \rangle_{\partial \mathcal{T}_h} \tag{5.3b}$$

$$- \langle [\![\vec{F}_v]\!], \hat{w} \rangle_{\mathcal{F}_h} \tag{5.3c}$$

$$\vec{F}_v = -\vec{t} + (\tau \hat{n})(v - \hat{v}). \tag{5.3d}$$

τ is a stabilization parameter that must be greater than 0 for stability[24]. In this thesis two methods of choosing the length scale are analyzed. The first HDG(h) uses the local length scale of the mesh, and the second HDG(L) uses a globally specified length scale L. The adjoint equation can also be written in mixed form

$$\vec{\varphi} - \nabla \psi = 0 \quad \text{in } \Omega \tag{5.4a}$$

$$-\nabla \cdot \vec{\varphi} = g \quad \text{in } \Omega \tag{5.4b}$$

$$\psi = 0 \quad \text{on } \partial\Omega. \tag{5.4c}$$

The spaces $\mathcal{V}_{h,p}$, $\mathcal{Q}_{h,p}$ and $\mathcal{M}_{h,p}$ are discrete counterparts to the infinite dimensional spaces $\mathcal{V}$, $\mathcal{Q}$ and $\mathcal{M}$,

$$\mathcal{V} \equiv L^2(\Omega) \tag{5.5a}$$

$$\mathcal{Q} \equiv [L^2(\Omega)]^d \tag{5.5b}$$

$$\mathcal{M} \equiv \{m \in [L^2(f)]^{d-1}, \quad \forall f \in \mathcal{F}_h\}. \tag{5.5c}$$

The collection of elemental discrete spaces is denoted $\mathcal{W}_{h,p} \equiv (\oplus_\kappa(\mathcal{V}_{h,p}(\kappa) \times \mathcal{Q}_{h,p}(\kappa)) \times \mathcal{M}_{h,p})$

5.2 Localization

Consider the following localization

$$r_\kappa(\mathbf{U},\mathbf{W}) = l_\kappa(w) - a_\kappa(\mathbf{U},\mathbf{W}) \tag{5.6a}$$

$$a_\kappa(\mathbf{U},\mathbf{W}) = (\vec{q}, \nabla w)_\kappa + \langle \vec{F}\cdot\hat{n}, w\rangle_{\partial\kappa} \tag{5.6b}$$

$$+ (\vec{q}, \vec{s})_\kappa + (u, \nabla\cdot\vec{s})_\kappa - \langle \hat{u}, \vec{s}\cdot\hat{n}\rangle_{\partial\kappa} \tag{5.6c}$$

$$-\frac{1}{2}\langle [\![\vec{F}]\!], \hat{w}\rangle_{\partial\kappa}, \tag{5.6d}$$

which closely follows the global form except for apportioning half the jump term to the two elements adjacent to each trace. Using this apportionment, the sum of the local residuals can be readily shown to equal the global residual.

LEMMA 29. HDG Extended Local Consistency

$$r_\kappa(\mathbf{U},\mathbf{W}) = 0,\ \forall \mathbf{W} \in (\mathcal{V}(\kappa) \times \mathcal{Q}(\kappa) \times \mathcal{M}(\partial\kappa))$$
$$r^\psi_\kappa(\mathbf{W},\mathbf{\Psi}) = 0,\ \forall \mathbf{W} \in (\mathcal{V}(\kappa) \times \mathcal{Q}(\kappa) \times \mathcal{M}(\partial\kappa)),$$

where $\mathcal{V}(\kappa)$, $\mathcal{Q}(\kappa)$ and $\mathcal{M}(\partial\kappa))$ are the elemental restrictions of $\mathcal{V}$, $\mathcal{Q}$ and $\mathcal{M}$.

Proof. $\vec{F} \equiv -\vec{q} + (\tau\hat{n})(u-\hat{u})$ occurs only in trace integrals thus $\vec{F} \equiv -\vec{q}$,

$$r_\kappa(u,\vec{q},\hat{u}; w,\vec{s},\hat{w}) = (f, w)_\kappa - (\vec{q}, \nabla w)_\kappa - \langle \vec{F}\cdot\hat{n}, w\rangle_{\partial\kappa} \tag{5.7a}$$

$$- (\vec{q}, \vec{s})_\kappa - (u, \nabla\cdot\vec{s})_\kappa + \langle \hat{u}, \vec{s}\cdot\hat{n}\rangle_{\partial\kappa} \tag{5.7b}$$

$$+\frac{1}{2}\langle [\![\vec{F}]\!], \hat{w}\rangle_{\partial\kappa} \tag{5.7c}$$

$$= (f + \nabla\cdot\vec{q}, w)_\kappa - \langle (\vec{F}+\vec{q})\cdot\hat{n}, w\rangle_{\partial\kappa} \tag{5.7d}$$

$$- (\vec{q} - \nabla u, \vec{s})_\kappa - \langle u - \hat{u}, \vec{s}\cdot\hat{n}\rangle_{\partial\kappa} \tag{5.7e}$$

$$+\frac{1}{2}\langle [\![\vec{F}]\!], \hat{w}\rangle_{\partial\kappa} = 0,\ \forall \mathbf{W} \in (\mathcal{V}(\kappa) \times \mathcal{Q}(\kappa) \times \mathcal{M}(\kappa)). \tag{5.7f}$$

□

The proof for the dual proceeds analagously.

Extended global consistency follows naturally from Lemma 29.

LEMMA 30. HDG Extended Global Consistency

$$R_h(\mathbf{U},\mathbf{W}) = 0,\ \forall \mathbf{W} \in (\oplus_\kappa(\mathcal{V}(\kappa) \times \mathcal{Q}(\kappa))\times \mathcal{M})$$
$$R_h^\psi(\mathbf{W},\mathbf{\Psi}) = 0,\ \forall \mathbf{W} \in (\oplus_\kappa(\mathcal{V}(\kappa) \times \mathcal{Q}(\kappa))\times \mathcal{M}).$$

The proof is a direct consequence of Lemma 29

Proof.

$$R_h(\mathbf{U},\mathbf{W}) = \sum_{\kappa\in\mathcal{T}_h} r_\kappa(\mathbf{U},\mathbf{W}) = 0,\ \forall \mathbf{W} \in (\oplus_\kappa(\mathcal{V}(\kappa) \times \mathcal{Q}(\kappa))\times \mathcal{M}) \tag{5.8a}$$

$$R_h^\psi(\mathbf{W},\mathbf{\Psi}) = \sum_{\kappa\in\mathcal{T}_h} r_\kappa^\psi(\mathbf{W},\mathbf{\Psi}) = 0,\ \forall \mathbf{W} \in (\oplus_\kappa(\mathcal{V}(\kappa) \times \mathcal{Q}(\kappa))\times \mathcal{M}). \tag{5.8b}$$

□

5.3 The Π_h^p Projector

To prove the convergence rates for the output error, the $\Pi_h^p(\vec{q},u) \equiv (\Pi_s^p\vec{q}, \Pi_w^p u)$ projector as introduced by Cockburn *et al.* [18] is used. The projector is defined for use with the primal problem, but it can also be applied to the adjoint.

The projector gives bounds on the local and the global solution errors of the HDG discretization in terms of semi norms on the exact quantities, whilst accounting for τ dependencies.

DEFINITION 31. The Π_h^p Projector

$$\begin{aligned}
(\Pi_s^p\vec{t},\vec{s})_\kappa &= (\vec{t},\vec{s})_\kappa, && \forall \vec{s} \in [\mathbb{P}^{p-1}(\kappa)]^d\\
(\Pi_w^p v, w)_\kappa &= (v,w)_\kappa, && \forall w \in \mathbb{P}^{p-1}(\kappa)\\
\langle \Pi_s^p\vec{t}\cdot\hat{n} + \tau\Pi_w^p v, \hat{w}\rangle_{\partial\kappa} &= \langle \vec{t}\cdot\hat{n} + \tau v, \hat{w}\rangle_{\partial\kappa}, && \forall \hat{w} \in \mathbb{P}^p(\partial\kappa),
\end{aligned}$$

The domain of Π_h^p *is a subset of* $\mathcal{Q}_{h,p} \times \mathcal{V}_{h,p}$.

The Π_h^p projector can be related to the $P_\mathcal{M}^p$ projector, defined as the L^2 projection in p onto $\mathcal{M}(f)$

$$P^p_{\mathcal{M}}(\vec{t}\cdot\hat{n}) = \vec{\Pi}^p_s\vec{t}\cdot\hat{n} + \tau(\Pi^p_w v - P^p_{\mathcal{M}} v). \tag{5.9}$$

DEFINITION 32. Error bounds for the Π^p_h Projector

For $0 \le m \le 1$ *[18, Theorem 3.1, Theorem 4.1],*

Primal

$$\|\Pi^p_w u - u_{h,p}\|_{H^m(\kappa)} \lesssim h^{\min\{p,1\}}\|\Pi^p_s\vec{q} - \vec{q}\|_{H^m(\kappa)} \tag{5.10}$$

$$\|\Pi^p_s\vec{q} - \vec{q}_{h,p}\|_{H^m(\kappa)} \le \|\Pi^p_s\vec{q} - \vec{q}\|_{H^m(\kappa)} \tag{5.11}$$

$$\|P^p_{\mathcal{M}}(\vec{q}\cdot\hat{n}) - \vec{F}_u\cdot\hat{n}\|_{h(\kappa)} \lesssim \|\Pi^p_s\vec{q} - \vec{q}\|_{H^m(\tilde{\kappa})} \tag{5.12}$$

$$\|P^p_{\mathcal{M}} u - \hat{u}_{h,p}\|_{h(\kappa)} \lesssim h\|\Pi^p_s\vec{q} - \vec{q}\|_{H^m(\tilde{\kappa})}. \tag{5.13}$$

The $\|\cdot\|_{h(\kappa)}$ *norm is defined as* $\|\mu\|^2_{h(\kappa)} = h\|\mu\|^2_{L^2(\partial\kappa)} : \mu \in L^2(\partial\kappa)$*, thus*

$$\|\mu\|_{L^2(\partial\kappa)} = h^{-\frac{1}{2}}\|\mu\|_{h(\kappa)}. \tag{5.14}$$

Adjoint

$$\|\Pi^p_w\psi - \psi_{h,p}\|_{H^m(\kappa)} \lesssim h^{\min\{p,1\}}\|\Pi^p_s\vec{\varphi} - \vec{\varphi}\|_{H^m(\kappa)} \tag{5.15}$$

$$\|\Pi^p_s\vec{\varphi} - \vec{\varphi}_{h,p}\|_{H^m(\kappa)} \le \|\Pi^p_s\vec{\varphi} - \vec{\varphi}\|_{H^m(\kappa)} \tag{5.16}$$

$$\|P^p_{\mathcal{M}}(\vec{\varphi}\cdot\hat{n}) - \vec{F}_\psi\cdot\hat{n}\|_{h(\kappa)} \lesssim \|\Pi^p_s\vec{\varphi} - \vec{\varphi}\|_{H^m(\tilde{\kappa})} \tag{5.17}$$

$$\|P^p_{\mathcal{M}}\psi - \hat{\psi}_{h,p}\|_{h(\kappa)} \lesssim h\|\Pi^p_s\vec{\varphi} - \vec{\varphi}\|_{H^m(\tilde{\kappa})}. \tag{5.18}$$

Equations (5.11), (5.12), (5.16), *and* (5.17) *are Theorem 3.1 and Equations* (5.10), (5.13), (5.15), *and* (5.18) *are Theorem 4.1.* $\vec{F}_u$ *and* $\vec{F}_\psi$ *are the numerical flux defined for the primal and adjoint respectively, thus in* $\vec{F}$ *in Equation* (5.3) *is equivalent to* $\vec{F}_u$*.*

Using the trace theorem[15, Theorem 1.6.6] the L^2 projection on a trace can be related to the semi norm over the volume,

$$\|v - P^p_{\mathcal{M}} v\|_{L^2(f)} \lesssim h^{p+\frac{1}{2}}|v|_{H^{p+1}(\kappa_f)}. \tag{5.19}$$

These error bounds can be combined with bounds for the interpolation error of the projector

DEFINITION 33. Π_h^p Projector Error Convergence rates [17, Theorem 2.1]

Primal

$$||\Pi_s^{p1}\vec{q} - \vec{q}||_{H^m(\kappa)} \lesssim h^{p1+1-m}|\vec{q}|_{H^{p1+1}(\kappa)} + h^{p1+1-m}\tau|u|_{H^{p1+1}(\kappa)}$$

$$||\Pi_w^{p1}u - u||_{H^m(\kappa)} \lesssim h^{p1+1-m}|u|_{H^{p1+1}(\kappa)} + \frac{h^{p1+1-m}}{\tau}|\nabla \cdot \vec{q}|_{H^{p1}(\kappa)}.$$

Adjoint

$$||\Pi_s^{p2}\vec{\varphi} - \vec{\varphi}||_{H^m(\kappa)} \lesssim h^{p2+1-m}|\vec{\varphi}|_{H^{p2+1}(\kappa)} + h^{p2+1-m}\tau|\psi|_{H^{p2+1}(\kappa)}$$

$$||\Pi_w^{p2}\psi - \psi||_{H^m(\kappa)} \lesssim h^{p2+1-m}|\psi|_{H^{p2+1}(\kappa)} + \frac{h^{p2+1-m}}{\tau}|\nabla \cdot \vec{\varphi}|_{H^{p2}(\kappa)}.$$

We make the assumption that τ is single valued on a trace and of sufficient smoothness in u and ψ. Given $\vec{q} \equiv \nabla u$ in Equation (5.1), combined with the regularity and smoothness assumptions from Chapter 2, more compact expressions are

Primal

$$||\Pi_s^{p1}\vec{q} - \vec{q}||_{H^m(\kappa)} \lesssim h^{p1+1-m}(|u|_{H^{p1+2}(\kappa)} + \tau|u|_{H^{p1+1}(\kappa)}) \tag{5.20a}$$

$$||\Pi_w^{p1}u - u||_{H^m(\kappa)} \lesssim h^{p1+1-m}(|u|_{H^{p1+1}(\kappa)} + \frac{1}{\tau}|u|_{H^{p1+2}(\kappa)}). \tag{5.20b}$$

Adjoint

$$||\Pi_s^{p2}\vec{\varphi} - \vec{\varphi}||_{H^m(\kappa)} \lesssim h^{p2+1-m}(|\psi|_{H^{p2+2}(\kappa)} + \tau|\psi|_{H^{p2+1}(\kappa)}) \tag{5.21a}$$

$$||\Pi_w^{p2}\psi - \psi||_{H^m(\kappa)} \lesssim h^{p2+1-m}(|\psi|_{H^{p2+1}(\kappa)} + \frac{1}{\tau}|\psi|_{H^{p2+2}(\kappa)}). \tag{5.21b}$$

5.4 Bilinear Error Bounds

From Definition 5, to bound the global bilinear error, it suffices to bound the local

LEMMA 34. HDG Local Bilinear Error Bound

$$a_\kappa(\mathbf{U}-\mathbf{U}_{h,p1},\mathbf{\Psi}-\mathbf{\Psi}_{h,p2}) \lesssim h^{p1+p2+1}\Big(|u|_{H^{p1+2}(\tilde{\kappa})}|\psi|_{H^{p2+1}(\kappa)} + (|u|_{H^{p1+1}(\kappa)}+\frac{1}{\tau}|u|_{H^{p1+2}(\kappa)})(|\psi|_{H^{p2+2}(\kappa)}+\tau|\psi|_{H^{p2+1}(\kappa)}) + (|u|_{H^{p1+2}(\kappa)}+\tau|u|_{H^{p1+1}(\kappa)})(|\psi|_{H^{p2+1}(\kappa)}+\frac{1}{\tau}|\psi|_{H^{p2+2}(\kappa)})\Big),$$

where $(\mathbf{U}_{h,p1},\mathbf{\Psi}_{h,p2})$ *are finite element solutions of order* $p1$ *and* $p2$ *and* τ *is the stabilization parameter, assumed to satisfy* $h\tau \lesssim 1$.

$$a_\kappa(\mathbf{U}-\mathbf{U}_{h,p1},\mathbf{\Psi}-\mathbf{\Psi}_{h,p2}) \lesssim \Big(\frac{1}{\tau}+\tau\Big)h^{p1+p2+1+d}.$$

Proof.

$$\begin{aligned}
&a_\kappa(\mathbf{U}-\mathbf{U}_{h,p1},\mathbf{\Psi}-\mathbf{\Psi}_{h,p2})\\
&= \underbrace{(\vec{q}-\vec{q}_{h,p1},\nabla(\psi-\psi_{h,p2}))_\kappa}_{\mathbf{I}} - \underbrace{\langle(\vec{q}-\vec{F})\cdot\hat{n},\psi-\psi_{h,p2}\rangle_{\partial\kappa}}_{\mathbf{II}}\\
&+ \underbrace{(\vec{q}-\vec{q}_{h,p1},\vec{\varphi}-\vec{\varphi}_{h,p2})_\kappa}_{\mathbf{III}} + \underbrace{(u-u_{h,p1},\nabla\cdot(\vec{\varphi}-\vec{\varphi}_{h,p2}))_\kappa}_{\mathbf{IV}}\\
&- \underbrace{\langle u-\hat{u}_{h,p1},(\vec{\varphi}-\vec{\varphi}_{h,p2})\cdot\hat{n}\rangle_{\partial\kappa}}_{\mathbf{V}} - \frac{1}{2}\underbrace{\langle[\![\vec{q}-\vec{F}]\!],\psi-\hat{\psi}_{h,p2}\rangle_{\partial\kappa\setminus\partial\Omega}}_{\mathbf{VI}}.
\end{aligned}$$

To bound the whole it suffices to bound each of the components individually.

(I):

(5.22a) $\quad (\vec{q}-\vec{q}_{h,p1},\nabla(\psi-\psi_{h,p2}))_\kappa$

(5.22b) $\quad \le \|\vec{q}-\vec{q}_{h,p1}\|_{L^2(\kappa)}\|\psi-\psi_{h,p2}\|_{H^1(\kappa)}$

(5.22c) $\quad \le \Big(\|\Pi_s^{p1}\vec{q}-\vec{q}_{h,p1}\|_{L^2(\kappa)}+\|\Pi_s^{p1}\vec{q}-\vec{q}\|_{L^2(\kappa)}\Big)\Big(\|\Pi_w^{p2}\psi-\psi_{h,p2}\|_{H^1(\kappa)}+\|\Pi_w^{p2}\psi-\psi\|_{H^1(\kappa)}\Big)$

(5.22d) $\quad \lesssim \|\Pi_s^{p1}\vec{q}-\vec{q}\|_{L^2(\kappa)}(h\|\Pi_s^{p2}\vec{\varphi}-\vec{\varphi}\|_{H^1(\kappa)}+\|\Pi_w^{p2}\psi-\psi\|_{H^1(\kappa)})$

(5.22e) $\quad \lesssim h^{p1+p2+1}(|u|_{H^{p1+2}(\kappa)}+\tau|u|_{H^{p1+1}(\kappa)})$
$\qquad (h(|\psi|_{H^{p2+2}(\kappa)}+\tau|\psi|_{H^{p2+1}(\kappa)})+(|\psi|_{H^{p2+1}(\kappa)}+\frac{1}{\tau}|\psi|_{H^{p2+2}(\kappa)}))$

(5.22f) $\quad \lesssim h^{p1+p2+1}(|u|_{H^{p1+2}(\kappa)}+\tau|u|_{H^{p1+1}(\kappa)})(|\psi|_{H^{p2+1}(\kappa)}+\frac{1}{\tau}|\psi|_{H^{p2+2}(\kappa)}).$

(II):

$$
\begin{aligned}
&(5.23a) && \langle(\vec{q}-\vec{F})\cdot\hat{n}, \psi-\psi_{h,p2}\rangle_{\partial\kappa} \\
&(5.23b) && \le \|(\vec{q}-\vec{F})\cdot\hat{n}\|_{L^2(\partial\kappa)}\|\psi-\psi_{h,p2}\|_{L^2(\partial\kappa)} \\
&(5.23c) && \lesssim \Big(\|(\vec{q}-P^{p1}_{\mathcal{M}}\vec{q})\cdot\hat{n}\|_{L^2(\partial\kappa)}+\|(P^{p1}_{\mathcal{M}}\vec{q}-\vec{F})\cdot\hat{n}\|_{L^2(\partial\kappa)}\Big)h^{-\frac{1}{2}}\|\psi-\psi_{h,p2}\|_{L^2(\kappa)} \\
&(5.23d) && \lesssim h^{-\frac{1}{2}}\Big(\|(\vec{q}-P^{p1}_{\mathcal{M}}\vec{q})\cdot\hat{n}\|_{L^2(\partial\kappa)}+h^{-\frac{1}{2}}\|\Pi^{p1}_s\vec{q}-\vec{q}\|_{L^2(\kappa)}\Big) \\
& && \quad\Big(\|\Pi^{p2}_w\psi-\psi\|_{L^2(\kappa)}+h\|\Pi^{p2}_s\vec{\varphi}-\vec{\varphi}\|_{L^2(\kappa)}\Big) \\
&(5.23e) && \lesssim \Big(h^{p1+\frac{1}{2}}(|u|_{H^{p1+2}(\kappa)}+\tau|u|_{H^{p1+1}(\kappa)})\Big) \\
& && \quad(h^{p2+\frac{1}{2}}(|\psi|_{H^{p2+1}(\kappa)}+\frac{1}{\tau}|\psi|_{H^{p2+2}(\kappa)})+h^{p2+\frac{3}{2}}(|\psi|_{H^{p2+2}(\kappa)}+\tau|\psi|_{H^{p2+1}(\kappa)})) \\
&(5.23f) && \lesssim h^{p1+p2+1}(|u|_{H^{p1+2}(\kappa)}+\tau|u|_{H^{p1+1}(\kappa)})(|\psi|_{H^{p2+1}(\kappa)}+\frac{1}{\tau}|\psi|_{H^{p2+2}(\kappa)}).
\end{aligned}
$$

(III):

$$
\begin{aligned}
&(5.24a) && (\vec{q}-\vec{q}_{h,p1},\vec{\varphi}-\vec{\varphi}_{h,p2})_\kappa \\
&(5.24b) && \le \|(\vec{q}-\Pi^{p1}_s\vec{q})+(\Pi^{p1}_s\vec{q}-\vec{q}_{h,p1})\|_{L^2(\kappa)}\|(\vec{\varphi}-\Pi^{p2}_s\vec{\varphi})+(\Pi^{p2}_s\vec{\varphi}-\vec{\varphi}_{h,p2})\|_{L^2(\kappa)} \\
&(5.24c) && \lesssim \|\Pi^{p1}_s\vec{q}-\vec{q}\|_{L^2(\kappa)}\|\Pi^{p2}_s\vec{\varphi}-\vec{\varphi}\|_{L^2(\kappa)} \\
&(5.24d) && \lesssim h^{p1+p2+2}(|u|_{H^{p1+2}(\kappa)}+\tau|u|_{H^{p1+1}(\kappa)})(|\psi|_{H^{p2+2}(\kappa)}+\tau|\psi|_{H^{p2+1}(\kappa)}).
\end{aligned}
$$

(IV):

$$
\begin{aligned}
&(5.25a) && (u-u_{h,p1},\nabla\cdot(\vec{\varphi}-\vec{\varphi}_{h,p2}))_\kappa \\
&(5.25b) && \le \|u-u_{h,p1}\|_{L^2(\kappa)}\|\nabla\cdot(\vec{\varphi}-\vec{\varphi}_{h,p2})\|_{L^2(\kappa)} \\
&(5.25c) && \le \Big(\|u-\Pi^{p1}_w u\|_{L^2(\kappa)}+\|\Pi^{p1}_w u-u_{h,p1}\|_{L^2(\kappa)}\Big)\|\vec{\varphi}-\vec{\varphi}_{h,p2}\|_{H^1(\kappa)} \\
&(5.25d) && \lesssim \Big(\|u-\Pi^{p1}_w u\|_{L^2(\kappa)}+h\|\Pi^{p1}_s\vec{q}-\vec{q}\|_{L^2(\kappa)}\Big)\Big(\|\vec{\varphi}-\Pi^{p2}_s\vec{\varphi}\|_{H^1(\kappa)}+\|\Pi^{p2}_s\vec{\varphi}-\vec{\varphi}_{h,p2}\|_{H^1(\kappa)}\Big) \\
&(5.25e) && \lesssim \Big(\|u-\Pi^{p1}_w u\|_{L^2(\kappa)}+h\|\Pi^{p1}_s\vec{q}-\vec{q}\|_{L^2(\kappa)}\Big)\|\Pi^{p2}_s\vec{\varphi}-\vec{\varphi}\|_{H^1(\kappa)} \\
&(5.25f) && \lesssim \Big(h^{p1+1}(|u|_{H^{p1+1}(\kappa)}+\frac{1}{\tau}|u|_{H^{p1+2}(\kappa)})+h^{p1+2}(|u|_{H^{p1+2}(\kappa)}+\tau|u|_{H^{p1+1}(\kappa)})\Big) \\
& && \quad h^{p2}\Big(|\psi|_{H^{p2+2}(\kappa)}+\tau|\psi|_{H^{p2+1}(\kappa)}\Big) \\
&(5.25g) && \lesssim h^{p1+p2+1}(|u|_{H^{p1+1}(\kappa)}+\frac{1}{\tau}|u|_{H^{p1+2}(\kappa)})(|\psi|_{H^{p2+2}(\kappa)}+\tau|\psi|_{H^{p2+1}(\kappa)}).
\end{aligned}
$$

(V):

$$\langle u - \hat{u}_{h,p1}, (\vec{\varphi} - \vec{\varphi}_{h,p2}) \cdot \hat{n} \rangle_{\partial\kappa} \tag{5.26a}$$

$$\lesssim h^{-\frac{1}{2}} \|(u - P_{\mathcal{M}}^{p1} u) + (P_{\mathcal{M}}^{p1} u - \hat{u}_{h,p})\|_{L^2(\partial\kappa)} \|\Pi_s^{p2} \vec{\varphi} - \vec{\varphi}\|_{L^2(\kappa)} \tag{5.26b}$$

$$\lesssim h^{-\frac{1}{2}} \Big(\|u - P_{\mathcal{M}}^{p1} u\|_{L^2(\partial\kappa)} + h^{-\frac{1}{2}} \|P_{\mathcal{M}}^{p1} u - \hat{u}_{h,p}\|_{h(\kappa)} \Big) \|\Pi_s^{p2} \vec{\varphi} - \vec{\varphi}\|_{L^2(\kappa)} \tag{5.26c}$$

$$\lesssim h^{-\frac{1}{2}} \Big(\|u - P_{\mathcal{M}}^{p1} u\|_{L^2(\partial\kappa)} + h^{\frac{1}{2}} \|\Pi_s^{p1} \vec{q} - \vec{q}\|_{L^2(\kappa)} \Big) \|\Pi_s^{p2} \vec{\varphi} - \vec{\varphi}\|_{L^2(\kappa)} \tag{5.26d}$$

$$\lesssim h^{p1} \Big(|u|_{H^{p1+1}(\kappa)} + h(|u|_{H^{p1+2}(\kappa)} + \tau |u|_{H^{p1+1}(\kappa)}) \Big) h^{p2+1} \Big(|\psi|_{H^{p2+2}(\kappa)} + \tau |\psi|_{H^{p2+1}(\kappa)} \Big) \tag{5.26e}$$

$$\lesssim h^{p1+p2+1} |u|_{H^{p1+1}(\kappa)} \Big(|\psi|_{H^{p2+2}(\kappa)} + \tau |\psi|_{H^{p2+1}(\kappa)} \Big). \tag{5.26f}$$

(VI)

(5.27a)

$$\langle [\![\vec{q} - \vec{F}]\!], \psi - \hat{\psi}_{h,p2} \rangle_{\partial\kappa \setminus \partial\Omega}$$

(5.27b)

$$\leq \|[\![\vec{q} - \vec{F}]\!]\|_{L^2(\partial\kappa)} \|\psi - \hat{\psi}_{h,p2}\|_{L^2(\partial\kappa)}$$

(5.27c)

$$\leq \Big(\|[\![\vec{q} - P_{\mathcal{M}}^{p1} \vec{q}]\!]\|_{L^2(\partial\kappa)} + \|[\![P_{\mathcal{M}}^{p1} \vec{q} - \vec{F}]\!]\|_{L^2(\partial\kappa)} \Big) \Big(\|\psi - P_{\mathcal{M}}^{p2} \psi\|_{L^2(\partial\kappa)} + \|P_{\mathcal{M}}^{p2} \psi - \hat{\psi}_{h,p2}\|_{L^2(\partial\kappa)} \Big)$$

(5.27d)

$$\lesssim \Big(h^{p1+\frac{1}{2}} |u|_{H^{p1+2}(\tilde{\kappa})} + h^{-\frac{1}{2}} \|\Pi_s^{p1} \vec{q} - \vec{q}\|_{L^2(\tilde{\kappa})} \Big) \Big(h^{p2+\frac{1}{2}} |\psi|_{H^{p2+1}(\kappa)} + h^{-\frac{1}{2}} \|P_{\mathcal{M}}^{p2} \psi - \hat{\psi}_{h,p2}\|_{h(\kappa)} \Big)$$

(5.27e)

$$\lesssim \Big(h^{p1+\frac{1}{2}} |u|_{H^{p1+2}(\tilde{\kappa})} + h^{-\frac{1}{2}} \|\Pi_s^{p1} \vec{q} - \vec{q}\|_{L^2(\tilde{\kappa})} \Big) \Big(h^{p2+\frac{1}{2}} |\psi|_{H^{p2+1}(\kappa)} + h^{\frac{1}{2}} \|\Pi_s^{p2} \vec{\varphi} - \vec{\varphi}_{h,p2}\|_{L^2(\kappa)} \Big)$$

$$\lesssim h^{p1+p2+1} \Big(|u|_{H^{p1+2}(\tilde{\kappa})} + \tau |u|_{H^{p1+1}(\tilde{\kappa})} \Big) \Big(|\psi|_{H^{p2+1}(\kappa)} + h(|\psi|_{H^{p2+2}(\kappa)} + \tau |\psi|_{H^{p2+1}(\kappa)}) \Big)$$

(5.27f)

$$\lesssim h^{p1+p2+1} |u|_{H^{p1+2}(\tilde{\kappa})} |\psi|_{H^{p2+1}(\kappa)}.$$

Combining these together,

$$\begin{aligned} a_\kappa(\mathbf{U} - \mathbf{U}_{h,p1}, \mathbf{\Psi} - \mathbf{\Psi}_{h,p2}) \lesssim h^{p1+p2+1} \Big(& |u|_{H^{p1+2}(\tilde{\kappa})} |\psi|_{H^{p2+1}(\kappa)} \\ & + (|u|_{H^{p1+1}(\kappa)} + \frac{1}{\tau} |u|_{H^{p1+2}(\kappa)})(|\psi|_{H^{p2+2}(\kappa)} + \tau |\psi|_{H^{p2+1}(\kappa)}) \\ & + (|u|_{H^{p1+2}(\kappa)} + \tau |u|_{H^{p1+1}(\kappa)})(|\psi|_{H^{p2+1}(\kappa)} + \frac{1}{\tau} |\psi|_{H^{p2+2}(\kappa)}) \Big). \end{aligned}$$

The semi norms on an element converge with order $O(h^{\frac{d}{2}})$ and they always occur in pairs. This gives rise to an additional $O(h^d)$ convergence of the local bilinear form, thus it can be more descriptively written as

□

$$a_\kappa(\mathbf{U} - \mathbf{U}_{h,p1}, \mathbf{\Psi} - \mathbf{\Psi}_{h,p2}) \lesssim \Big(\frac{1}{\tau} + \tau\Big) h^{p1+p2+1+d}.$$

Using Lemma 34 the Global Bilinear Error Bound can be proven.

LEMMA 35. HDG Global Bilinear Error Bound

$$\begin{aligned} &a_h(\mathbf{U} - \mathbf{U}_{h,p1}, \mathbf{\Psi} - \mathbf{\Psi}_{h,p2}) \\ &\qquad \lesssim h^{p1+p2+1}(|u|_{H^{p1+1}(\Omega)} + \frac{1}{\tau}|u|_{H^{p1+2}(\Omega)})(|\psi|_{H^{p2+2}(\Omega)} + \tau|\psi|_{H^{p2+1}(\Omega)}) \\ &\qquad \lesssim h^{p1+p2+1}\Big(\frac{1}{\tau} + \tau\Big), \end{aligned}$$

where $(\mathbf{U}_{h,p1}, \mathbf{\Psi}_{h,p2})$ *are finite element solutions of order* $p1$ *and* $p2$ *and* τ *is the stabilization parameter, assumed to satisfy* $h\tau \lesssim 1$.

Proof.

$$a_h(\mathbf{U} - \mathbf{U}_{h,p1}, \mathbf{\Psi} - \mathbf{\Psi}_{h,p2}) = R_h(\mathbf{U}_{h,p1}, \mathbf{\Psi} - \mathbf{\Psi}_{h,p2}) \tag{5.28a}$$

$$= \sum_{\kappa \in \mathcal{T}_h} r_\kappa(\mathbf{U}_{h,p1}, \mathbf{\Psi} - \mathbf{\Psi}_{h,p2}) \tag{5.28b}$$

$$= \sum_{\kappa \in \mathcal{T}_h} a_\kappa(\mathbf{U} - \mathbf{U}_{h,p1}, \mathbf{\Psi} - \mathbf{\Psi}_{h,p2}) \quad \text{via Lemma 29} \tag{5.28c}$$

$$\lesssim h^{p1+p2+1}(|u|_{H^{p1+1}(\Omega)} + \frac{1}{\tau}|u|_{H^{p1+2}(\Omega)})(|\psi|_{H^{p2+2}(\Omega)} + \tau|\psi|_{H^{p2+1}(\Omega)}) \tag{5.28d}$$

$$\lesssim h^{p1+p2+1}\Big(\frac{1}{\tau} + \tau\Big). \tag{5.28e}$$

□

5.5 Global Error Bound

In this section Lemma 35 is used to derive asymptotic convergence rates for $\mathcal{E}$ and $\mathcal{E} - \tilde{\mathcal{E}}$ for the HDG discretization.

THEOREM 36. HDG Global Error Bound

$$\begin{aligned}|\mathcal{E}| &\lesssim h^{2p+1}(|u|_{H^{p+1}(\Omega)} + \frac{1}{\tau}|u|_{H^{p+2}(\Omega)})(|\psi|_{H^{p+2}(\Omega)} + \tau|\psi|_{H^{p+1}(\Omega)}) \\ &\lesssim h^{2p+1}\Big(\frac{1}{\tau} + \tau\Big),\end{aligned}$$

where τ is the stabilization parameter, assumed to satisfy $h\tau \lesssim 1$.

Proof.

$$\begin{aligned}
&(5.29a) && |\mathcal{E}| = |R_h(\mathbf{U}_{h,p}, \mathbf{\Psi} - \mathbf{W}_{h,p})|,\ \forall \mathbf{W}_{h,p} \in \mathcal{W}_{h,p} \\
&(5.29b) && \quad = |R_h(\mathbf{U}_{h,p}, \mathbf{\Psi} - \mathbf{\Psi}_{h,p})| \\
&(5.29c) && \quad = |a_h(\mathbf{U} - \mathbf{U}_{h,p}, \mathbf{\Psi} - \mathbf{\Psi}_{h,p})| \quad \text{via Lemma 4} \\
&(5.29d) && \quad \lesssim h^{2p+1}(|u|_{H^{p+1}(\Omega)} + \frac{1}{\tau}|u|_{H^{p+2}(\Omega)})(|\psi|_{H^{p+2}(\Omega)} + \tau|\psi|_{H^{p+1}(\Omega)}) \\
&(5.29e) && \quad \lesssim h^{2p+1}\Big(\frac{1}{\tau} + \tau\Big) \quad \text{via Lemma 35.}
\end{aligned}$$

□

THEOREM 37. HDG Global Error Estimate Error Bound

$$\begin{aligned}|\mathcal{E} - \tilde{\mathcal{E}}| &\lesssim h^{2p'+1}(|u|_{H^{p'+1}(\Omega)} + \frac{1}{\tau}|u|_{H^{p'+2}(\Omega)})(|\psi|_{H^{p'+2}(\Omega)} + \tau|\psi|_{H^{p'+1}(\Omega)}) \\ &\lesssim h^{2p'+1}\Big(\frac{1}{\tau} + \tau\Big),\end{aligned}$$

where τ is the stabilization parameter, assumed to satisfy $h\tau \lesssim 1$.

Proof.

$$\begin{aligned}
&(5.30a) && |\mathcal{E} - \tilde{\mathcal{E}}| = |R_h(\mathbf{U}_{h,p}, \mathbf{\Psi} - \mathbf{W}_{h,p}) - R(\mathbf{U}_{h,p}, \mathbf{\Psi}_{h,p'} - \mathbf{W}_{h,p})|,\ \forall \mathbf{W}_{h,p} \in \mathcal{W}_{h,p} \\
&(5.30b) && \quad = |R_h(\mathbf{U}_{h,p}, \mathbf{\Psi} - \mathbf{\Psi}_{h,p'})| \\
&(5.30c) && \quad = |R_h^{\psi}(\mathbf{U} - \mathbf{U}_{h,p}, \mathbf{\Psi}_{h,p'})| \quad \text{via Lemma 4} \\
&(5.30d) && \quad = |R_h^{\psi}(\mathbf{U} - \mathbf{W}_{h,p'}, \mathbf{\Psi}_{h,p'})|,\ \forall \mathbf{W}_{h,p'} \in \mathcal{W}_{h,p'} \quad \text{via orthogonality} \\
&(5.30e) && \quad = |a_h(\mathbf{U} - \mathbf{W}_{h,p'}, \mathbf{\Psi} - \mathbf{\Psi}_{h,p'})|,\ \forall \mathbf{W}_{h,p'} \in \mathcal{W}_{h,p'} \quad \text{via Lemma 4} \\
&(5.30f) && \quad \lesssim h^{2p'+1}(|u|_{H^{p'+1}(\Omega)} + \frac{1}{\tau}|u|_{H^{p'+2}(\Omega)})(|\psi|_{H^{p'+2}(\Omega)} + \tau|\psi|_{H^{p'+1}(\Omega)}) \\
&(5.30g) && \quad \lesssim h^{2p'+1}\Big(\frac{1}{\tau} + \tau\Big) \quad \text{via Lemma 35.}
\end{aligned}$$

□

COROLLARY 38. HDG Global Error Estimate Effectivity Bound

$$\frac{|\mathcal{E} - \tilde{\mathcal{E}}|}{|\mathcal{E}|} \lesssim h^{2p_{inc}}.$$

Proof.

$$\frac{|\mathcal{E}-\tilde{\mathcal{E}}|}{|\mathcal{E}|} \lesssim \frac{h^{2p'}\left(\frac{1}{\tau}+\tau\right)}{h^{2p}\left(\frac{1}{\tau}+\tau\right)} \lesssim h^{2p_{inc}}. \tag{5.31}$$

□

5.6 Local Error Bound

In this section Lemma 34 is used to derive asymptotic convergence rates for η_κ and $\eta_\kappa - \tilde{\eta}_\kappa$ for the HDG discretization. In common with the global results, all that is necessary to bound the relevant formulae are Lemmas 7 and 21. Unlike CG (see Theorem 15), the HDG localized residual is the same as the global residual, aside from the local restriction of test functions and the factor of $\frac{1}{2}$ on the jump condition, as such $r_\kappa(\mathbf{U}_{h,p}, \mathbf{W}_{h,p}) = 0$, $\forall \mathbf{W}_{h,p} \in \mathcal{W}_{h,p}(\kappa)$, where $\mathcal{W}_{h,p}(\kappa)$ is the elemental restriction of $\mathcal{W}_{h,p}$.

Theorems 39 and 40 contains semi-norms on the element κ, these semi norms also converge to 0 with order $O(h^{\frac{d}{2}})$, thus when combined in a pair they give an additional $O(h^d)$ rate of convergence to the local estimate.

THEOREM 39. HDG Local Error Bound

$$\begin{aligned}
|\eta_\kappa| \lesssim h^{2p+1}\Big(&|u|_{H^{p+2}(\tilde{\kappa})}|\psi|_{H^{p+1}(\kappa)} \\
&+ (|u|_{H^{p+1}(\kappa)} + \frac{1}{\tau}|u|_{H^{p+2}(\kappa)})(|\psi|_{H^{p+2}(\kappa)} + \tau|\psi|_{H^{p+1}(\kappa)}) \\
&+ (|u|_{H^{p+2}(\kappa)} + \tau|u|_{H^{p+1}(\kappa)})(|\psi|_{H^{p+1}(\kappa)} + \frac{1}{\tau}|\psi|_{H^{p+2}(\kappa)})\Big) \\
\lesssim \Big(\frac{1}{\tau}+\tau\Big)&h^{2p+1+d},
\end{aligned}$$

where τ is the stabilization parameter, assumed to satisfy $h\tau \lesssim 1$.

Proof.

$$\begin{aligned}
&\text{(5.32a)} && |\eta_\kappa| = |r_\kappa(\mathbf{U}_{h,p}, \mathbf{\Psi} - \mathbf{W}_{h,p})|, \ \forall \mathbf{W}_{h,p} \in \mathcal{W}_{h,p}(\kappa) \\
&\text{(5.32b)} && \quad = |r_\kappa(\mathbf{U}_{h,p}, \mathbf{\Psi} - \mathbf{\Psi}_{h,p})| \\
&\text{(5.32c)} && \quad = |a_\kappa(\mathbf{U} - \mathbf{U}_{h,p}, \mathbf{\Psi} - \mathbf{\Psi}_{h,p})| \quad \text{via Lemma 7} \\
&\text{(5.32d)} && \quad \lesssim h^{2p+1}\Big(|u|_{H^{p+2}(\tilde{\kappa})}|\psi|_{H^{p+1}(\kappa)} \\
& && \qquad + (|u|_{H^{p+1}(\kappa)} + \frac{1}{\tau}|u|_{H^{p+2}(\kappa)})(|\psi|_{H^{p+2}(\kappa)} + \tau|\psi|_{H^{p+1}(\kappa)}) \\
& && \qquad + (|u|_{H^{p+2}(\kappa)} + \tau|u|_{H^{p+1}(\kappa)})(|\psi|_{H^{p+1}(\kappa)} + \frac{1}{\tau}|\psi|_{H^{p+2}(\kappa)})\Big) \\
&\text{(5.32e)} && \quad \lesssim \Big(\frac{1}{\tau} + \tau\Big)h^{2p+1+d} \quad \text{via Lemma 34.}
\end{aligned}$$

□

THEOREM 40. HDG Local Estimate Error Bound

$$\begin{aligned}
|\eta_\kappa - \tilde{\eta}_\kappa| &\lesssim h^{p+p'+1}\Big(|u|_{H^{p+2}(\tilde{\kappa})}|\psi|_{H^{p'+1}(\kappa)} \\
&\quad + (|u|_{H^{p+1}(\kappa)} + \frac{1}{\tau}|u|_{H^{p+2}(\kappa)})(|\psi|_{H^{p'+2}(\kappa)} + \tau|\psi|_{H^{p'+1}(\kappa)}) \\
&\quad + (|u|_{H^{p+2}(\kappa)} + \tau|u|_{H^{p+1}(\kappa)})(|\psi|_{H^{p'+1}(\kappa)} + \frac{1}{\tau}|\psi|_{H^{p'+2}(\kappa)})\Big) \\
&\lesssim \Big(\frac{1}{\tau} + \tau\Big)h^{p+p'+1+d},
\end{aligned}$$

where τ is the stabilization parameter, assumed to satisfy $h\tau \lesssim 1$.

Proof.

$$\begin{aligned}
&\text{(5.33a)} && |\eta_\kappa - \tilde{\eta}_\kappa| = |r_\kappa(\mathbf{U}_{h,p}, \mathbf{\Psi} - \mathbf{W}_{h,p}) - r_\kappa(\mathbf{U}_{h,p}, \mathbf{\Psi}_{h,p'} - \mathbf{W}_{h,p})|, \ \forall \mathbf{W}_{h,p} \in \mathcal{W}_{h,p}(\kappa) \\
&\text{(5.33b)} && \quad = |r_\kappa(\mathbf{U}_{h,p}, \mathbf{\Psi} - \mathbf{\Psi}_{h,p'})| \\
&\text{(5.33c)} && \quad = |a_\kappa(\mathbf{U} - \mathbf{U}_{h,p}, \mathbf{\Psi} - \mathbf{\Psi}_{h,p'})| \quad \text{via Lemma 7} \\
&\text{(5.33d)} && \quad \lesssim h^{p+p'+1}\Big(|u|_{H^{p+2}(\tilde{\kappa})}|\psi|_{H^{p'+1}(\kappa)} \\
& && \qquad + (|u|_{H^{p+1}(\kappa)} + \frac{1}{\tau}|u|_{H^{p+2}(\kappa)})(|\psi|_{H^{p'+2}(\kappa)} + \tau|\psi|_{H^{p'+1}(\kappa)}) \\
& && \qquad + (|u|_{H^{p+2}(\kappa)} + \tau|u|_{H^{p+1}(\kappa)})(|\psi|_{H^{p'+1}(\kappa)} + \frac{1}{\tau}|\psi|_{H^{p'+2}(\kappa)})\Big) \\
&\text{(5.33e)} && \quad \lesssim \Big(\frac{1}{\tau} + \tau\Big)h^{p+p'+1+d} \quad \text{via Lemma 34.}
\end{aligned}$$

□

COROLLARY 41. HDG Local Error Estimate Effectivity Bound

$$\frac{|\eta_\kappa - \tilde{\eta}_\kappa|}{|\eta_\kappa|} \lesssim h^{p_{inc}}.$$

Proof.

$$\frac{|\eta_\kappa - \tilde{\eta}_\kappa|}{|\eta_\kappa|} \lesssim \frac{h^{p+p'}\left(\frac{1}{\tau}+\tau\right)}{h^{2p}\left(\frac{1}{\tau}+\tau\right)} \lesssim h^{p_{inc}}. \tag{5.34}$$

□

CHAPTER 6

NUMERICAL RESULTS

To demonstrate the theoretical convergenc rates, exact primal and dual solutions with sufficient smoothness are required. To do this, the forcing functions f and g are chosen to give solutions $u,\ \psi \in C^\infty(\Omega)$. Averages of absolute values of the local quantities are used to measure the convergence of the local error estimates.

$$\mathcal{E}_{\text{avg}} = \frac{\sum_{\kappa\in\mathcal{T}_h} |\eta_\kappa|}{N}, \quad \Delta\tilde{\mathcal{E}}_{\text{avg}} = \frac{\sum_{\kappa\in\mathcal{T}_h} |\eta_\kappa - \tilde{\eta}_\kappa|}{N}, \quad \Theta_{\text{avg}} = \frac{\Delta\tilde{\mathcal{E}}_{\text{avg}}}{\mathcal{E}_{\text{avg}}}. \tag{6.1}$$

These are in contrast to their global equivalents

$$\mathcal{E}_{\text{glob}} = |\mathcal{E}|, \quad \Delta\tilde{\mathcal{E}}_{\text{glob}} = |\mathcal{E} - \tilde{\mathcal{E}}|, \quad \Theta_{\text{glob}} = \frac{\Delta\tilde{\mathcal{E}}_{\text{glob}}}{\mathcal{E}_{\text{glob}}} \tag{6.2}$$

Θ_{avg} and Θ_{glob} are the relative error of the estimate with respect to the true error, the rate of convergence ought to be independent of the polynomial order of approximation, being only a function of the increase in polynomial order over the primal for the adjoint approximation. Table 6-1 shows a summary of the expected rates of convergence for all of the error estimates and schemes analyzed in Chapters 3 to 5, and is thus the reference against which the numerical results will be compared. The additional $O(h^d)$ convergence for the local quantities is from the $O(h^{\frac{d}{2}})$ scaling of the semi norms involved in the estimates, which always occur in pairs.

Table 6-1: A priori *convergence rates for global and local error and estimate error*

	$\mathcal{E}_{\text{glob}}$	$\Delta\tilde{\mathcal{E}}_{\text{glob}}$	$\mathcal{E}_{\text{avg}}$	$\Delta\tilde{\mathcal{E}}_{\text{avg}}$
CG	h^{2p}	$h^{2p'}$	h^{2p+d}	$h^{p+p'+d}$
DG	h^{2p}	$h^{2p'}$	h^{2p+d}	$h^{p+p'+d}$
HDG(h)	h^{2p}	$h^{2p'}$	h^{2p+d}	$h^{p+p'+d}$
HDG(L)	h^{2p+1}	$h^{2p'+1}$	h^{2p+1+d}	$h^{p+p'+1+d}$

Table 6-2: A priori *convergence rates for global and local error and estimate error in 1D*

	$\mathcal{E}_{\text{glob}}$	$\Delta\tilde{\mathcal{E}}_{\text{glob}}$	$\mathcal{E}_{\text{avg}}$	$\Delta\tilde{\mathcal{E}}_{\text{avg}}$
CG	h^{2p}	$h^{2p'}$	h^{2p+d}	$h^{2p'+d}$
DG	h^{2p}	$h^{2p'}$	h^{2p+d}	$h^{2p'+d}$
HDG(h)	h^{2p}	$h^{2p'}$	h^{2p+d}	$h^{2p'+d}$
HDG(L)	h^{2p+1}	$h^{2p'+1}$	h^{2p+1+d}	$h^{2p'+1+d}$

6.1 1D Results

This section numerically verifies the results of the *a priori* analysis presented in Chapters 3 to 5 for the Poisson problem. The particular test case chosen for 1D is

$$u = (1-x)(e^{5x}-1), \quad \text{in } (0,1) \tag{6.3a}$$

$$\psi = \sin(\pi x), \quad \text{in } (0,1) \tag{6.3b}$$

which corresponds to an output functional of

$$\mathcal{J}(u) = (\pi^2 \sin(\pi x), u)_\Omega \tag{6.4}$$

this test case was chosen for being relatively pathological as a result of the adjoint being a simple sine wave. $\int_0^1 \sin(n\pi x)\sin(m\pi x) = \delta_{n,m}$ ensures only odd components of the Fourier modes of primal will return non zeroes. The expected rates of convergence for the estimates as a result of the *a priori* analysis are given in Table 6-2 and the analytical solutions and data are shown in Fig. 6-1.

In this section the convergence rates of CG, DG, HDG(h) and HDG(L) are compared. The h and L specify the length scale used in the stabilization constant τ, both satisfy the assumption $h\tau \lesssim 1$, thus the analysis of Chapter 5 holds.

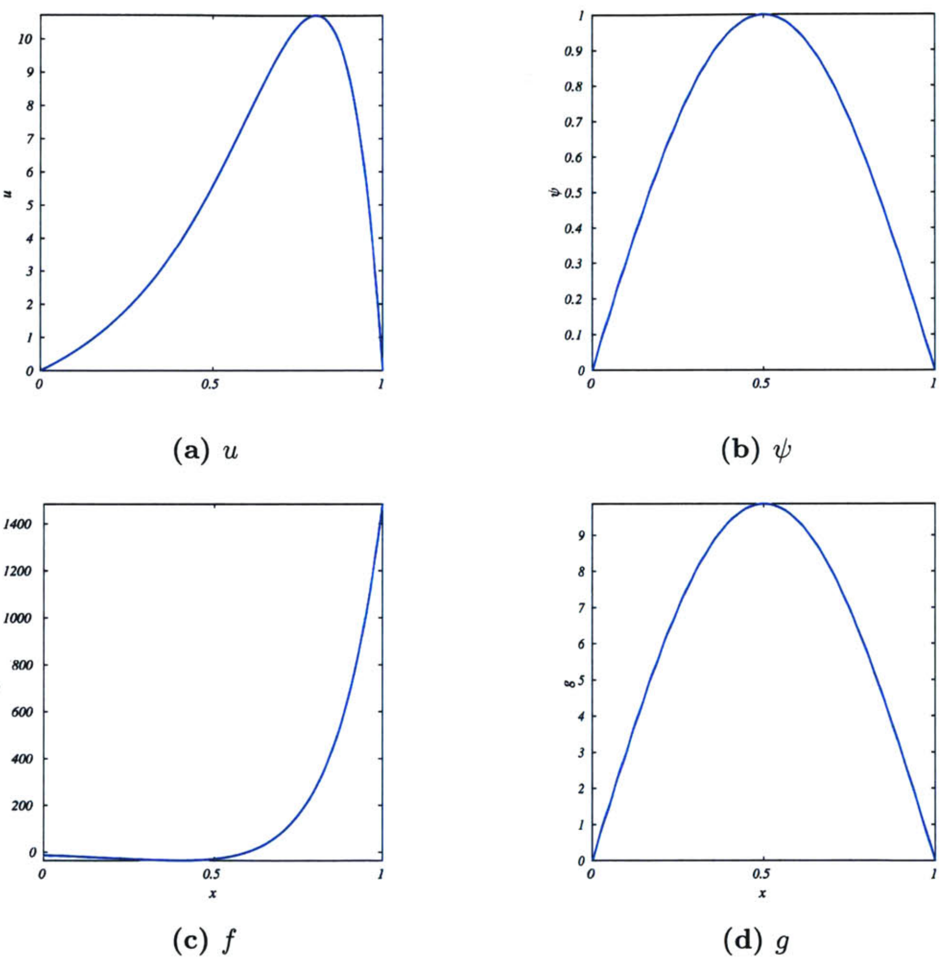

(a) u (b) ψ

(c) f (d) g

Figure 6-1: *1D Solutions and Data*

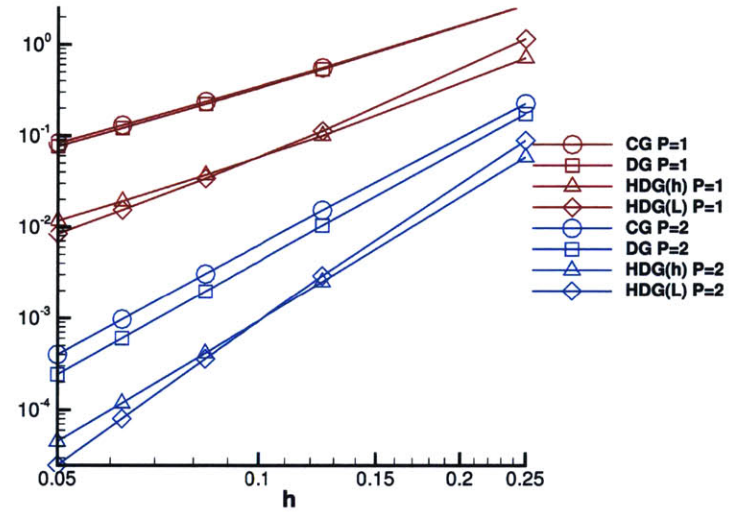

(a) $\mathcal{E}_{glob}$

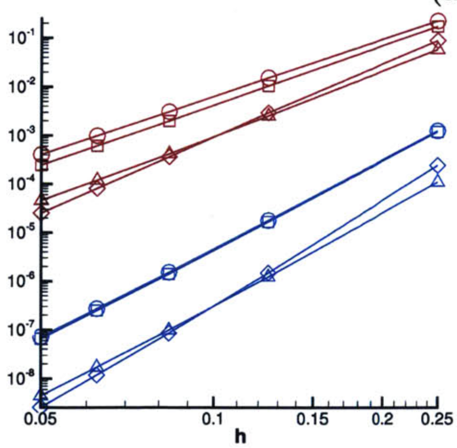

(b) $\Delta\tilde{\mathcal{E}}_{glob} : p_{inc} = 1$

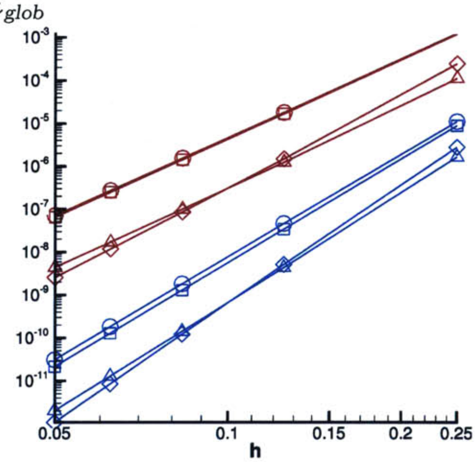

(c) $\Delta\tilde{\mathcal{E}}_{glob} : p_{inc} = 2$

Figure 6-2: *Global error ($\mathcal{E}_{\text{glob}}$) and estimate error ($\Delta\tilde{\mathcal{E}}_{\text{glob}}$) : $u = (1-x)(e^{5x}-1)$, $\psi = \sin(\pi x)$*

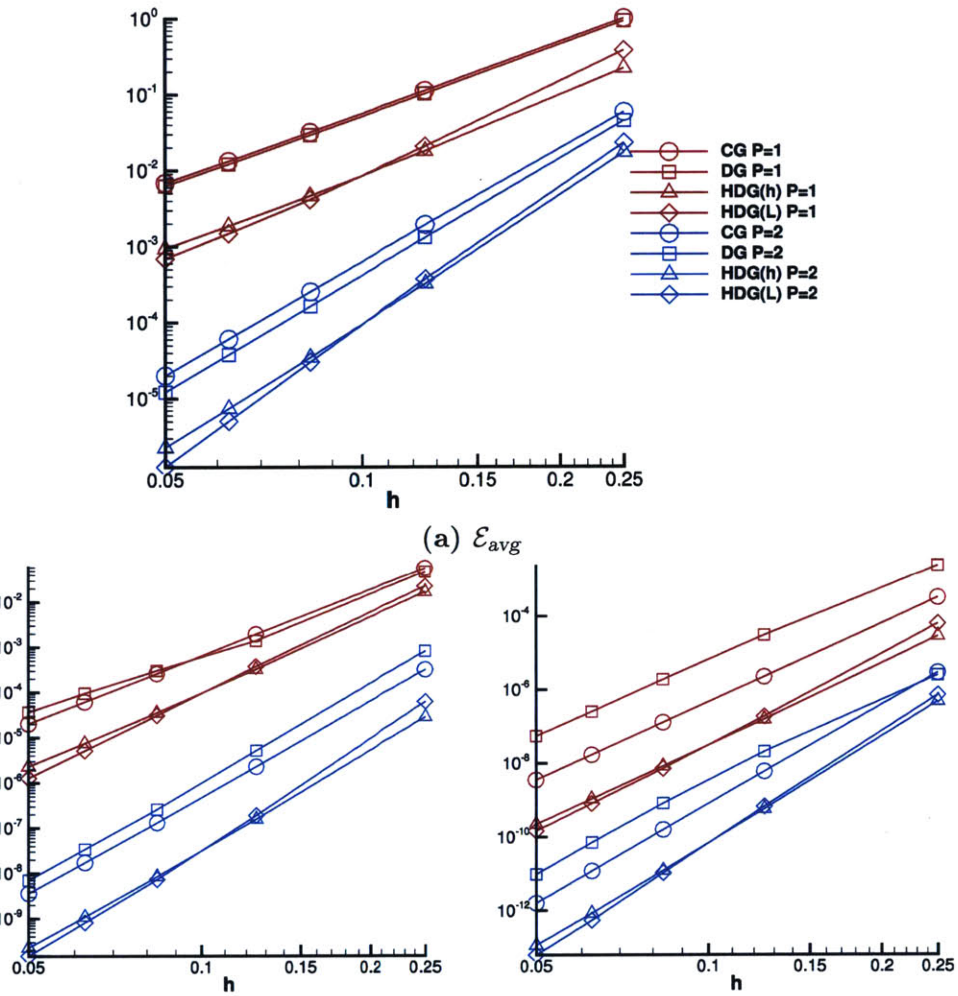

(a) $\mathcal{E}_{\text{avg}}$

(b) $\Delta\tilde{\mathcal{E}}_{\text{avg}}$: $p_{inc} = 1$

(c) $\Delta\tilde{\mathcal{E}}_{\text{avg}}$: $p_{inc} = 2$

Figure 6-3: *Local error ($\mathcal{E}_{\text{avg}}$) and estimate error ($\Delta\tilde{\mathcal{E}}_{\text{avg}}$) : $u = (1-x)(e^{5x}-1)$, $\psi = \sin(\pi x)$*

Figures 6-2a to 6-2c show the global error, error in the error estimate with $p_{\text{inc}} = 1$ and error in the error estimate with $p_{\text{inc}} = 2$ for CG, DG, HDG(h) and HDG(L). The global length scale was taken to be $\frac{1}{10}$ for HDG(L), this corresponds to half of the distance between the right boundary and the peak value. All of the estimates considered are converging exactly as expected. Discerning the difference for the two HDG estimates is difficult using the figures alone, thus the data for generating the plots is presented in Appendix A.1.

All of the discretizations and their estimates are converging exactly in line with Table 6-2. HDG also achieves an order of magnitude less error, both in the computed output functional, $\mathcal{E}_{\text{glob}}$, and in the estimate $\Delta\tilde{\mathcal{E}}_{\text{glob}}$ for the same grid, the exact cause of this is unclear. All of the data used for generating these plots are presented in Tables A-1 to A-4 and A-9 to A-12.

Figures 6-3a to 6-3c show the local error, error in the error estimate with $p_{\text{inc}} = 1$ and error in the error estimate with $p_{\text{inc}} = 2$. The local average estimates and their errors are converging at the expected rates from Table 6-2.

HDG gives an order of magnitude less error than CG for all values of p and p_{inc}, with HDG(h) and HDG(L) having approximately the same error despite HDG(L) converging $O(h)$ faster, this is as a result of the choice of the global length scale. The choice of global length scale is relatively simple for linear one dimensional case such as this, but for multi-dimensional cases or those with anisotropic features (for example a boundary layer), it is difficult to know *a priori* what length scale to choose. Choosing a length scale too small ensures the asymptotic convergence rate, but at the cost of the initial error being larger, and vice versa. Figures 6-3b and 6-3c show that choosing the reference length scale of the order of the grid spacing is a viable alternative that would require no *a priori* knowledge of the important underlying flow features.

The DG estimate performs the worst of all of the schemes considered, for $p_{\text{inc}} = 1$ it is approximately the same as CG, but for $p_{\text{inc}} = 2$ it is an order of magnitude worse for the same mesh. This suggests that DG estimates have more of a cancelation effect than the other two discretizations given it performs well for the global but is significantly affected by the introduction of the absolute value into the summation of $\Delta\tilde{\mathcal{E}}_{\text{avg}}$.

In summary, all of the schemes converge exactly as predicted by the *a priori* analysis, with the DG and HDG discretizations also inheriting the 'super convergent' properties of the CG local estimate shown in Chapter 3. All of the data used for generating these plots are presented in Tables A-5 to A-8 and A-13 to A-16.

6.1.1 Statically Condensed Estimation

The p dependent estimates introduced by Yano [29] were shown to be incomplete approximations of the true estimate in Chapter 4, in that they fail to completely account for the error in the approximation of $\vec{r}^{F}_{h,p}$. In order to make comparisons of the estimates, the weighted residual can be separated into scalar and auxilliary components

$$R_h(\mathbf{U}_{h,p}, \mathbf{\Psi}_{h,p'}) = R^u_h(\mathbf{U}_{h,p}, \psi_{h,p'}) + R^{\vec{r}^F}_h(\mathbf{U}_{h,p}, \vec{\sigma}^f_{h,p'}). \tag{6.5}$$

Failing to include the lifting operator error in an estimate results in $\tilde{\mathcal{E}}^u = R^u_h(\mathbf{U}_{h,p}, \psi_{h,p'})$ with it's

Table 6-3: A priori *convergence rates for DG global and local error and estimate error in 1D*

	$\tilde{\mathcal{E}}$, $\tilde{\eta}_\kappa$	$\tilde{\mathcal{E}}^u$, $\tilde{\eta}^u_\kappa$	$\tilde{\mathcal{E}}^1$, $\tilde{\eta}^1_\kappa$	$\tilde{\mathcal{E}}^2$, $\tilde{\eta}^2_\kappa$
$\Delta\tilde{\mathcal{E}}_{\text{glob}}$	$h^{2p'}$	$h^{p+p'}$	$h^{p+p'}$	$h^{2p'}$
$\Delta\tilde{\mathcal{E}}_{\text{avg}}$	$h^{2p'+d}$	$h^{p+p'+d}$	$h^{p+p'+d}$	h^{p+d}

corresponding localized equivalent $\tilde{\eta}^u_\kappa$, it is thus possible to assess the statically condensed estimates with respect to $\tilde{\mathcal{E}}^u$ and $\tilde{\mathcal{E}}$.

The 1D analysis from Chapter 3 ought to apply for any truly adjoint consistent estimate, as a result the true local estimate ought to recover the optimal asymptotic global convergence for all p and p_{inc}. Figures 6-4a to 6-4c show the effect of the static condensantion evaluation on the global error estimates.

Global Estimation

Fig. 6-4a shows the computed values for $\mathcal{E}_{\text{glob}}$ which is independent of the estimation method. Fig. 6-4b shows the results for $p_{\text{inc}} = 1$ and Fig. 6-4c shows the results for $p_{\text{inc}} = 2$.

As can be seen from the plots, $\Delta\tilde{\mathcal{E}}_{\text{glob}} \equiv \Delta\tilde{\mathcal{E}}^2_{\text{glob}}$ and $\Delta\tilde{\mathcal{E}}^u_{\text{glob}} \equiv \Delta\tilde{\mathcal{E}}^1_{\text{glob}}$, with the lines perfectly aligning for all p and p_{inc}. This is expected as a result of the analysis in Chapter 4, wherein it was shown that both $\tilde{\mathcal{E}}^1$ and $\tilde{\mathcal{E}}^2$ fail to weight the lifting operator residual with the corresponding adjoint auxilliary variable $\vec{\sigma}^f_{h,p'}$. However by recalculating $\vec{r}^F_{h,p'}$ as a function of $[\![u_{h,p}]\!]$, the primal auxilliary lifting operator residual is made orthogonal to the space $\mathcal{S}^F_{h,p'}$ for $\tilde{\mathcal{E}}^2$. This means that $\Delta\tilde{\mathcal{E}}^2_{\text{glob}} = R^u(\mathbf{U}_{h,p}, \psi_{h,p'}) + R^{\vec{r}^F}_h(\mathbf{U}_{h,p}, \vec{\phi}^F_{h,p'})\ \forall\phi^F_{h,p'} \in \mathcal{S}^F_{h,p'} \equiv R_f(\mathbf{U}_{h,p}, \mathbf{\Psi}_{h,p'})$ which is $\Delta\tilde{\mathcal{E}}_{\text{glob}}$.

$\Delta\tilde{\mathcal{E}}^u_{\text{glob}} \equiv \Delta\tilde{\mathcal{E}}^1_{\text{glob}}$ gives a marginally worse approximation than $\Delta\tilde{\mathcal{E}}_{\text{glob}}$ for $p_{\text{inc}} = 1$ which grows worse with grid refinement. This is because $R^{\vec{r}^F}_h(\mathbf{U}_{h,p}, \vec{\sigma}^f_{h,p'})$ ought to grow as a proportion of the error as the grid is refined and the solution primarily occupies the even modes. This also explains why for $p = 2$ and $p_{\text{inc}} = 1$ it performs better than the other estimate given $\lim_{h\to 0} \Delta\tilde{\mathcal{E}}^{\vec{r}^F}_{\text{glob}} = 0$, thus $\Delta\tilde{\mathcal{E}}^u_{\text{glob}}$ ought to make up the majority of the error for any sufficiently fine grid. For $p_{\text{inc}} = 2$, it is an extremely poor approximation with 4 orders of magnitude more error than $\Delta\tilde{\mathcal{E}}_{\text{glob}}$. The predicted sub optimal rate of $O(h^{p+p'})$ is observed for $p_{\text{inc}} = 2$, verifying the *a priori* analysis.

In summary, all of the observed rates are in accordance with Table 6-3, as seen in Tables A-25 to A-28. $\Delta\tilde{\mathcal{E}}_{\text{glob}} \equiv \Delta\tilde{\mathcal{E}}^2_{\text{glob}}$ achieve $O(h^{2p'})$, the optimal convergence rate, whilst $\Delta\tilde{\mathcal{E}}^u_{\text{glob}} \equiv \Delta\tilde{\mathcal{E}}^1_{\text{glob}}$ achieve the sub optimal $O(h^{p+p'})$, as expected.

Local Estimation

Fig. 6-5a shows the computed values for $\mathcal{E}_{\text{avg}}$ which is independent of the estimation method.

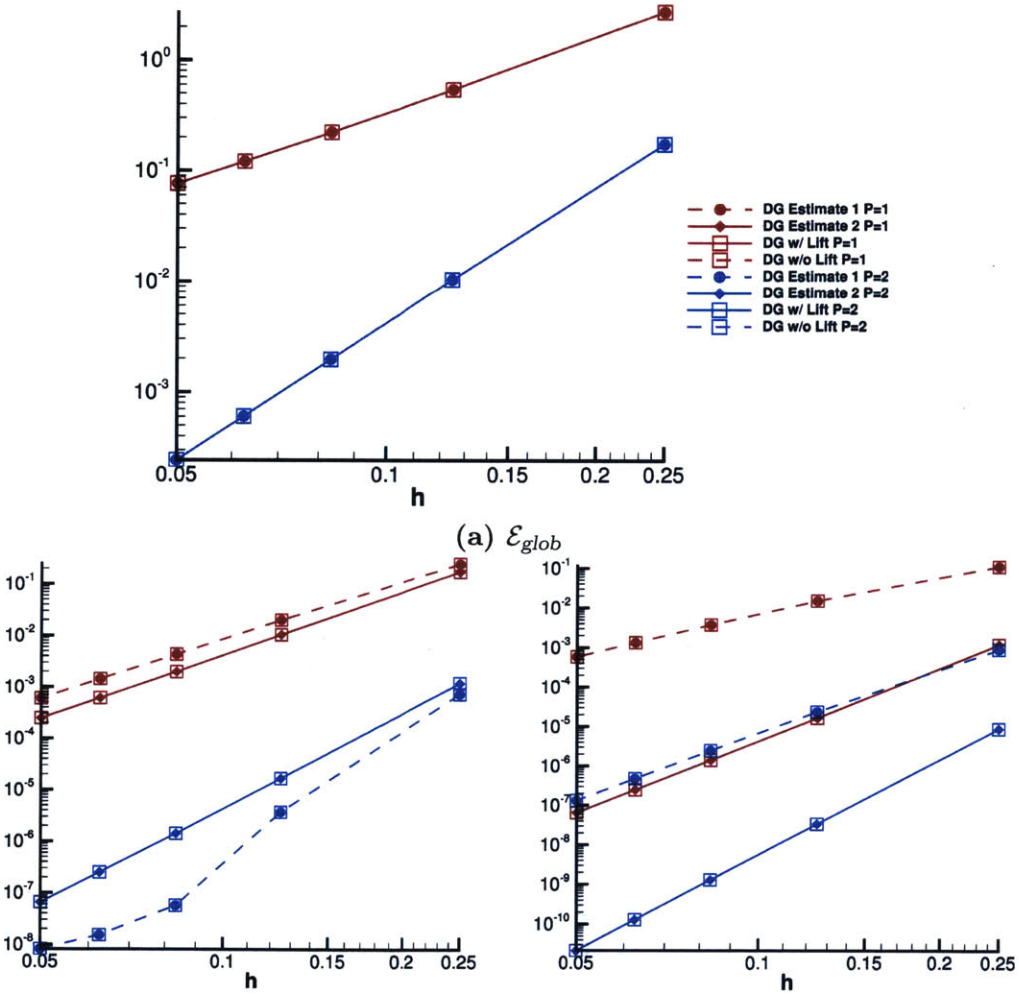

(a) $\mathcal{E}_{glob}$

(b) $\Delta\tilde{\mathcal{E}}_{glob} : p_{inc} = 1$

(c) $\Delta\tilde{\mathcal{E}}_{glob} : p_{inc} = 2$

Figure 6-4: *Global error* ($\mathcal{E}_{\text{glob}}$) *and estimate error* ($\Delta\tilde{\mathcal{E}}_{\text{glob}}$) : $u = (1-x)(e^{5x}-1)$, $\psi = \sin(\pi x)$

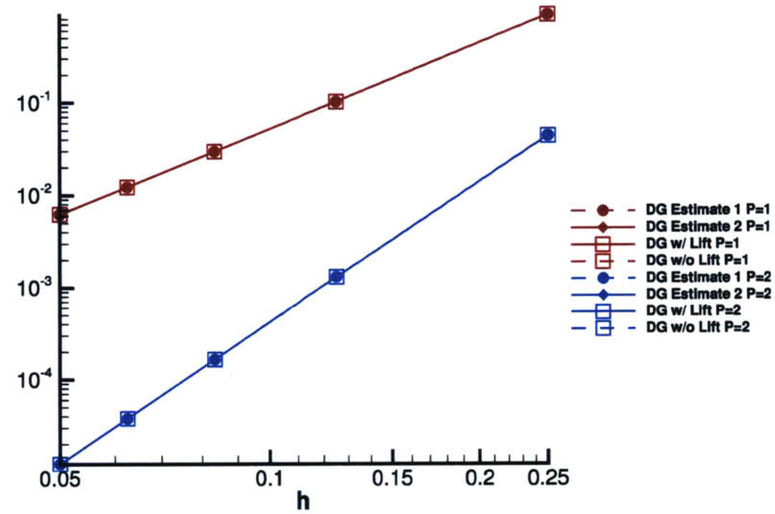

(a) $\mathcal{E}_{\text{avg}}$

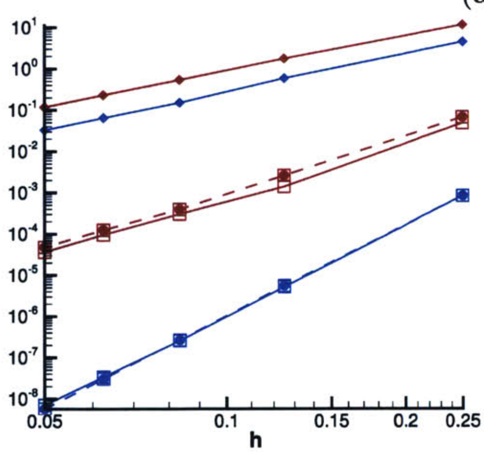

(b) $\Delta\tilde{\mathcal{E}}_{\text{avg}} : p_{inc} = 1$

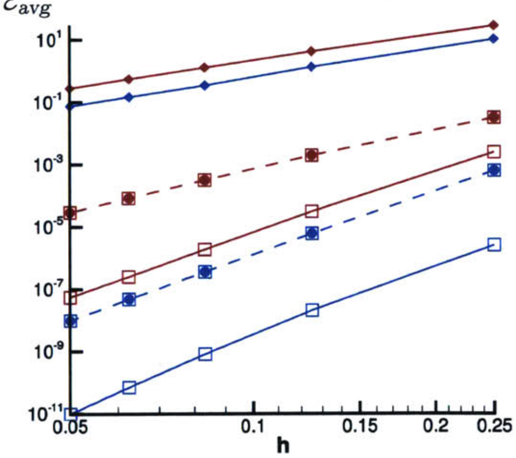

(c) $\Delta\tilde{\mathcal{E}}_{\text{avg}} : p_{inc} = 2$

Figure 6-5: *Local error ($\mathcal{E}_{\text{avg}}$) and estimate error ($\Delta\tilde{\mathcal{E}}_{\text{avg}}$) :* $u = (1-x)(e^{5x} - 1)$, $\psi = \sin(\pi x)$

Fig. 6-5b shows the results for $p_{\text{inc}} = 1$ and Fig. 6-5c shows the results for $p_{\text{inc}} = 2$ which though not typically used for estimation, is useful for verifying the analysis.

The plots confirm the hypothesis of Chapter 4 that $\Delta\tilde{\mathcal{E}}^{u}_{\text{avg}} \equiv \Delta\tilde{\mathcal{E}}^{1}_{\text{avg}}$, with both failing to account for the error in the auxilliary equation. $\Delta\tilde{\mathcal{E}}_{\text{avg}}$ has the lowest error for $p = 1,\ 2$ and $p_{\text{inc}} = 1,\ 2$. For $p_{\text{inc}} = 1$ the benefit over $\Delta\tilde{\mathcal{E}}^{u}_{\text{avg}} \equiv \Delta\tilde{\mathcal{E}}^{1}_{\text{avg}}$ is minimal, in particular for $p_{\text{inc}} = 1,\ p = 1$, the three are practically identical, thus $\tilde{\eta}^{\vec{q}}_{\kappa}$ does not make up much of the local error. However for $p_{\text{inc}} = 2$ the effect is significant, with $\Delta\tilde{\mathcal{E}}^{u}_{\text{avg}} \equiv \Delta\tilde{\mathcal{E}}^{1}_{\text{avg}}$ being 2 orders of magnitude worse than $\Delta\tilde{\mathcal{E}}_{\text{avg}}$, this supports the conclusion that failing to account for the error in the primal auxilliary variable can reduce the quality of the estimate.

$\Delta\tilde{\mathcal{E}}^{2}_{\text{avg}}$ is far worse than the other estimates, in accordance with the *a priori* thus $\Delta\tilde{\mathcal{E}}^{2}_{\text{avg}}$ converges only because of the primal variables. This results in the sub-optimal $O(h^{p+d})$ rate of convergence. Thus all of the observed rates are in accordance with Table 6-3. All of the data used for generating these plots are presented in Tables A-21 to A-24 and A-29 to A-32.

6.2 2D Results

The primal and adjoint equations are

$$u = (1-x)(1-y)(1-e^{3xy}), \quad \text{in } (0,1)^2 \tag{6.6a}$$

$$\psi = \sin(\pi x)\sin(\pi y), \quad \text{in } (0,1)^2 \tag{6.6b}$$

which corresponds to an output functional of

$$\mathcal{J}(u) = (\pi^2 \sin(\pi x)\sin(\pi y), u). \tag{6.7}$$

The solutions and forcing functions are shown in Figures 6-6a to 6-6d.

Global Estimation

Figures 6-7a to 6-7c show the global error, error in the error estimate with $p_{\text{inc}} = 1$ and error in the error estimate with $p_{\text{inc}} = 2$ for CG, DG, HDG(h) and HDG(L). The global length scale was

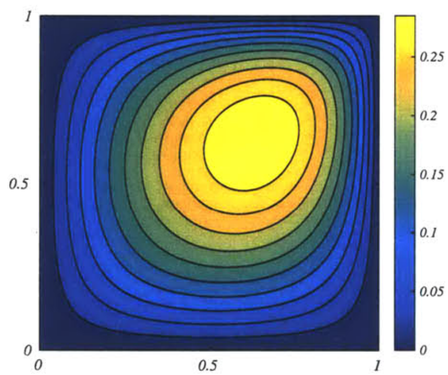

(a) u

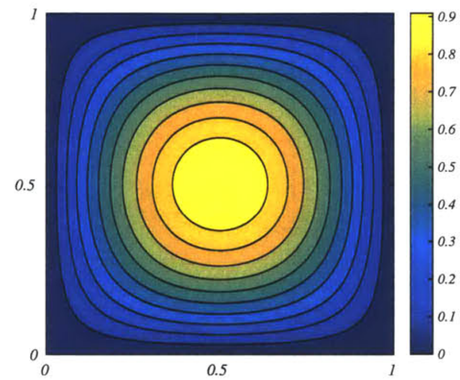

(b) ψ

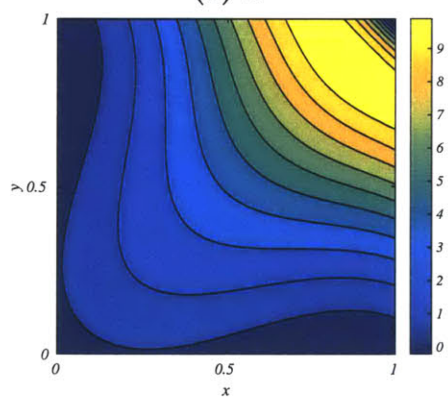

(c) f

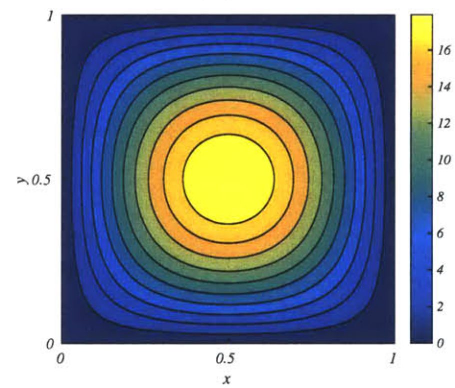

(d) g

Figure 6-6: *2D Solutions and Data*

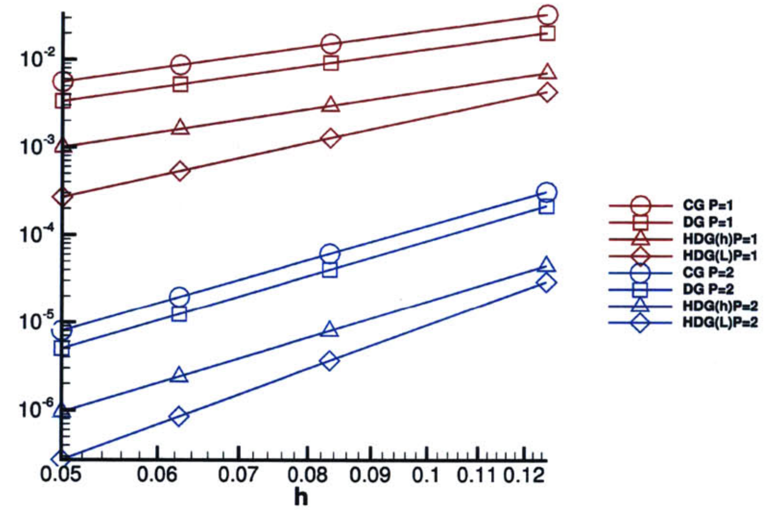

(a) $\mathcal{E}_{glob}$

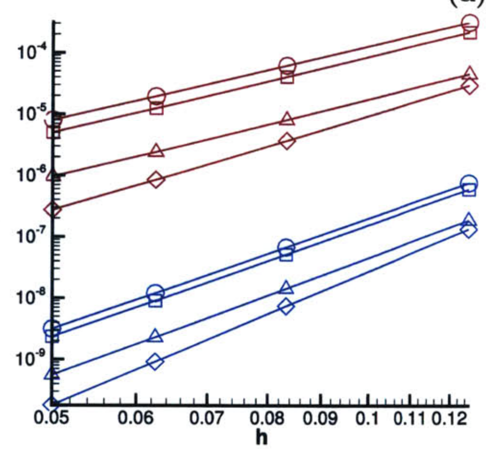

(b) $\Delta\tilde{\mathcal{E}}_{glob} : p_{inc} = 1$

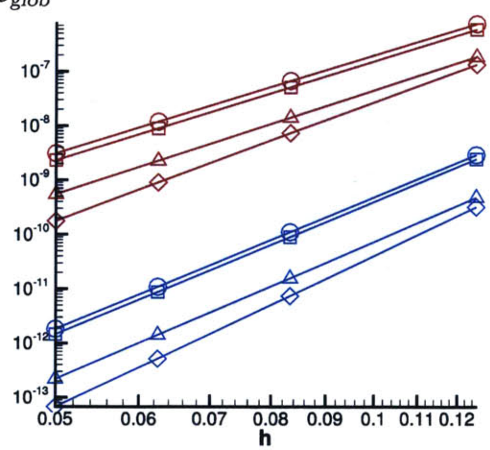

(c) $\Delta\tilde{\mathcal{E}}_{glob} : p_{inc} = 2$

Figure 6-7: *Global error* ($\mathcal{E}_{glob}$) *and estimate error* ($\Delta\tilde{\mathcal{E}}_{glob}$) : $u = (1-x)(1-y)(1-e^{3xy})$, $\psi = \sin(\pi x)\sin(\pi y)$

taken to be $\frac{1}{10}$ for HDG(L). All of the estimates considered are converging exactly as expected. Discerning the difference for the two HDG estimates is difficult using the figures alone, thus the data for generating the plots is presented in Appendix A.3.

HDG(h) has approximately an order of magnitude less error and error in the estimate than CG and DG for $p = 1,\ 2$ and $p_{\text{inc}} = 1,\ 2$. CG and DG are approximately equal, with DG having slightly less error than CG for a given mesh. HDG(L) has approximately half the error of HDG(h) and the ratio increases as the grid is refined with HDG(L) performing better relatively because of the additional $O(h)$ convergence of HDG(L) compared to HDG(h).

All of the discretizations and their estimates are converging exactly in line with Table 6-1. HDG also achieves an order of magnitude less error, both in the computed output functional, $\mathcal{E}_{\text{glob}}$, and in the estimate $\Delta\tilde{\mathcal{E}}_{\text{glob}}$ for the same grid, the exact cause of this is unclear. All of the data used for generating these plots are presented in Tables A-33 to A-36 and A-41 to A-44.

Local Estimation

Figures 6-8a to 6-8c show the local error, error in the error estimate with $p_{\text{inc}} = 1$ and error in the error estimate with $p_{\text{inc}} = 2$. The expected rates of convergence for $\mathcal{E}_{\text{avg}}$ and $\Delta\tilde{\mathcal{E}}_{\text{avg}}$ are given in Table 6-1. $\Delta\tilde{\mathcal{E}}_{\text{avg}}$ are all converging on average $p_{\text{inc}}/2$ faster than expected. This is possibly because whilst the absolute value ought to prevent Galerkin orthogonality occuring, if $\eta_\kappa - \tilde{\eta}_\kappa$ were all the same sign, the absolute value would have no effect on the summation and the global estimate would be recovered. Thus the convergence rates of Table 6-1 for $\Delta\tilde{\mathcal{E}}_{\text{avg}}$ are pessimistic and assume the worst case scenario for the application of the absolute value.

HDG(h) has approximately an order of magnitude less error than CG and DG in $\mathcal{E}_{\text{avg}}$, with HDG(L) having about half an order of magnitude less error than HDG(h). HDG(L) has increasingly better error than HDG(h) with mesh refinement because of the additional $O(h)$ convergence rate. For $\Delta\tilde{\mathcal{E}}_{\text{avg}}$, HDG($L$) also has about half an order of magnitude less error than HDG(h), HDG(L) also has increasingly smaller error than HDG(h) due to the additional $O(h)$ convergence rate. CG and DG have approximately half an order of magnitude less error than HDG(h) for $p_{\text{inc}} = 1$, but for $p_{\text{inc}} = 2$ CG has almost the same as HDG(h).

The choice of global length scale, L, for HDG(L) is relatively simple for a linear one dimensional case, but for multi-dimensional cases or those with anistropic features (for example a boundary layer), it is difficult to know *a priori* what length scale to choose. Choosing a length scale too small ensures the asymptotic convergence rate, but at the cost of the initial error being larger, and vice versa, thus the correct choice of L is difficult *a priori*. Figures 6-8b and 6-8c shows that instead choosing the reference length scale of the order of the grid spacing is a viable alternative that would

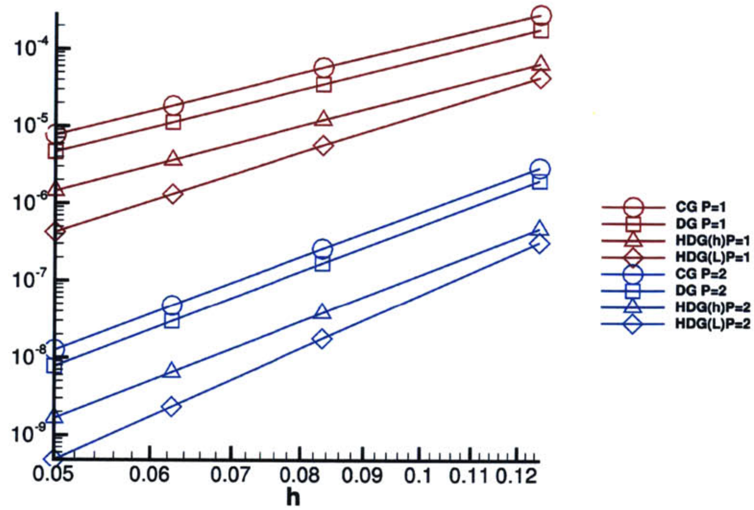

(a) $\mathcal{E}_{\text{avg}}$

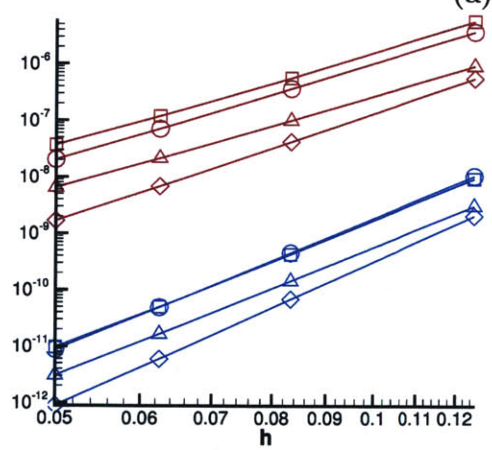

(b) $\Delta\tilde{\mathcal{E}}_{\text{avg}} : p_{inc} = 1$

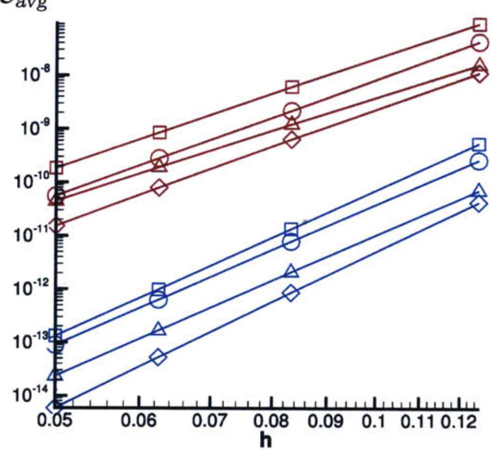

(c) $\Delta\tilde{\mathcal{E}}_{\text{avg}} : p_{inc} = 2$

Figure 6-8: *Local error* ($\mathcal{E}_{\text{avg}}$) *and estimate error* ($\Delta\tilde{\mathcal{E}}_{\text{avg}}$) : $u = (1-x)(1-y)(1-e^{3xy})$, $\psi = \sin(\pi x)\sin(\pi y)$

Table 6-4: A priori *convergence rates for DG global and local error and estimate error in 2D*

	$\tilde{\mathcal{E}}$, $\tilde{\eta}_\kappa$	$\tilde{\mathcal{E}}^u$, $\tilde{\eta}^u_\kappa$	$\tilde{\mathcal{E}}^1$, $\tilde{\eta}^1_\kappa$	$\tilde{\mathcal{E}}^2$, $\tilde{\eta}^2_\kappa$
$\Delta\tilde{\mathcal{E}}_{\text{glob}}$	$h^{2p'}$	$h^{p+p'}$	$h^{p+p'}$	$h^{2p'}$
$\Delta\tilde{\mathcal{E}}_{\text{avg}}$	$h^{p+p'+d}$	$h^{p+p'+d}$	$h^{p+p'+d}$	h^{p+d}

require no *a priori* knowledge of the important underlying flow features.

In summary, all of the schemes converge as predicted by the *a priori* analysis, or slightly better. All of the data used for generating these plots are presented in Tables A-5 to A-8 and A-13 to A-16.

6.2.1 Statically Condensed Estimation

Fig. 6-9a shows the computed values for $\mathcal{E}_{\text{glob}}$ which is independent of the estimation method. Fig. 6-9b shows the results for $p_{\text{inc}} = 1$ and Fig. 6-9c shows the results for $p_{\text{inc}} = 2$ which though not typically used for estimation, is useful for verifying the analysis.

As can be seen from the plots, $\Delta\tilde{\mathcal{E}}_{\text{glob}} \equiv \Delta\tilde{\mathcal{E}}^2_{\text{glob}}$ and $\Delta\tilde{\mathcal{E}}^u_{\text{glob}} \equiv \Delta\tilde{\mathcal{E}}^1_{\text{glob}}$, with the lines perfectly aligning for all p and p_{inc}. This is expected as a result of the analysis in Chapter 4.

$\Delta\tilde{\mathcal{E}}^u_{\text{glob}} \equiv \Delta\tilde{\mathcal{E}}^1_{\text{glob}}$ gives a marginally worse approximation than $\Delta\tilde{\mathcal{E}}_{\text{glob}}$ for p_1, $p_{\text{inc}} = 1$ which gets worse with grid refinement. For $p_{\text{inc}} = 2$, it is an extremely poor approximation with 4 orders of magnitude more error than $\Delta\tilde{\mathcal{E}}_{\text{glob}}$. The predicted sub optimal rate of $O(h^{p+p'})$ is observed for $p_{\text{inc}} = 2$.

In summary, all of the observed rates are in accordance with Table 6-4, as seen in Tables A-57 to A-60.

Fig. 6-10a shows the computed values for $\mathcal{E}_{\text{avg}}$ which is independent of the estimation method. Fig. 6-10b shows the results for $p_{\text{inc}} = 1$ and Fig. 6-10c shows the results for $p_{\text{inc}} = 2$.

The plots confirm the hypothesis of Chapter 4 that $\Delta\tilde{\mathcal{E}}^u_{\text{avg}} \equiv \Delta\tilde{\mathcal{E}}^1_{\text{avg}}$, with both failing to account for the error in the auxilliary equation. $\Delta\tilde{\mathcal{E}}_{\text{avg}}$ has the lowest error for $p = 1,\ 2$ and $p_{\text{inc}} = 1,\ 2$. For $p_{\text{inc}} = 1$ the benefit over $\Delta\tilde{\mathcal{E}}^u_{\text{avg}} \equiv \Delta\tilde{\mathcal{E}}^1_{\text{avg}}$ is minimal, in particular for $p_{\text{inc}} = 1,\ p = 1$, the three are practically identical, thus $\tilde{\eta}^{\vec{r}}_\kappa$ does not make up much of the local error. However for $p_{\text{inc}} = 2$ the effect is significant, with $\Delta\tilde{\mathcal{E}}^u_{\text{avg}} \equiv \Delta\tilde{\mathcal{E}}^1_{\text{avg}}$ being 2 orders of magnitude worse than $\Delta\tilde{\mathcal{E}}_{\text{avg}}$, this supports the conclusion that failing to account for the error in the primal auxilliary variable can reduce the quality of the estimate.

$\Delta\tilde{\mathcal{E}}^2_{\text{avg}}$ is far worse than the other estimates, in accordance with the *a priori* thus $\Delta\tilde{\mathcal{E}}^2_{\text{avg}}$ converges

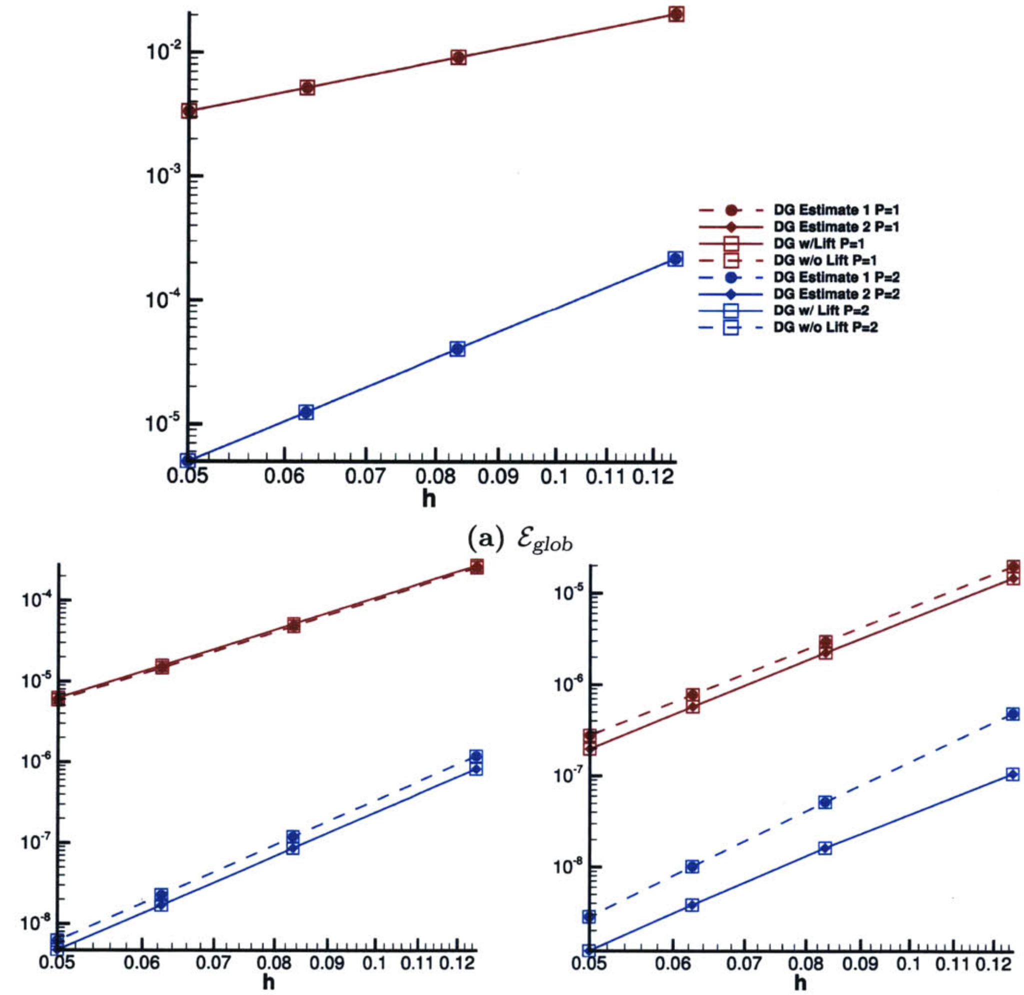

(a) $\mathcal{E}_{glob}$

(b) $\Delta\tilde{\mathcal{E}}_{glob}$: $p_{inc} = 1$

(c) $\Delta\tilde{\mathcal{E}}_{glob}$: $p_{inc} = 2$

Figure 6-9: *Global error* ($\mathcal{E}_{glob}$) *and estimate error* ($\Delta\tilde{\mathcal{E}}_{glob}$) : $u = (1-x)(1-y)(1-e^{3xy})$, $\psi = \sin(\pi x)\sin(\pi y)$

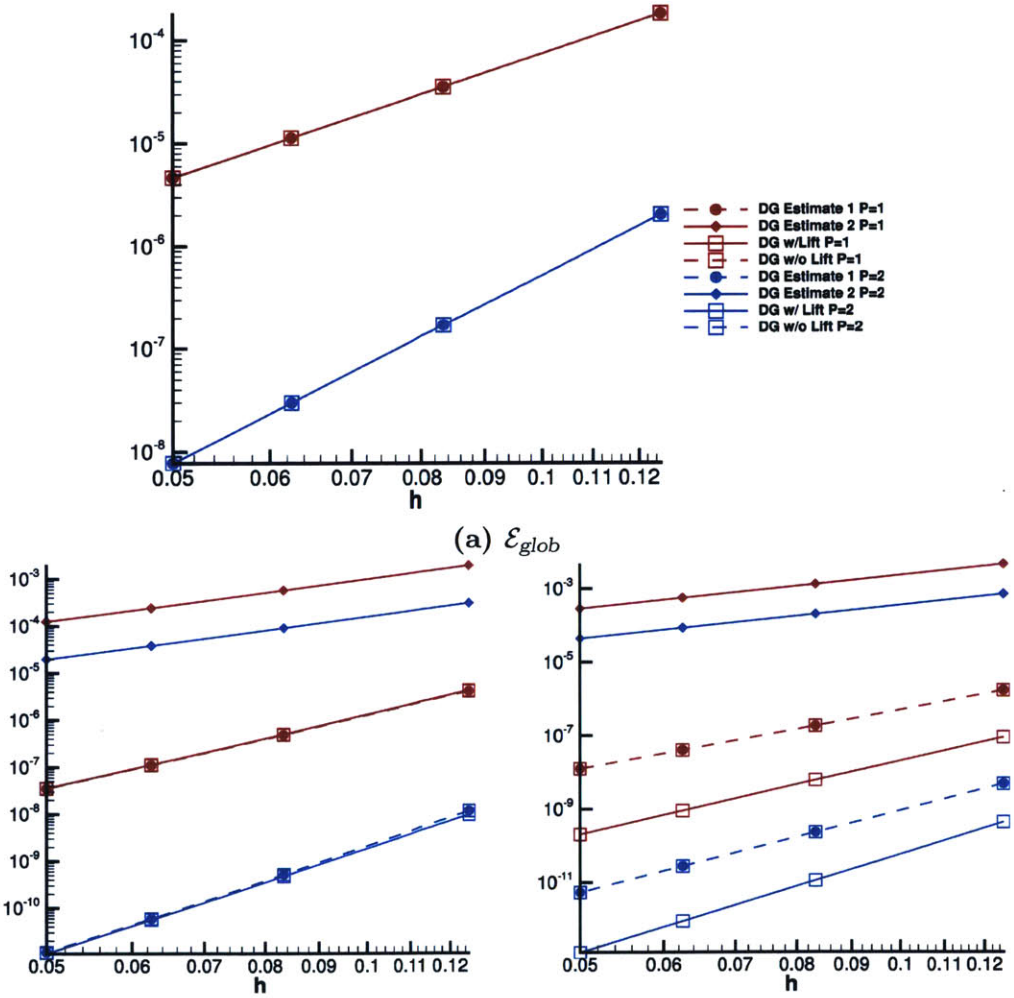

(a) $\mathcal{E}_{glob}$

(b) $\Delta\tilde{\mathcal{E}}_{glob} : p_{inc} = 1$

(c) $\Delta\tilde{\mathcal{E}}_{glob} : p_{inc} = 2$

Figure 6-10: *Local error* ($\mathcal{E}_{\text{glob}}$) *and estimate error* ($\Delta\tilde{\mathcal{E}}_{\text{glob}}$) : $u = (1-x)(1-y)(1-e^{3xy})$, $\psi = \sin(\pi x)\sin(\pi y)$

only because of the primal variables. This results in the sub-optimal $O(h^{p+d})$ rate of convergence. Thus all of the observed rates are in accordance with Table 6-4. All of the data used for generating these plots are presented in Tables A-53 to A-56 and A-61 to A-64.

Chapter 7

Conclusion

In this thesis a common framework for analyzing localizations of Dual-Weighted Residual Error Estimates is outlined. The framework enables *a priori* analysis of the asymptotic convergence rates of output functional error, estimates and error in these estimates within the context of the Poisson problem. The framework requries the proof of Extended Local Consistency (Definitions 5 and 6) and a local bilinear error bound (Lemmas 10, 21 and 34). Subsequently, this method can be used to prove convergence for any other local estimate based upon Galerkin methods for which these properties can be shown.

Using this analysis we have demonstrated that the classical weighted strong form residual error for CG converges optimally, and that the estimate converges to the true estimate asymptotically.

Within the DG context, the structure of the analysis was used to devise a novel post-processing procedure for the lifting-operator variable in the BR2 scheme[11]. The new estimate exhibits an improved convergence rate in the Global Estimate compared to the results within the literature. This is as a consequence of correctly accounting for the error in the calculation of the lifting operator such that Galerkin orthogonality can be exploited. The use of this analysis in directing research to devise such a scheme demonstrates the usefulness of the approach within this thesis and suggests applicability to other similar DG methods as described in Arnold *et al.* [2].

For HDG a new result for the convergence of volume output functionals was derived. Making use of projection based analysis[18], it is possible to account for the variation of the error as a function of the stabilization length scale τ. The choice of whether to use a globally defined length scale or a locally defined length scale has an impact on the asymptotic convergence rate, though the reduction in convergence of $O(\tau + \frac{1}{\tau})$ is less than initially suspected given the previously observed reduction in the convergence rate of $\|\vec{q} - \vec{q}_{h,p}\|_{L^2(\kappa)}$.

Finally numerical results are presented that verified the *a priori* analysis; with all of the schemes demonstrating the expected asymptotic convergence rates. Attention is drawn to the fact that HDG exhibits an order of magnitude less error than either CG or DG for a given mesh, even when a locally defined reference length scale is used in the stabilization constant τ. The cause for this superior performance and to what degree this performance is PDE dependent is unclear and suggests future analysis or numerical experimentation using other PDEs.

Chapter A

Results Tables

A.1 1D Results

A.2 1D Statically Condensed DG Estimation

A.3 2D Results

A.4 2D Statically Condensed DG Estimation

Table A-1: *1D CG Global Results* – $p_{inc} = 1$

p	h	$\mathcal{E}_{\text{glob}}$	Rate	$\Delta\tilde{\mathcal{E}}_{\text{glob}}$	Rate	Θ_{glob}	Rate
1	$2.50{\cdot}10^{-1}$	2.701^{0}	–	2.260^{-1}	–	7.72^{-2}	–
	$1.25{\cdot}10^{-1}$	5.535^{-1}	2.29	1.530^{-2}	3.88	2.69^{-2}	1.52
	$8.33{\cdot}10^{-2}$	2.346^{-1}	2.12	3.065^{-3}	3.97	1.29^{-2}	1.81
	$6.25{\cdot}10^{-2}$	1.297^{-1}	2.06	9.744^{-4}	3.98	7.46^{-3}	1.9
	$5.00{\cdot}10^{-2}$	8.232^{-2}	2.04	4.000^{-4}	3.99	4.84^{-3}	1.94
2	$2.50{\cdot}10^{-1}$	2.260^{-1}	–	1.261^{-3}	–	5.61^{-3}	–
	$1.25{\cdot}10^{-1}$	1.530^{-2}	3.88	1.795^{-5}	6.13	1.17^{-3}	2.26
	$8.33{\cdot}10^{-2}$	3.065^{-3}	3.97	1.544^{-6}	6.05	5.04^{-4}	2.09
	$6.25{\cdot}10^{-2}$	9.744^{-4}	3.98	2.727^{-7}	6.03	2.80^{-4}	2.04
	$5.00{\cdot}10^{-2}$	4.000^{-4}	3.99	7.124^{-8}	6.02	1.78^{-4}	2.03

Table A-2: *1D DG Global Results* – $p_{inc} = 1$

p	h	$\mathcal{E}_{\text{glob}}$	Rate	$\Delta\tilde{\mathcal{E}}_{\text{glob}}$	Rate	Θ_{glob}	Rate
1	$2.50{\cdot}10^{-1}$	2.691^{0}	–	1.742^{-1}	–	6.08^{-2}	–
	$1.25{\cdot}10^{-1}$	5.344^{-1}	2.33	1.042^{-2}	4.06	1.91^{-2}	1.67
	$8.33{\cdot}10^{-2}$	2.209^{-1}	2.18	1.970^{-3}	4.11	8.84^{-3}	1.9
	$6.25{\cdot}10^{-2}$	1.206^{-1}	2.11	6.054^{-4}	4.1	5.00^{-3}	1.98
	$5.00{\cdot}10^{-2}$	7.599^{-2}	2.07	2.431^{-4}	4.09	3.19^{-3}	2.01
2	$2.50{\cdot}10^{-1}$	1.742^{-1}	–	1.203^{-3}	–	6.95^{-3}	–
	$1.25{\cdot}10^{-1}$	1.042^{-2}	4.06	1.677^{-5}	6.16	1.61^{-3}	2.11
	$8.33{\cdot}10^{-2}$	1.970^{-3}	4.11	1.425^{-6}	6.08	7.24^{-4}	1.97
	$6.25{\cdot}10^{-2}$	6.054^{-4}	4.1	2.503^{-7}	6.05	4.14^{-4}	1.95
	$5.00{\cdot}10^{-2}$	2.431^{-4}	4.09	6.518^{-8}	6.03	2.68^{-4}	1.94

Table A-3: *1D HDG-h Global Results* – $p_{inc} = 1$

p	h	$\mathcal{E}_{\text{glob}}$	Rate	$\Delta\tilde{\mathcal{E}}_{\text{glob}}$	Rate	Θ_{glob}	Rate
1	$2.50{\cdot}10^{-1}$	7.122^{-1}	–	5.857^{-2}	–	8.22^{-2}	–
	$1.25{\cdot}10^{-1}$	9.958^{-2}	2.84	2.524^{-3}	4.54	2.53^{-2}	1.7
	$8.33{\cdot}10^{-2}$	3.698^{-2}	2.44	4.161^{-4}	4.45	1.12^{-2}	2
	$6.25{\cdot}10^{-2}$	1.913^{-2}	2.29	1.186^{-4}	4.36	6.20^{-3}	2.07
	$5.00{\cdot}10^{-2}$	1.169^{-2}	2.21	4.537^{-5}	4.3	3.88^{-3}	2.1
2	$2.50{\cdot}10^{-1}$	5.857^{-2}	–	1.113^{-4}	–	1.90^{-3}	–
	$1.25{\cdot}10^{-1}$	2.524^{-3}	4.54	1.236^{-6}	6.49	4.90^{-4}	1.96
	$8.33{\cdot}10^{-2}$	4.161^{-4}	4.45	1.002^{-7}	6.2	2.41^{-4}	1.75
	$6.25{\cdot}10^{-2}$	1.186^{-4}	4.36	1.726^{-8}	6.11	1.46^{-4}	1.75
	$5.00{\cdot}10^{-2}$	4.537^{-5}	4.3	4.448^{-9}	6.08	9.80^{-5}	1.77

Table A-4: *1D HDG-L Global Results* – $p_{inc} = 1$

p	h	$\mathcal{E}_{\text{glob}}$	Rate	$\Delta\tilde{\mathcal{E}}_{\text{glob}}$	Rate	Θ_{glob}	Rate
1	$2.50{\cdot}10^{-1}$	1.154^{0}	–	8.928^{-2}	–	7.74^{-2}	–
	$1.25{\cdot}10^{-1}$	1.122^{-1}	3.36	2.935^{-3}	4.93	2.62^{-2}	1.56
	$8.33{\cdot}10^{-2}$	3.388^{-2}	2.95	3.614^{-4}	5.17	1.07^{-2}	2.21
	$6.25{\cdot}10^{-2}$	1.535^{-2}	2.75	8.038^{-5}	5.23	5.24^{-3}	2.47
	$5.00{\cdot}10^{-2}$	8.416^{-3}	2.69	2.497^{-5}	5.24	2.97^{-3}	2.55
2	$2.50{\cdot}10^{-1}$	8.928^{-2}	–	2.453^{-4}	–	2.75^{-3}	–
	$1.25{\cdot}10^{-1}$	2.935^{-3}	4.93	1.495^{-6}	7.36	5.09^{-4}	2.43
	$8.33{\cdot}10^{-2}$	3.614^{-4}	5.17	8.653^{-8}	7.03	2.39^{-4}	1.86
	$6.25{\cdot}10^{-2}$	8.038^{-5}	5.23	1.191^{-8}	6.89	1.48^{-4}	1.67
	$5.00{\cdot}10^{-2}$	2.497^{-5}	5.24	2.582^{-9}	6.85	1.03^{-4}	1.61

Table A-5: *1D CG Local Results* – $p_{inc} = 1$

p	h	$\frac{\mathcal{E}_{agg}}{N}$	Rate	$\frac{\Delta\tilde{\mathcal{E}}_{agg}}{N}$	Rate	Θ_{agg}	Rate
1	$2.50{\cdot}10^{-1}$	9.644^{-1}	–	5.651^{-2}	–	5.86^{-2}	–
	$1.25{\cdot}10^{-1}$	1.113^{-1}	3.12	1.915^{-3}	4.88	1.72^{-2}	1.77
	$8.33{\cdot}10^{-2}$	3.204^{-2}	3.07	2.557^{-4}	4.97	7.98^{-3}	1.9
	$6.25{\cdot}10^{-2}$	1.333^{-2}	3.05	6.096^{-5}	4.98	4.57^{-3}	1.93
	$5.00{\cdot}10^{-2}$	6.822^{-3}	3	2.002^{-5}	4.99	2.93^{-3}	1.99
2	$2.50{\cdot}10^{-1}$	5.651^{-2}	–	3.162^{-4}	–	5.60^{-3}	–
	$1.25{\cdot}10^{-1}$	1.915^{-3}	4.88	2.248^{-6}	7.14	1.17^{-3}	2.25
	$8.33{\cdot}10^{-2}$	2.557^{-4}	4.97	1.289^{-7}	7.05	5.04^{-4}	2.08
	$6.25{\cdot}10^{-2}$	6.096^{-5}	4.98	1.708^{-8}	7.03	2.80^{-4}	2.04
	$5.00{\cdot}10^{-2}$	2.002^{-5}	4.99	3.569^{-9}	7.02	1.78^{-4}	2.03

Table A-6: *1D DG Local Results* – $p_{inc} = 1$

p	h	$\frac{\mathcal{E}_{agg}}{N}$	Rate	$\frac{\Delta\tilde{\mathcal{E}}_{agg}}{N}$	Rate	Θ_{agg}	Rate
1	$2.50{\cdot}10^{-1}$	8.898^{-1}	–	4.725^{-2}	–	5.31^{-2}	–
	$1.25{\cdot}10^{-1}$	1.015^{-1}	3.13	1.375^{-3}	5.1	1.35^{-2}	1.97
	$8.33{\cdot}10^{-2}$	2.945^{-2}	3.05	2.997^{-4}	3.76	1.02^{-2}	0.71
	$6.25{\cdot}10^{-2}$	1.218^{-2}	3.07	9.462^{-5}	4.01	7.77^{-3}	0.94
	$5.00{\cdot}10^{-2}$	6.233^{-3}	3	3.616^{-5}	4.31	5.80^{-3}	1.31
2	$2.50{\cdot}10^{-1}$	4.355^{-2}	–	8.132^{-4}	–	1.87^{-2}	–
	$1.25{\cdot}10^{-1}$	1.304^{-3}	5.06	5.101^{-6}	7.32	3.91^{-3}	2.25
	$8.33{\cdot}10^{-2}$	1.643^{-4}	5.11	2.553^{-7}	7.39	1.55^{-3}	2.28
	$6.25{\cdot}10^{-2}$	3.787^{-5}	5.1	3.368^{-8}	7.04	8.90^{-4}	1.94
	$5.00{\cdot}10^{-2}$	1.216^{-5}	5.09	6.962^{-9}	7.07	5.72^{-4}	1.98

Table A-7: *1D HDG-h Local Results – $p_{inc} = 1$*

p	h	$\frac{\mathcal{E}_{agg}}{N}$	Rate	$\frac{\Delta\tilde{\mathcal{E}}_{agg}}{N}$	Rate	Θ_{agg}	Rate
1	$2.50 \cdot 10^{-1}$	2.130^{-1}	–	1.674^{-2}	–	7.86^{-2}	–
	$1.25 \cdot 10^{-1}$	1.784^{-2}	3.58	3.214^{-4}	5.7	1.80^{-2}	2.13
	$8.33 \cdot 10^{-2}$	4.686^{-3}	3.3	3.490^{-5}	5.48	7.45^{-3}	2.18
	$6.25 \cdot 10^{-2}$	1.868^{-3}	3.2	7.437^{-6}	5.37	3.98^{-3}	2.18
	$5.00 \cdot 10^{-2}$	9.344^{-4}	3.1	2.274^{-6}	5.31	2.43^{-3}	2.21
2	$2.50 \cdot 10^{-1}$	1.674^{-2}	–	2.815^{-5}	–	1.68^{-3}	–
	$1.25 \cdot 10^{-1}$	3.214^{-4}	5.7	1.552^{-7}	7.5	4.83^{-4}	1.8
	$8.33 \cdot 10^{-2}$	3.490^{-5}	5.48	8.377^{-9}	7.2	2.40^{-4}	1.72
	$6.25 \cdot 10^{-2}$	7.437^{-6}	5.37	1.081^{-9}	7.12	1.45^{-4}	1.74
	$5.00 \cdot 10^{-2}$	2.274^{-6}	5.31	2.229^{-10}	7.08	9.80^{-5}	1.77

Table A-8: *1D HDG-L Local Results – $p_{inc} = 1$*

p	h	$\frac{\mathcal{E}_{agg}}{N}$	Rate	$\frac{\Delta\tilde{\mathcal{E}}_{agg}}{N}$	Rate	Θ_{agg}	Rate
1	$2.50 \cdot 10^{-1}$	3.664^{-1}	–	2.238^{-2}	–	6.11^{-2}	–
	$1.25 \cdot 10^{-1}$	2.059^{-2}	4.15	3.708^{-4}	5.92	1.80^{-2}	1.76
	$8.33 \cdot 10^{-2}$	4.185^{-3}	3.93	3.043^{-5}	6.17	7.27^{-3}	2.24
	$6.25 \cdot 10^{-2}$	1.489^{-3}	3.59	5.078^{-6}	6.22	3.41^{-3}	2.63
	$5.00 \cdot 10^{-2}$	6.879^{-4}	3.46	1.263^{-6}	6.23	1.84^{-3}	2.77
2	$2.50 \cdot 10^{-1}$	2.238^{-2}	–	6.162^{-5}	–	2.75^{-3}	–
	$1.25 \cdot 10^{-1}$	3.708^{-4}	5.92	1.876^{-7}	8.36	5.06^{-4}	2.44
	$8.33 \cdot 10^{-2}$	3.043^{-5}	6.17	7.235^{-9}	8.03	2.38^{-4}	1.86
	$6.25 \cdot 10^{-2}$	5.078^{-6}	6.22	8.087^{-10}	7.62	1.59^{-4}	1.39
	$5.00 \cdot 10^{-2}$	1.263^{-6}	6.23	1.466^{-10}	7.65	1.16^{-4}	1.42

Table A-9: *1D CG Global Results – $p_{inc} = 2$*

p	h	$\mathcal{E}_{\text{glob}}$	Rate	$\Delta\tilde{\mathcal{E}}_{\text{glob}}$	Rate	Θ_{glob}	Rate
1	$2.50{\cdot}10^{-1}$	2.701^{0}	–	1.261^{-3}	–	4.67^{-4}	–
	$1.25{\cdot}10^{-1}$	5.535^{-1}	2.29	1.795^{-5}	6.13	3.24^{-5}	3.85
	$8.33{\cdot}10^{-2}$	2.346^{-1}	2.12	1.544^{-6}	6.05	6.58^{-6}	3.93
	$6.25{\cdot}10^{-2}$	1.297^{-1}	2.06	2.727^{-7}	6.03	2.10^{-6}	3.97
	$5.00{\cdot}10^{-2}$	8.232^{-2}	2.04	7.124^{-8}	6.02	8.65^{-7}	3.98
2	$2.50{\cdot}10^{-1}$	2.260^{-1}	–	1.105^{-5}	–	4.89^{-5}	–
	$1.25{\cdot}10^{-1}$	1.530^{-2}	3.88	4.675^{-8}	7.88	3.06^{-6}	4
	$8.33{\cdot}10^{-2}$	3.065^{-3}	3.97	1.850^{-9}	7.97	6.04^{-7}	4
	$6.25{\cdot}10^{-2}$	9.744^{-4}	3.98	1.861^{-10}	7.98	1.91^{-7}	4
	$5.00{\cdot}10^{-2}$	4.000^{-4}	3.99	3.130^{-11}	7.99	7.82^{-8}	4

Table A-10: *1D DG Global Results – $p_{inc} = 2$*

p	h	$\mathcal{E}_{\text{glob}}$	Rate	$\Delta\tilde{\mathcal{E}}_{\text{glob}}$	Rate	Θ_{glob}	Rate
1	$2.50{\cdot}10^{-1}$	2.691^{0}	–	1.203^{-3}	–	4.47^{-4}	–
	$1.25{\cdot}10^{-1}$	5.344^{-1}	2.33	1.677^{-5}	6.16	3.14^{-5}	3.83
	$8.33{\cdot}10^{-2}$	2.209^{-1}	2.18	1.425^{-6}	6.08	6.45^{-6}	3.9
	$6.25{\cdot}10^{-2}$	1.206^{-1}	2.11	2.503^{-7}	6.05	2.08^{-6}	3.94
	$5.00{\cdot}10^{-2}$	7.599^{-2}	2.07	6.518^{-8}	6.03	8.58^{-7}	3.96
2	$2.50{\cdot}10^{-1}$	1.742^{-1}	–	8.901^{-6}	–	5.11^{-5}	–
	$1.25{\cdot}10^{-1}$	1.042^{-2}	4.06	3.468^{-8}	8	3.33^{-6}	3.94
	$8.33{\cdot}10^{-2}$	1.970^{-3}	4.11	1.323^{-9}	8.05	6.72^{-7}	3.95
	$6.25{\cdot}10^{-2}$	6.054^{-4}	4.1	1.304^{-10}	8.05	2.15^{-7}	3.95
	$5.00{\cdot}10^{-2}$	2.431^{-4}	4.09	2.164^{-11}	8.05	8.90^{-8}	3.96

Table A-11: *1D HDG-h Global Results – $p_{inc} = 2$*

p	h	$\mathcal{E}_{\text{glob}}$	Rate	$\Delta\tilde{\mathcal{E}}_{\text{glob}}$	Rate	Θ_{glob}	Rate
1	$2.50 \cdot 10^{-1}$	7.122^{-1}	–	1.113^{-4}	–	1.56^{-4}	–
	$1.25 \cdot 10^{-1}$	9.958^{-2}	2.84	1.236^{-6}	6.49	1.24^{-5}	3.65
	$8.33 \cdot 10^{-2}$	3.698^{-2}	2.44	1.002^{-7}	6.2	2.71^{-6}	3.75
	$6.25 \cdot 10^{-2}$	1.913^{-2}	2.29	1.726^{-8}	6.11	9.02^{-7}	3.82
	$5.00 \cdot 10^{-2}$	1.169^{-2}	2.21	4.448^{-9}	6.08	3.80^{-7}	3.87
2	$2.50 \cdot 10^{-1}$	5.857^{-2}	–	1.651^{-6}	–	2.82^{-5}	–
	$1.25 \cdot 10^{-1}$	2.524^{-3}	4.54	4.426^{-9}	8.54	1.75^{-6}	4.01
	$8.33 \cdot 10^{-2}$	4.161^{-4}	4.45	1.445^{-10}	8.44	3.47^{-7}	3.99
	$6.25 \cdot 10^{-2}$	1.186^{-4}	4.36	1.304^{-11}	8.36	1.10^{-7}	4
	$5.00 \cdot 10^{-2}$	4.537^{-5}	4.3	2.040^{-12}	8.31	4.50^{-8}	4.01

Table A-12: *1D HDG-L Global Results – $p_{inc} = 2$*

p	h	$\mathcal{E}_{\text{glob}}$	Rate	$\Delta\tilde{\mathcal{E}}_{\text{glob}}$	Rate	Θ_{glob}	Rate
1	$2.50 \cdot 10^{-1}$	1.154^{0}	–	2.453^{-4}	–	2.13^{-4}	–
	$1.25 \cdot 10^{-1}$	1.122^{-1}	3.36	1.495^{-6}	7.36	1.33^{-5}	4
	$8.33 \cdot 10^{-2}$	3.388^{-2}	2.95	8.653^{-8}	7.03	2.55^{-6}	4.08
	$6.25 \cdot 10^{-2}$	1.535^{-2}	2.75	1.191^{-8}	6.89	7.76^{-7}	4.14
	$5.00 \cdot 10^{-2}$	8.416^{-3}	2.69	2.582^{-9}	6.85	3.07^{-7}	4.16
2	$2.50 \cdot 10^{-1}$	8.928^{-2}	–	2.788^{-6}	–	3.12^{-5}	–
	$1.25 \cdot 10^{-1}$	2.935^{-3}	4.93	5.250^{-9}	9.05	1.79^{-6}	4.13
	$8.33 \cdot 10^{-2}$	3.614^{-4}	5.17	1.238^{-10}	9.24	3.43^{-7}	4.08
	$6.25 \cdot 10^{-2}$	8.038^{-5}	5.23	8.593^{-12}	9.27	1.07^{-7}	4.05
	$5.00 \cdot 10^{-2}$	2.497^{-5}	5.24	1.089^{-12}	9.26	4.36^{-8}	4.02

Table A-13: *1D CG Local Results – $p_{inc} = 2$*

p	h	$\frac{\mathcal{E}_{agg}}{N}$	Rate	$\frac{\Delta\tilde{\mathcal{E}}_{agg}}{N}$	Rate	Θ_{agg}	Rate
1	$2.50{\cdot}10^{-1}$	9.644^{-1}	–	3.162^{-4}	–	3.28^{-4}	–
	$1.25{\cdot}10^{-1}$	1.113^{-1}	3.12	2.248^{-6}	7.14	2.02^{-5}	4.02
	$8.33{\cdot}10^{-2}$	3.204^{-2}	3.07	1.289^{-7}	7.05	4.02^{-6}	3.98
	$6.25{\cdot}10^{-2}$	1.333^{-2}	3.05	1.708^{-8}	7.03	1.28^{-6}	3.98
	$5.00{\cdot}10^{-2}$	6.822^{-3}	3	3.569^{-9}	7.02	5.23^{-7}	4.01
2	$2.50{\cdot}10^{-1}$	5.651^{-2}	–	2.856^{-6}	–	5.05^{-5}	–
	$1.25{\cdot}10^{-1}$	1.915^{-3}	4.88	6.004^{-9}	8.89	3.13^{-6}	4.01
	$8.33{\cdot}10^{-2}$	2.557^{-4}	4.97	1.582^{-10}	8.97	6.19^{-7}	4
	$6.25{\cdot}10^{-2}$	6.096^{-5}	4.98	1.193^{-11}	8.98	1.96^{-7}	4
	$5.00{\cdot}10^{-2}$	2.002^{-5}	4.99	1.605^{-12}	8.99	8.02^{-8}	4

Table A-14: *1D DG Local Results – $p_{inc} = 2$*

p	h	$\frac{\mathcal{E}_{agg}}{N}$	Rate	$\frac{\Delta\tilde{\mathcal{E}}_{agg}}{N}$	Rate	Θ_{agg}	Rate
1	$2.50{\cdot}10^{-1}$	8.898^{-1}	–	2.360^{-3}	–	2.65^{-3}	–
	$1.25{\cdot}10^{-1}$	1.015^{-1}	3.13	3.078^{-5}	6.26	3.03^{-4}	3.13
	$8.33{\cdot}10^{-2}$	2.945^{-2}	3.05	1.903^{-6}	6.87	6.46^{-5}	3.81
	$6.25{\cdot}10^{-2}$	1.218^{-2}	3.07	2.520^{-7}	7.03	2.07^{-5}	3.96
	$5.00{\cdot}10^{-2}$	6.233^{-3}	3	5.502^{-8}	6.82	8.83^{-6}	3.82
2	$2.50{\cdot}10^{-1}$	4.355^{-2}	–	2.443^{-6}	–	5.61^{-5}	–
	$1.25{\cdot}10^{-1}$	1.304^{-3}	5.06	2.069^{-8}	6.88	1.59^{-5}	1.82
	$8.33{\cdot}10^{-2}$	1.643^{-4}	5.11	8.217^{-10}	7.96	5.00^{-6}	2.85
	$6.25{\cdot}10^{-2}$	3.787^{-5}	5.1	7.050^{-11}	8.54	1.86^{-6}	3.43
	$5.00{\cdot}10^{-2}$	1.216^{-5}	5.09	9.705^{-12}	8.89	7.98^{-7}	3.8

Table A-15: *1D HDG-h Local Results – $p_{inc} = 2$*

p	h	$\frac{\mathcal{E}_{\text{agg}}}{N}$	Rate	$\frac{\Delta\tilde{\mathcal{E}}_{\text{agg}}}{N}$	Rate	Θ_{agg}	Rate
1	$2.50{\cdot}10^{-1}$	2.130^{-1}	–	2.815^{-5}	–	1.32^{-4}	–
	$1.25{\cdot}10^{-1}$	1.784^{-2}	3.58	1.552^{-7}	7.5	8.70^{-6}	3.92
	$8.33{\cdot}10^{-2}$	4.686^{-3}	3.3	8.377^{-9}	7.2	1.79^{-6}	3.9
	$6.25{\cdot}10^{-2}$	1.868^{-3}	3.2	1.081^{-9}	7.12	5.79^{-7}	3.92
	$5.00{\cdot}10^{-2}$	9.344^{-4}	3.1	2.229^{-10}	7.08	2.39^{-7}	3.97
2	$2.50{\cdot}10^{-1}$	1.674^{-2}	–	4.763^{-7}	–	2.84^{-5}	–
	$1.25{\cdot}10^{-1}$	3.214^{-4}	5.7	5.727^{-10}	9.7	1.78^{-6}	4
	$8.33{\cdot}10^{-2}$	3.490^{-5}	5.48	1.234^{-11}	9.47	3.53^{-7}	3.99
	$6.25{\cdot}10^{-2}$	7.437^{-6}	5.37	8.543^{-13}	9.28	1.15^{-7}	3.91
	$5.00{\cdot}10^{-2}$	2.274^{-6}	5.31	1.149^{-13}	8.99	5.05^{-8}	3.68

Table A-16: *1D HDG-L Local Results – $p_{inc} = 2$*

p	h	$\frac{\mathcal{E}_{\text{agg}}}{N}$	Rate	$\frac{\Delta\tilde{\mathcal{E}}_{\text{agg}}}{N}$	Rate	Θ_{agg}	Rate
1	$2.50{\cdot}10^{-1}$	3.664^{-1}	–	6.162^{-5}	–	1.68^{-4}	–
	$1.25{\cdot}10^{-1}$	2.059^{-2}	4.15	1.876^{-7}	8.36	9.11^{-6}	4.21
	$8.33{\cdot}10^{-2}$	4.185^{-3}	3.93	7.235^{-9}	8.03	1.73^{-6}	4.1
	$6.25{\cdot}10^{-2}$	1.489^{-3}	3.59	8.087^{-10}	7.62	5.43^{-7}	4.03
	$5.00{\cdot}10^{-2}$	6.879^{-4}	3.46	1.466^{-10}	7.65	2.13^{-7}	4.19
2	$2.50{\cdot}10^{-1}$	2.238^{-2}	–	7.114^{-7}	–	3.18^{-5}	–
	$1.25{\cdot}10^{-1}$	3.708^{-4}	5.92	6.719^{-10}	10.05	1.81^{-6}	4.13
	$8.33{\cdot}10^{-2}$	3.043^{-5}	6.17	1.062^{-11}	10.23	3.49^{-7}	4.06
	$6.25{\cdot}10^{-2}$	5.078^{-6}	6.22	5.476^{-13}	10.31	1.08^{-7}	4.08
	$5.00{\cdot}10^{-2}$	1.263^{-6}	6.23	6.234^{-14}	9.74	4.94^{-8}	3.5

Table A-17: *1D DG with Lifting Operator Error Global Results* – $p_{\text{inc}} = 1$

p	h	$\mathcal{E}_{\text{glob}}$	Rate	$\Delta\tilde{\mathcal{E}}_{\text{glob}}$	Rate	Θ_{glob}	Rate
1	$2.50{\cdot}10^{-1}$	2.691^{0}	–	1.742^{-1}	–	6.08^{-2}	–
	$1.25{\cdot}10^{-1}$	5.344^{-1}	2.33	1.042^{-2}	4.06	1.91^{-2}	1.67
	$8.33{\cdot}10^{-2}$	2.209^{-1}	2.18	1.970^{-3}	4.11	8.84^{-3}	1.9
	$6.25{\cdot}10^{-2}$	1.206^{-1}	2.11	6.054^{-4}	4.1	5.00^{-3}	1.98
	$5.00{\cdot}10^{-2}$	7.599^{-2}	2.07	2.431^{-4}	4.09	3.19^{-3}	2.01
2	$2.50{\cdot}10^{-1}$	1.742^{-1}	–	1.203^{-3}	–	6.95^{-3}	–
	$1.25{\cdot}10^{-1}$	1.042^{-2}	4.06	1.677^{-5}	6.16	1.61^{-3}	2.11
	$8.33{\cdot}10^{-2}$	1.970^{-3}	4.11	1.425^{-6}	6.08	7.24^{-4}	1.97
	$6.25{\cdot}10^{-2}$	6.054^{-4}	4.1	2.503^{-7}	6.05	4.14^{-4}	1.95
	$5.00{\cdot}10^{-2}$	2.431^{-4}	4.09	6.518^{-8}	6.03	2.68^{-4}	1.94

Table A-18: *1D DG without Lifting Operator Error Global Results* – $p_{\text{inc}} = 1$

p	h	$\mathcal{E}_{\text{glob}}$	Rate	$\Delta\tilde{\mathcal{E}}_{\text{glob}}$	Rate	Θ_{glob}	Rate
1	$2.50{\cdot}10^{-1}$	2.691^{0}	–	2.486^{-1}	–	8.46^{-2}	–
	$1.25{\cdot}10^{-1}$	5.344^{-1}	2.33	2.007^{-2}	3.63	3.62^{-2}	1.22
	$8.33{\cdot}10^{-2}$	2.209^{-1}	2.18	4.307^{-3}	3.8	1.91^{-2}	1.57
	$6.25{\cdot}10^{-2}$	1.206^{-1}	2.11	1.420^{-3}	3.86	1.16^{-2}	1.73
	$5.00{\cdot}10^{-2}$	7.599^{-2}	2.07	5.960^{-4}	3.89	7.78^{-3}	1.8
2	$2.50{\cdot}10^{-1}$	1.742^{-1}	–	7.423^{-4}	–	4.28^{-3}	–
	$1.25{\cdot}10^{-1}$	1.042^{-2}	4.06	3.720^{-6}	7.64	3.57^{-4}	3.58
	$8.33{\cdot}10^{-2}$	1.970^{-3}	4.11	5.720^{-8}	10.3	2.90^{-5}	6.19
	$6.25{\cdot}10^{-2}$	6.054^{-4}	4.1	1.524^{-8}	4.6	2.52^{-5}	0.5
	$5.00{\cdot}10^{-2}$	2.431^{-4}	4.09	8.126^{-9}	2.82	3.34^{-5}	−1.27

Table A-19: *1D DG Estimate 1 Global Results* – $p_{inc} = 1$

p	h	$\mathcal{E}_{\text{glob}}$	Rate	$\Delta\tilde{\mathcal{E}}_{\text{glob}}$	Rate	Θ_{glob}	Rate
1	$2.50{\cdot}10^{-1}$	2.691^{0}	–	2.486^{-1}	–	8.46^{-2}	–
	$1.25{\cdot}10^{-1}$	5.344^{-1}	2.33	2.007^{-2}	3.63	3.62^{-2}	1.22
	$8.33{\cdot}10^{-2}$	2.209^{-1}	2.18	4.307^{-3}	3.8	1.91^{-2}	1.57
	$6.25{\cdot}10^{-2}$	1.206^{-1}	2.11	1.420^{-3}	3.86	1.16^{-2}	1.73
	$5.00{\cdot}10^{-2}$	7.599^{-2}	2.07	5.960^{-4}	3.89	7.78^{-3}	1.8
2	$2.50{\cdot}10^{-1}$	1.742^{-1}	–	7.423^{-4}	–	4.28^{-3}	–
	$1.25{\cdot}10^{-1}$	1.042^{-2}	4.06	3.720^{-6}	7.64	3.57^{-4}	3.58
	$8.33{\cdot}10^{-2}$	1.970^{-3}	4.11	5.720^{-8}	10.3	2.90^{-5}	6.19
	$6.25{\cdot}10^{-2}$	6.054^{-4}	4.1	1.524^{-8}	4.6	2.52^{-5}	0.5
	$5.00{\cdot}10^{-2}$	2.431^{-4}	4.09	8.126^{-9}	2.82	3.34^{-5}	−1.27

Table A-20: *1D DG Estimate 2 Global Results* – $p_{inc} = 1$

p	h	$\mathcal{E}_{\text{glob}}$	Rate	$\Delta\tilde{\mathcal{E}}_{\text{glob}}$	Rate	Θ_{glob}	Rate
1	$2.50{\cdot}10^{-1}$	2.691^{0}	–	1.742^{-1}	–	6.08^{-2}	–
	$1.25{\cdot}10^{-1}$	5.344^{-1}	2.33	1.042^{-2}	4.06	1.91^{-2}	1.67
	$8.33{\cdot}10^{-2}$	2.209^{-1}	2.18	1.970^{-3}	4.11	8.84^{-3}	1.9
	$6.25{\cdot}10^{-2}$	1.206^{-1}	2.11	6.054^{-4}	4.1	5.00^{-3}	1.98
	$5.00{\cdot}10^{-2}$	7.599^{-2}	2.07	2.431^{-4}	4.09	3.19^{-3}	2.01
2	$2.50{\cdot}10^{-1}$	1.742^{-1}	–	1.203^{-3}	–	6.95^{-3}	–
	$1.25{\cdot}10^{-1}$	1.042^{-2}	4.06	1.677^{-5}	6.16	1.61^{-3}	2.11
	$8.33{\cdot}10^{-2}$	1.970^{-3}	4.11	1.425^{-6}	6.08	7.24^{-4}	1.97
	$6.25{\cdot}10^{-2}$	6.054^{-4}	4.1	2.503^{-7}	6.05	4.14^{-4}	1.95
	$5.00{\cdot}10^{-2}$	2.431^{-4}	4.09	6.518^{-8}	6.03	2.68^{-4}	1.94

Table A-21: *1D DG with Lifting Operator Error Local Results* – $p_{inc} = 1$

p	h	$\frac{\mathcal{E}_{agg}}{N}$	Rate	$\frac{\Delta\tilde{\mathcal{E}}_{agg}}{N}$	Rate	Θ_{agg}	Rate
1	$2.50 \cdot 10^{-1}$	8.898^{-1}	–	4.725^{-2}	–	5.31^{-2}	–
	$1.25 \cdot 10^{-1}$	1.015^{-1}	3.13	1.375^{-3}	5.1	1.35^{-2}	1.97
	$8.33 \cdot 10^{-2}$	2.945^{-2}	3.05	2.997^{-4}	3.76	1.02^{-2}	0.71
	$6.25 \cdot 10^{-2}$	1.218^{-2}	3.07	9.462^{-5}	4.01	7.77^{-3}	0.94
	$5.00 \cdot 10^{-2}$	6.233^{-3}	3	3.616^{-5}	4.31	5.80^{-3}	1.31
2	$2.50 \cdot 10^{-1}$	4.355^{-2}	–	8.132^{-4}	–	1.87^{-2}	–
	$1.25 \cdot 10^{-1}$	1.304^{-3}	5.06	5.101^{-6}	7.32	3.91^{-3}	2.25
	$8.33 \cdot 10^{-2}$	1.643^{-4}	5.11	2.553^{-7}	7.39	1.55^{-3}	2.28
	$6.25 \cdot 10^{-2}$	3.787^{-5}	5.1	3.368^{-8}	7.04	8.90^{-4}	1.94
	$5.00 \cdot 10^{-2}$	1.216^{-5}	5.09	6.962^{-9}	7.07	5.72^{-4}	1.98

Table A-22: *1D DG without Lifting Operator Error Local Results* – $p_{inc} = 1$

p	h	$\frac{\mathcal{E}_{agg}}{N}$	Rate	$\frac{\Delta\tilde{\mathcal{E}}_{agg}}{N}$	Rate	Θ_{agg}	Rate
1	$2.50 \cdot 10^{-1}$	8.898^{-1}	–	6.551^{-2}	–	7.36^{-2}	–
	$1.25 \cdot 10^{-1}$	1.015^{-1}	3.13	2.572^{-3}	4.67	2.53^{-2}	1.54
	$8.33 \cdot 10^{-2}$	2.945^{-2}	3.05	3.884^{-4}	4.66	1.32^{-2}	1.61
	$6.25 \cdot 10^{-2}$	1.218^{-2}	3.07	1.234^{-4}	3.99	1.01^{-2}	0.92
	$5.00 \cdot 10^{-2}$	6.233^{-3}	3	4.745^{-5}	4.28	7.61^{-3}	1.28
2	$2.50 \cdot 10^{-1}$	4.355^{-2}	–	8.132^{-4}	–	1.87^{-2}	–
	$1.25 \cdot 10^{-1}$	1.304^{-3}	5.06	5.493^{-6}	7.21	4.21^{-3}	2.15
	$8.33 \cdot 10^{-2}$	1.643^{-4}	5.11	2.651^{-7}	7.48	1.61^{-3}	2.37
	$6.25 \cdot 10^{-2}$	3.787^{-5}	5.1	3.016^{-8}	7.56	7.96^{-4}	2.45
	$5.00 \cdot 10^{-2}$	1.216^{-5}	5.09	5.666^{-9}	7.49	4.66^{-4}	2.4

Table A-23: *1D DG Estimate 1 Local Results –* $p_{inc} = 1$

p	h	$\frac{\mathcal{E}_{\text{agg}}}{N}$	Rate	$\frac{\Delta\tilde{\mathcal{E}}_{\text{agg}}}{N}$	Rate	Θ_{agg}	Rate
1	$2.50{\cdot}10^{-1}$	8.898^{-1}	–	6.551^{-2}	–	7.36^{-2}	–
	$1.25{\cdot}10^{-1}$	1.015^{-1}	3.13	2.572^{-3}	4.67	2.53^{-2}	1.54
	$8.33{\cdot}10^{-2}$	2.945^{-2}	3.05	3.884^{-4}	4.66	1.32^{-2}	1.61
	$6.25{\cdot}10^{-2}$	1.218^{-2}	3.07	1.234^{-4}	3.99	1.01^{-2}	0.92
	$5.00{\cdot}10^{-2}$	6.233^{-3}	3	4.745^{-5}	4.28	7.61^{-3}	1.28
2	$2.50{\cdot}10^{-1}$	4.355^{-2}	–	8.132^{-4}	–	1.87^{-2}	–
	$1.25{\cdot}10^{-1}$	1.304^{-3}	5.06	5.493^{-6}	7.21	4.21^{-3}	2.15
	$8.33{\cdot}10^{-2}$	1.643^{-4}	5.11	2.651^{-7}	7.48	1.61^{-3}	2.37
	$6.25{\cdot}10^{-2}$	3.787^{-5}	5.1	3.016^{-8}	7.56	7.96^{-4}	2.45
	$5.00{\cdot}10^{-2}$	1.216^{-5}	5.09	5.666^{-9}	7.49	4.66^{-4}	2.4

Table A-24: *1D DG Estimate 2 Local Results –* $p_{inc} = 1$

p	h	$\frac{\mathcal{E}_{\text{agg}}}{N}$	Rate	$\frac{\Delta\tilde{\mathcal{E}}_{\text{agg}}}{N}$	Rate	Θ_{agg}	Rate
1	$2.50{\cdot}10^{-1}$	8.898^{-1}	–	1.125^{1}	–	1.26^{1}	–
	$1.25{\cdot}10^{-1}$	1.015^{-1}	3.13	1.738^{0}	2.69	1.71^{1}	−0.44
	$8.33{\cdot}10^{-2}$	2.945^{-2}	3.05	5.324^{-1}	2.92	1.81^{1}	−0.13
	$6.25{\cdot}10^{-2}$	1.218^{-2}	3.07	2.289^{-1}	2.93	1.88^{1}	−0.14
	$5.00{\cdot}10^{-2}$	6.233^{-3}	3	1.161^{-1}	3.04	1.86^{1}	$4.07 \cdot 10^{-2}$
2	$2.50{\cdot}10^{-1}$	4.355^{-2}	–	4.331^{0}	–	9.94^{1}	–
	$1.25{\cdot}10^{-1}$	1.304^{-3}	5.06	5.791^{-1}	2.9	4.44^{2}	−2.16
	$8.33{\cdot}10^{-2}$	1.643^{-4}	5.11	1.489^{-1}	3.35	9.07^{2}	−1.76
	$6.25{\cdot}10^{-2}$	3.787^{-5}	5.1	6.364^{-2}	2.96	1.68^{3}	−2.15
	$5.00{\cdot}10^{-2}$	1.216^{-5}	5.09	3.236^{-2}	3.03	2.66^{3}	−2.06

Table A-25: *1D DG with Lifting Operator Error Global Results* – $p_{inc} = 2$

p	h	$\mathcal{E}_{glob}$	Rate	$\Delta\tilde{\mathcal{E}}_{glob}$	Rate	Θ_{glob}	Rate
1	$2.50{\cdot}10^{-1}$	2.691^{0}	–	1.203^{-3}	–	4.47^{-4}	–
	$1.25{\cdot}10^{-1}$	5.344^{-1}	2.33	1.677^{-5}	6.16	3.14^{-5}	3.83
	$8.33{\cdot}10^{-2}$	2.209^{-1}	2.18	1.425^{-6}	6.08	6.45^{-6}	3.9
	$6.25{\cdot}10^{-2}$	1.206^{-1}	2.11	2.503^{-7}	6.05	2.08^{-6}	3.94
	$5.00{\cdot}10^{-2}$	7.599^{-2}	2.07	6.518^{-8}	6.03	8.58^{-7}	3.96
2	$2.50{\cdot}10^{-1}$	1.742^{-1}	–	8.901^{-6}	–	5.11^{-5}	–
	$1.25{\cdot}10^{-1}$	1.042^{-2}	4.06	3.468^{-8}	8	3.33^{-6}	3.94
	$8.33{\cdot}10^{-2}$	1.970^{-3}	4.11	1.323^{-9}	8.05	6.72^{-7}	3.95
	$6.25{\cdot}10^{-2}$	6.054^{-4}	4.1	1.304^{-10}	8.05	2.15^{-7}	3.95
	$5.00{\cdot}10^{-2}$	2.431^{-4}	4.09	2.164^{-11}	8.05	8.90^{-8}	3.96

Table A-26: *1D DG without Lifting Operator Error Global Results* – $p_{inc} = 2$

p	h	$\mathcal{E}_{glob}$	Rate	$\Delta\tilde{\mathcal{E}}_{glob}$	Rate	Θ_{glob}	Rate
1	$2.50{\cdot}10^{-1}$	2.691^{0}	–	1.146^{-1}	–	4.09^{-2}	–
	$1.25{\cdot}10^{-1}$	5.344^{-1}	2.33	1.547^{-2}	2.89	2.81^{-2}	0.54
	$8.33{\cdot}10^{-2}$	2.209^{-1}	2.18	3.794^{-3}	3.47	1.69^{-2}	1.26
	$6.25{\cdot}10^{-2}$	1.206^{-1}	2.11	1.331^{-3}	3.64	1.09^{-2}	1.52
	$5.00{\cdot}10^{-2}$	7.599^{-2}	2.07	5.790^{-4}	3.73	7.56^{-3}	1.65
2	$2.50{\cdot}10^{-1}$	1.742^{-1}	–	9.061^{-4}	–	5.17^{-3}	–
	$1.25{\cdot}10^{-1}$	1.042^{-2}	4.06	2.432^{-5}	5.22	2.33^{-3}	1.15
	$8.33{\cdot}10^{-2}$	1.970^{-3}	4.11	2.512^{-6}	5.6	1.27^{-3}	1.49
	$6.25{\cdot}10^{-2}$	6.054^{-4}	4.1	4.841^{-7}	5.72	7.99^{-4}	1.62
	$5.00{\cdot}10^{-2}$	2.431^{-4}	4.09	1.331^{-7}	5.79	5.47^{-4}	1.7

Table A-27: *1D DG Estimate 1 Global Results* – $p_{\text{inc}} = 2$

p	h	$\mathcal{E}_{\text{glob}}$	Rate	$\Delta\tilde{\mathcal{E}}_{\text{glob}}$	Rate	Θ_{glob}	Rate
1	$2.50{\cdot}10^{-1}$	2.691^{0}	–	1.146^{-1}	–	4.09^{-2}	–
	$1.25{\cdot}10^{-1}$	5.344^{-1}	2.33	1.547^{-2}	2.89	2.81^{-2}	0.54
	$8.33{\cdot}10^{-2}$	2.209^{-1}	2.18	3.794^{-3}	3.47	1.69^{-2}	1.26
	$6.25{\cdot}10^{-2}$	1.206^{-1}	2.11	1.331^{-3}	3.64	1.09^{-2}	1.52
	$5.00{\cdot}10^{-2}$	7.599^{-2}	2.07	5.790^{-4}	3.73	7.56^{-3}	1.65
2	$2.50{\cdot}10^{-1}$	1.742^{-1}	–	9.061^{-4}	–	5.17^{-3}	–
	$1.25{\cdot}10^{-1}$	1.042^{-2}	4.06	2.432^{-5}	5.22	2.33^{-3}	1.15
	$8.33{\cdot}10^{-2}$	1.970^{-3}	4.11	2.512^{-6}	5.6	1.27^{-3}	1.49
	$6.25{\cdot}10^{-2}$	6.054^{-4}	4.1	4.841^{-7}	5.72	7.99^{-4}	1.62
	$5.00{\cdot}10^{-2}$	2.431^{-4}	4.09	1.331^{-7}	5.79	5.47^{-4}	1.7

Table A-28: *1D DG Estimate 2 Global Results* – $p_{\text{inc}} = 2$

p	h	$\mathcal{E}_{\text{glob}}$	Rate	$\Delta\tilde{\mathcal{E}}_{\text{glob}}$	Rate	Θ_{glob}	Rate
1	$2.50{\cdot}10^{-1}$	2.691^{0}	–	1.203^{-3}	–	4.47^{-4}	–
	$1.25{\cdot}10^{-1}$	5.344^{-1}	2.33	1.677^{-5}	6.16	3.14^{-5}	3.83
	$8.33{\cdot}10^{-2}$	2.209^{-1}	2.18	1.425^{-6}	6.08	6.45^{-6}	3.9
	$6.25{\cdot}10^{-2}$	1.206^{-1}	2.11	2.503^{-7}	6.05	2.08^{-6}	3.94
	$5.00{\cdot}10^{-2}$	7.599^{-2}	2.07	6.518^{-8}	6.03	8.58^{-7}	3.96
2	$2.50{\cdot}10^{-1}$	1.742^{-1}	–	8.901^{-6}	–	5.11^{-5}	–
	$1.25{\cdot}10^{-1}$	1.042^{-2}	4.06	3.468^{-8}	8	3.33^{-6}	3.94
	$8.33{\cdot}10^{-2}$	1.970^{-3}	4.11	1.323^{-9}	8.05	6.72^{-7}	3.95
	$6.25{\cdot}10^{-2}$	6.054^{-4}	4.1	1.304^{-10}	8.05	2.15^{-7}	3.95
	$5.00{\cdot}10^{-2}$	2.431^{-4}	4.09	2.164^{-11}	8.05	8.91^{-8}	3.96

Table A-29: *1D DG with Lifting Operator Error Local Results* – $p_{inc} = 2$

p	h	$\frac{\mathcal{E}_{agg}}{N}$	Rate	$\frac{\Delta\tilde{\mathcal{E}}_{agg}}{N}$	Rate	Θ_{agg}	Rate
1	$2.50{\cdot}10^{-1}$	8.898^{-1}	–	2.360^{-3}	–	2.65^{-3}	–
	$1.25{\cdot}10^{-1}$	1.015^{-1}	3.13	3.078^{-5}	6.26	3.03^{-4}	3.13
	$8.33{\cdot}10^{-2}$	2.945^{-2}	3.05	1.903^{-6}	6.87	6.46^{-5}	3.81
	$6.25{\cdot}10^{-2}$	1.218^{-2}	3.07	2.520^{-7}	7.03	2.07^{-5}	3.96
	$5.00{\cdot}10^{-2}$	6.233^{-3}	3	5.502^{-8}	6.82	8.83^{-6}	3.82
2	$2.50{\cdot}10^{-1}$	4.355^{-2}	–	2.443^{-6}	–	5.61^{-5}	–
	$1.25{\cdot}10^{-1}$	1.304^{-3}	5.06	2.069^{-8}	6.88	1.59^{-5}	1.82
	$8.33{\cdot}10^{-2}$	1.643^{-4}	5.11	8.217^{-10}	7.96	5.00^{-6}	2.85
	$6.25{\cdot}10^{-2}$	3.787^{-5}	5.1	7.050^{-11}	8.54	1.86^{-6}	3.43
	$5.00{\cdot}10^{-2}$	1.216^{-5}	5.09	9.705^{-12}	8.89	7.98^{-7}	3.8

Table A-30: *1D DG without Lifting Operator Error Local Results* – $p_{inc} = 2$

p	h	$\frac{\mathcal{E}_{agg}}{N}$	Rate	$\frac{\Delta\tilde{\mathcal{E}}_{agg}}{N}$	Rate	Θ_{agg}	Rate
1	$2.50{\cdot}10^{-1}$	8.898^{-1}	–	3.015^{-2}	–	3.39^{-2}	–
	$1.25{\cdot}10^{-1}$	1.015^{-1}	3.13	1.942^{-3}	3.96	1.91^{-2}	0.82
	$8.33{\cdot}10^{-2}$	2.945^{-2}	3.05	3.168^{-4}	4.47	1.08^{-2}	1.42
	$6.25{\cdot}10^{-2}$	1.218^{-2}	3.07	8.330^{-5}	4.64	6.84^{-3}	1.57
	$5.00{\cdot}10^{-2}$	6.233^{-3}	3	2.899^{-5}	4.73	4.65^{-3}	1.73
2	$2.50{\cdot}10^{-1}$	4.355^{-2}	–	6.006^{-4}	–	1.38^{-2}	–
	$1.25{\cdot}10^{-1}$	1.304^{-3}	5.06	6.022^{-6}	6.64	4.62^{-3}	1.58
	$8.33{\cdot}10^{-2}$	1.643^{-4}	5.11	3.595^{-7}	6.95	2.19^{-3}	1.84
	$6.25{\cdot}10^{-2}$	3.787^{-5}	5.1	4.741^{-8}	7.04	1.25^{-3}	1.94
	$5.00{\cdot}10^{-2}$	1.216^{-5}	5.09	9.773^{-9}	7.08	8.03^{-4}	1.99

Table A-31: *1D DG Estimate 1 Local Results – $p_{inc} = 2$*

p	h	$\frac{\mathcal{E}_{agg}}{N}$	Rate	$\frac{\Delta\tilde{\mathcal{E}}_{agg}}{N}$	Rate	Θ_{agg}	Rate
1	$2.50 \cdot 10^{-1}$	8.898^{-1}	–	3.015^{-2}	–	3.39^{-2}	–
	$1.25 \cdot 10^{-1}$	1.015^{-1}	3.13	1.942^{-3}	3.96	1.91^{-2}	0.82
	$8.33 \cdot 10^{-2}$	2.945^{-2}	3.05	3.168^{-4}	4.47	1.08^{-2}	1.42
	$6.25 \cdot 10^{-2}$	1.218^{-2}	3.07	8.330^{-5}	4.64	6.84^{-3}	1.57
	$5.00 \cdot 10^{-2}$	6.233^{-3}	3	2.899^{-5}	4.73	4.65^{-3}	1.73
2	$2.50 \cdot 10^{-1}$	4.355^{-2}	–	6.006^{-4}	–	1.38^{-2}	–
	$1.25 \cdot 10^{-1}$	1.304^{-3}	5.06	6.022^{-6}	6.64	4.62^{-3}	1.58
	$8.33 \cdot 10^{-2}$	1.643^{-4}	5.11	3.595^{-7}	6.95	2.19^{-3}	1.84
	$6.25 \cdot 10^{-2}$	3.787^{-5}	5.1	4.741^{-8}	7.04	1.25^{-3}	1.94
	$5.00 \cdot 10^{-2}$	1.216^{-5}	5.09	9.773^{-9}	7.08	8.03^{-4}	1.99

Table A-32: *1D DG Estimate 2 Local Results – $p_{inc} = 2$*

p	h	$\frac{\mathcal{E}_{agg}}{N}$	Rate	$\frac{\Delta\tilde{\mathcal{E}}_{agg}}{N}$	Rate	Θ_{agg}	Rate
1	$2.50 \cdot 10^{-1}$	8.898^{-1}	–	2.707^{1}	–	3.04^{1}	–
	$1.25 \cdot 10^{-1}$	1.015^{-1}	3.13	4.168^{0}	2.7	4.11^{1}	−0.43
	$8.33 \cdot 10^{-2}$	2.945^{-2}	3.05	1.278^{0}	2.92	4.34^{1}	−0.13
	$6.25 \cdot 10^{-2}$	1.218^{-2}	3.07	5.492^{-1}	2.94	4.51^{1}	−0.13
	$5.00 \cdot 10^{-2}$	6.233^{-3}	3	2.785^{-1}	3.04	4.47^{1}	$4.03 \cdot 10^{-2}$
2	$2.50 \cdot 10^{-1}$	4.355^{-2}	–	9.897^{0}	–	2.27^{2}	–
	$1.25 \cdot 10^{-1}$	1.304^{-3}	5.06	1.324^{0}	2.9	1.02^{3}	−2.16
	$8.33 \cdot 10^{-2}$	1.643^{-4}	5.11	3.405^{-1}	3.35	2.07^{3}	−1.76
	$6.25 \cdot 10^{-2}$	3.787^{-5}	5.1	1.455^{-1}	2.96	3.84^{3}	−2.15
	$5.00 \cdot 10^{-2}$	1.216^{-5}	5.09	7.397^{-2}	3.03	6.08^{3}	−2.06

Table A-33: *2D CG Global Results – $p_{inc} = 1$*

p	h	$\mathcal{E}_{glob}$	Rate	$\Delta\tilde{\mathcal{E}}_{glob}$	Rate	Θ_{glob}	Rate
1	$1.25 \cdot 10^{-1}$	3.354^{-2}	–	3.162^{-4}	–	9.52^{-3}	–
	$8.33 \cdot 10^{-2}$	1.527^{-2}	1.94	6.188^{-5}	4.02	4.07^{-3}	2.09
	$6.25 \cdot 10^{-2}$	8.665^{-3}	1.97	1.951^{-5}	4.01	2.26^{-3}	2.05
	$5.00 \cdot 10^{-2}$	5.569^{-3}	1.98	7.976^{-6}	4.01	1.43^{-3}	2.03
2	$1.25 \cdot 10^{-1}$	3.162^{-4}	–	7.629^{-7}	–	2.41^{-3}	–
	$8.33 \cdot 10^{-2}$	6.188^{-5}	4.02	6.761^{-8}	5.98	1.09^{-3}	1.95
	$6.25 \cdot 10^{-2}$	1.951^{-5}	4.01	1.199^{-8}	6.01	6.14^{-4}	2
	$5.00 \cdot 10^{-2}$	7.976^{-6}	4.01	3.126^{-9}	6.02	3.92^{-4}	2.01

Table A-34: *2D DG Global Results – $p_{inc} = 1$*

p	h	$\mathcal{E}_{glob}$	Rate	$\Delta\tilde{\mathcal{E}}_{glob}$	Rate	Θ_{glob}	Rate
1	$1.25 \cdot 10^{-1}$	2.066^{-2}	–	2.190^{-4}	–	1.07^{-2}	–
	$8.33 \cdot 10^{-2}$	9.228^{-3}	1.99	4.049^{-5}	4.16	4.41^{-3}	2.19
	$6.25 \cdot 10^{-2}$	5.210^{-3}	1.99	1.243^{-5}	4.11	2.39^{-3}	2.13
	$5.00 \cdot 10^{-2}$	3.344^{-3}	1.99	5.004^{-6}	4.08	1.50^{-3}	2.09
2	$1.25 \cdot 10^{-1}$	2.190^{-4}	–	6.019^{-7}	–	2.74^{-3}	–
	$8.33 \cdot 10^{-2}$	4.049^{-5}	4.16	5.163^{-8}	6.06	1.27^{-3}	1.89
	$6.25 \cdot 10^{-2}$	1.243^{-5}	4.11	9.009^{-9}	6.07	7.24^{-4}	1.96
	$5.00 \cdot 10^{-2}$	5.004^{-6}	4.08	2.328^{-9}	6.07	4.65^{-4}	1.99

Table A-35: *2D HDG-h Global Results – $p_{inc} = 1$*

p	h	$\mathcal{E}_{\text{glob}}$	Rate	$\Delta\tilde{\mathcal{E}}_{\text{glob}}$	Rate	Θ_{glob}	Rate
1	$1.25{\cdot}10^{-1}$	7.159^{-3}	–	4.571^{-5}	–	6.39^{-3}	–
	$8.33{\cdot}10^{-2}$	2.992^{-3}	2.15	8.068^{-6}	4.28	2.70^{-3}	2.13
	$6.25{\cdot}10^{-2}$	1.613^{-3}	2.15	2.409^{-6}	4.2	1.49^{-3}	2.05
	$5.00{\cdot}10^{-2}$	1.002^{-3}	2.13	9.529^{-7}	4.16	9.51^{-4}	2.02
2	$1.25{\cdot}10^{-1}$	4.571^{-5}	–	1.890^{-7}	–	4.13^{-3}	–
	$8.33{\cdot}10^{-2}$	8.068^{-6}	4.28	1.427^{-8}	6.37	1.77^{-3}	2.09
	$6.25{\cdot}10^{-2}$	2.409^{-6}	4.2	2.281^{-9}	6.37	9.47^{-4}	2.17
	$5.00{\cdot}10^{-2}$	9.529^{-7}	4.16	5.528^{-10}	6.35	5.80^{-4}	2.19

Table A-36: *2D HDG-L Global Results – $p_{inc} = 1$*

p	h	$\mathcal{E}_{\text{glob}}$	Rate	$\Delta\tilde{\mathcal{E}}_{\text{glob}}$	Rate	Θ_{glob}	Rate
1	$1.25{\cdot}10^{-1}$	4.364^{-3}	–	2.987^{-5}	–	6.85^{-3}	–
	$8.33{\cdot}10^{-2}$	1.287^{-3}	3.01	3.690^{-6}	5.16	2.87^{-3}	2.15
	$6.25{\cdot}10^{-2}$	5.345^{-4}	3.06	8.477^{-7}	5.11	1.59^{-3}	2.06
	$5.00{\cdot}10^{-2}$	2.695^{-4}	3.07	2.725^{-7}	5.08	1.01^{-3}	2.02
2	$1.25{\cdot}10^{-1}$	2.987^{-5}	–	1.355^{-7}	–	4.54^{-3}	–
	$8.33{\cdot}10^{-2}$	3.690^{-6}	5.16	7.414^{-9}	7.17	2.01^{-3}	2.01
	$6.25{\cdot}10^{-2}$	8.477^{-7}	5.11	9.131^{-10}	7.28	1.08^{-3}	2.17
	$5.00{\cdot}10^{-2}$	2.725^{-7}	5.08	1.783^{-10}	7.32	6.54^{-4}	2.24

Table A-37: *2D CG Local Results – $p_{inc} = 1$*

p	h	$\frac{\mathcal{E}_{\text{agg}}}{N}$	Rate	$\frac{\Delta\tilde{\mathcal{E}}_{\text{agg}}}{N}$	Rate	Θ_{agg}	Rate
1	$1.25{\cdot}10^{-1}$	2.812^{-4}	–	3.758^{-6}	–	1.34^{-2}	–
	$8.33{\cdot}10^{-2}$	5.779^{-5}	3.9	3.670^{-7}	5.74	6.35^{-3}	1.83
	$6.25{\cdot}10^{-2}$	1.859^{-5}	3.94	7.104^{-8}	5.71	3.82^{-3}	1.77
	$5.00{\cdot}10^{-2}$	7.700^{-6}	3.95	2.021^{-8}	5.63	2.62^{-3}	1.68
2	$1.25{\cdot}10^{-1}$	2.955^{-6}	–	1.063^{-8}	–	3.60^{-3}	–
	$8.33{\cdot}10^{-2}$	2.651^{-7}	5.95	4.515^{-10}	7.79	1.70^{-3}	1.84
	$6.25{\cdot}10^{-2}$	4.739^{-8}	5.98	4.855^{-11}	7.75	1.02^{-3}	1.77
	$5.00{\cdot}10^{-2}$	1.248^{-8}	5.98	8.667^{-12}	7.72	6.95^{-4}	1.74

Table A-38: *2D DG Local Results – $p_{inc} = 1$*

p	h	$\frac{\mathcal{E}_{\text{agg}}}{N}$	Rate	$\frac{\Delta\tilde{\mathcal{E}}_{\text{agg}}}{N}$	Rate	Θ_{agg}	Rate
1	$1.25{\cdot}10^{-1}$	1.801^{-4}	–	5.791^{-6}	–	3.22^{-2}	–
	$8.33{\cdot}10^{-2}$	3.514^{-5}	4.03	5.641^{-7}	5.74	1.61^{-2}	1.71
	$6.25{\cdot}10^{-2}$	1.129^{-5}	3.95	1.195^{-7}	5.4	1.06^{-2}	1.45
	$5.00{\cdot}10^{-2}$	4.642^{-6}	3.98	3.677^{-8}	5.28	7.92^{-3}	1.3
2	$1.25{\cdot}10^{-1}$	2.018^{-6}	–	9.547^{-9}	–	4.73^{-3}	–
	$8.33{\cdot}10^{-2}$	1.707^{-7}	6.09	4.256^{-10}	7.67	2.49^{-3}	1.58
	$6.25{\cdot}10^{-2}$	2.980^{-8}	6.07	4.931^{-11}	7.49	1.65^{-3}	1.43
	$5.00{\cdot}10^{-2}$	7.719^{-9}	6.05	9.508^{-12}	7.38	1.23^{-3}	1.32

Table A-39: *2D HDG-h Local Results –* $p_{inc} = 1$

p	h	$\frac{\mathcal{E}_{agg}}{N}$	Rate	$\frac{\Delta\tilde{\mathcal{E}}_{agg}}{N}$	Rate	Θ_{agg}	Rate
1	$1.25{\cdot}10^{-1}$	6.493^{-5}	–	9.340^{-7}	–	1.44^{-2}	–
	$8.33{\cdot}10^{-2}$	1.215^{-5}	4.13	1.005^{-7}	5.5	8.27^{-3}	1.37
	$6.25{\cdot}10^{-2}$	3.659^{-6}	4.17	2.131^{-8}	5.39	5.82^{-3}	1.22
	$5.00{\cdot}10^{-2}$	1.444^{-6}	4.17	6.438^{-9}	5.36	4.46^{-3}	1.2
2	$1.25{\cdot}10^{-1}$	4.841^{-7}	–	3.108^{-9}	–	6.42^{-3}	–
	$8.33{\cdot}10^{-2}$	3.857^{-8}	6.24	1.433^{-10}	7.59	3.72^{-3}	1.35
	$6.25{\cdot}10^{-2}$	6.517^{-9}	6.18	1.632^{-11}	7.55	2.50^{-3}	1.37
	$5.00{\cdot}10^{-2}$	1.650^{-9}	6.15	3.019^{-12}	7.56	1.83^{-3}	1.41

Table A-40: *2D HDG-L Local Results –* $p_{inc} = 1$

p	h	$\frac{\mathcal{E}_{agg}}{N}$	Rate	$\frac{\Delta\tilde{\mathcal{E}}_{agg}}{N}$	Rate	Θ_{agg}	Rate
1	$1.25{\cdot}10^{-1}$	4.329^{-5}	–	5.649^{-7}	–	1.31^{-2}	–
	$8.33{\cdot}10^{-2}$	5.744^{-6}	4.98	4.209^{-8}	6.4	7.33^{-3}	1.42
	$6.25{\cdot}10^{-2}$	1.324^{-6}	5.1	6.782^{-9}	6.35	5.12^{-3}	1.24
	$5.00{\cdot}10^{-2}$	4.235^{-7}	5.11	1.664^{-9}	6.3	3.93^{-3}	1.19
2	$1.25{\cdot}10^{-1}$	3.214^{-7}	–	2.082^{-9}	–	6.48^{-3}	–
	$8.33{\cdot}10^{-2}$	1.795^{-8}	7.12	6.787^{-11}	8.44	3.78^{-3}	1.33
	$6.25{\cdot}10^{-2}$	2.332^{-9}	7.09	5.904^{-12}	8.49	2.53^{-3}	1.39
	$5.00{\cdot}10^{-2}$	4.795^{-10}	7.09	8.804^{-13}	8.53	1.84^{-3}	1.44

Table A-41: *2D CG Global Results –* $p_{inc} = 2$

p	h	$\mathcal{E}_{glob}$	Rate	$\Delta\tilde{\mathcal{E}}_{glob}$	Rate	Θ_{glob}	Rate
1	$1.25{\cdot}10^{-1}$	3.354^{-2}	–	7.629^{-7}	–	2.27^{-5}	–
	$8.33{\cdot}10^{-2}$	1.527^{-2}	1.94	6.761^{-8}	5.98	4.43^{-6}	4.04
	$6.25{\cdot}10^{-2}$	8.665^{-3}	1.97	1.199^{-8}	6.01	1.38^{-6}	4.04
	$5.00{\cdot}10^{-2}$	5.569^{-3}	1.98	3.126^{-9}	6.02	5.61^{-7}	4.04
2	$1.25{\cdot}10^{-1}$	3.162^{-4}	–	2.942^{-9}	–	9.31^{-6}	–
	$8.33{\cdot}10^{-2}$	6.188^{-5}	4.02	1.115^{-10}	8.07	1.80^{-6}	4.05
	$6.25{\cdot}10^{-2}$	1.951^{-5}	4.01	1.102^{-11}	8.04	5.65^{-7}	4.03
	$5.00{\cdot}10^{-2}$	7.976^{-6}	4.01	1.841^{-12}	8.02	2.31^{-7}	4.01

Table A-42: *2D DG Global Results –* $p_{inc} = 2$

p	h	$\mathcal{E}_{glob}$	Rate	$\Delta\tilde{\mathcal{E}}_{glob}$	Rate	Θ_{glob}	Rate
1	$1.25{\cdot}10^{-1}$	2.066^{-2}	–	6.019^{-7}	–	2.91^{-5}	–
	$8.33{\cdot}10^{-2}$	9.228^{-3}	1.99	5.163^{-8}	6.06	5.60^{-6}	4.07
	$6.25{\cdot}10^{-2}$	5.210^{-3}	1.99	9.009^{-9}	6.07	1.73^{-6}	4.08
	$5.00{\cdot}10^{-2}$	3.344^{-3}	1.99	2.328^{-9}	6.07	6.96^{-7}	4.08
2	$1.25{\cdot}10^{-1}$	2.190^{-4}	–	2.462^{-9}	–	1.12^{-5}	–
	$8.33{\cdot}10^{-2}$	4.049^{-5}	4.16	9.066^{-11}	8.14	2.24^{-6}	3.98
	$6.25{\cdot}10^{-2}$	1.243^{-5}	4.11	8.846^{-12}	8.09	7.12^{-7}	3.98
	$5.00{\cdot}10^{-2}$	5.004^{-6}	4.08	1.464^{-12}	8.06	2.93^{-7}	3.98

Table A-43: *2D HDG-h Global Results –* $p_{inc} = 2$

p	h	$\mathcal{E}_{\text{glob}}$	Rate	$\Delta\tilde{\mathcal{E}}_{\text{glob}}$	Rate	Θ_{glob}	Rate
1	$1.25{\cdot}10^{-1}$	7.159^{-3}	–	1.890^{-7}	–	2.64^{-5}	–
	$8.33{\cdot}10^{-2}$	2.992^{-3}	2.15	1.427^{-8}	6.37	4.77^{-6}	4.22
	$6.25{\cdot}10^{-2}$	1.613^{-3}	2.15	2.281^{-9}	6.37	1.41^{-6}	4.23
	$5.00{\cdot}10^{-2}$	1.002^{-3}	2.13	5.528^{-10}	6.35	5.52^{-7}	4.22
2	$1.25{\cdot}10^{-1}$	4.571^{-5}	–	4.833^{-10}	–	1.06^{-5}	–
	$8.33{\cdot}10^{-2}$	8.068^{-6}	4.28	1.581^{-11}	8.44	1.96^{-6}	4.16
	$6.25{\cdot}10^{-2}$	2.409^{-6}	4.2	1.435^{-12}	8.34	5.96^{-7}	4.14
	$5.00{\cdot}10^{-2}$	9.529^{-7}	4.16	2.196^{-13}	8.41	2.30^{-7}	4.25

Table A-44: *2D HDG-L Global Results –* $p_{inc} = 2$

p	h	$\mathcal{E}_{\text{glob}}$	Rate	$\Delta\tilde{\mathcal{E}}_{\text{glob}}$	Rate	Θ_{glob}	Rate
1	$1.25{\cdot}10^{-1}$	4.364^{-3}	–	1.355^{-7}	–	3.10^{-5}	–
	$8.33{\cdot}10^{-2}$	1.287^{-3}	3.01	7.414^{-9}	7.17	5.76^{-6}	4.16
	$6.25{\cdot}10^{-2}$	5.345^{-4}	3.06	9.131^{-10}	7.28	1.71^{-6}	4.22
	$5.00{\cdot}10^{-2}$	2.695^{-4}	3.07	1.783^{-10}	7.32	6.62^{-7}	4.25
2	$1.25{\cdot}10^{-1}$	2.987^{-5}	–	3.239^{-10}	–	1.08^{-5}	–
	$8.33{\cdot}10^{-2}$	3.690^{-6}	5.16	7.478^{-12}	9.29	2.03^{-6}	4.14
	$6.25{\cdot}10^{-2}$	8.477^{-7}	5.11	5.209^{-13}	9.26	6.15^{-7}	4.15
	$5.00{\cdot}10^{-2}$	2.725^{-7}	5.08	6.737^{-14}	9.17	2.47^{-7}	4.08

Table A-45: *2D CG Local Results –* $p_{inc} = 2$

p	h	$\frac{\mathcal{E}_{\text{agg}}}{N}$	Rate	$\frac{\Delta\tilde{\mathcal{E}}_{\text{agg}}}{N}$	Rate	Θ_{agg}	Rate
1	$1.25{\cdot}10^{-1}$	2.812^{-4}	–	4.307^{-8}	–	1.53^{-4}	–
	$8.33{\cdot}10^{-2}$	5.779^{-5}	3.9	2.215^{-9}	7.32	3.83^{-5}	3.42
	$6.25{\cdot}10^{-2}$	1.859^{-5}	3.94	2.844^{-10}	7.14	1.53^{-5}	3.19
	$5.00{\cdot}10^{-2}$	7.700^{-6}	3.95	5.600^{-11}	7.28	7.27^{-6}	3.33
2	$1.25{\cdot}10^{-1}$	2.955^{-6}	–	2.638^{-10}	–	8.93^{-5}	–
	$8.33{\cdot}10^{-2}$	2.651^{-7}	5.95	7.882^{-12}	8.66	2.97^{-5}	2.71
	$6.25{\cdot}10^{-2}$	4.739^{-8}	5.98	6.350^{-13}	8.76	1.34^{-5}	2.77
	$5.00{\cdot}10^{-2}$	1.248^{-8}	5.98	8.926^{-14}	8.79	7.15^{-6}	2.81

Table A-46: *2D DG Local Results –* $p_{inc} = 2$

p	h	$\frac{\mathcal{E}_{\text{agg}}}{N}$	Rate	$\frac{\Delta\tilde{\mathcal{E}}_{\text{agg}}}{N}$	Rate	Θ_{agg}	Rate
1	$1.25{\cdot}10^{-1}$	1.801^{-4}	–	9.365^{-8}	–	5.20^{-4}	–
	$8.33{\cdot}10^{-2}$	3.514^{-5}	4.03	6.222^{-9}	6.69	1.77^{-4}	2.66
	$6.25{\cdot}10^{-2}$	1.129^{-5}	3.95	8.605^{-10}	6.88	7.62^{-5}	2.93
	$5.00{\cdot}10^{-2}$	4.642^{-6}	3.98	1.850^{-10}	6.89	3.99^{-5}	2.9
2	$1.25{\cdot}10^{-1}$	2.018^{-6}	–	5.423^{-10}	–	2.69^{-4}	–
	$8.33{\cdot}10^{-2}$	1.707^{-7}	6.09	1.347^{-11}	9.11	7.89^{-5}	3.02
	$6.25{\cdot}10^{-2}$	2.980^{-8}	6.07	9.945^{-13}	9.06	3.34^{-5}	2.99
	$5.00{\cdot}10^{-2}$	7.719^{-9}	6.05	1.317^{-13}	9.06	1.71^{-5}	3

Table A-47: *2D HDG-h Local Results* – $p_{inc} = 2$

p	h	$\frac{\mathcal{E}_{agg}}{N}$	Rate	$\frac{\Delta\tilde{\mathcal{E}}_{agg}}{N}$	Rate	Θ_{agg}	Rate
1	$1.25{\cdot}10^{-1}$	6.493^{-5}	–	1.590^{-8}	–	2.45^{-4}	–
	$8.33{\cdot}10^{-2}$	1.215^{-5}	4.13	1.237^{-9}	6.3	1.02^{-4}	2.17
	$6.25{\cdot}10^{-2}$	3.659^{-6}	4.17	1.935^{-10}	6.45	5.29^{-5}	2.28
	$5.00{\cdot}10^{-2}$	1.444^{-6}	4.17	4.483^{-11}	6.55	3.11^{-5}	2.38
2	$1.25{\cdot}10^{-1}$	4.841^{-7}	–	7.083^{-11}	–	1.46^{-4}	–
	$8.33{\cdot}10^{-2}$	3.857^{-8}	6.24	2.104^{-12}	8.67	5.46^{-5}	2.43
	$6.25{\cdot}10^{-2}$	6.517^{-9}	6.18	1.683^{-13}	8.78	2.58^{-5}	2.6
	$5.00{\cdot}10^{-2}$	1.650^{-9}	6.15	2.345^{-14}	8.83	1.42^{-5}	2.68

Table A-48: *2D HDG-L Local Results* – $p_{inc} = 2$

p	h	$\frac{\mathcal{E}_{agg}}{N}$	Rate	$\frac{\Delta\tilde{\mathcal{E}}_{agg}}{N}$	Rate	Θ_{agg}	Rate
1	$1.25{\cdot}10^{-1}$	4.329^{-5}	–	1.125^{-8}	–	2.60^{-4}	–
	$8.33{\cdot}10^{-2}$	5.744^{-6}	4.98	6.470^{-10}	7.04	1.13^{-4}	2.06
	$6.25{\cdot}10^{-2}$	1.324^{-6}	5.1	8.007^{-11}	7.26	6.05^{-5}	2.16
	$5.00{\cdot}10^{-2}$	4.235^{-7}	5.11	1.533^{-11}	7.41	3.62^{-5}	2.3
2	$1.25{\cdot}10^{-1}$	3.214^{-7}	–	4.261^{-11}	–	1.33^{-4}	–
	$8.33{\cdot}10^{-2}$	1.795^{-8}	7.12	8.694^{-13}	9.6	4.84^{-5}	2.48
	$6.25{\cdot}10^{-2}$	2.332^{-9}	7.09	5.289^{-14}	9.73	2.27^{-5}	2.64
	$5.00{\cdot}10^{-2}$	4.795^{-10}	7.09	5.885^{-15}	9.84	1.23^{-5}	2.75

Table A-49: *2D DG with Lifting Operator Error Global Results* – $p_{inc} = 1$

p	h	$\mathcal{E}_{glob}$	Rate	$\Delta\tilde{\mathcal{E}}_{glob}$	Rate	Θ_{glob}	Rate
1	$1.25{\cdot}10^{-1}$	2.066^{-2}	–	2.190^{-4}	–	1.07^{-2}	–
	$8.33{\cdot}10^{-2}$	9.228^{-3}	1.99	4.049^{-5}	4.16	4.41^{-3}	2.19
	$6.25{\cdot}10^{-2}$	5.210^{-3}	1.99	1.243^{-5}	4.11	2.39^{-3}	2.13
	$5.00{\cdot}10^{-2}$	3.344^{-3}	1.99	5.004^{-6}	4.08	1.50^{-3}	2.09
2	$1.25{\cdot}10^{-1}$	2.190^{-4}	–	6.019^{-7}	–	2.74^{-3}	–
	$8.33{\cdot}10^{-2}$	4.049^{-5}	4.16	5.163^{-8}	6.06	1.27^{-3}	1.89
	$6.25{\cdot}10^{-2}$	1.243^{-5}	4.11	9.009^{-9}	6.07	7.24^{-4}	1.96
	$5.00{\cdot}10^{-2}$	5.004^{-6}	4.08	2.328^{-9}	6.07	4.65^{-4}	1.99

Table A-50: *2D DG without Lifting Operator Error Global Results* – $p_{inc} = 1$

p	h	$\mathcal{E}_{glob}$	Rate	$\Delta\tilde{\mathcal{E}}_{glob}$	Rate	Θ_{glob}	Rate
1	$1.25{\cdot}10^{-1}$	2.066^{-2}	–	2.036^{-4}	–	9.95^{-3}	–
	$8.33{\cdot}10^{-2}$	9.228^{-3}	1.99	3.701^{-5}	4.21	4.03^{-3}	2.23
	$6.25{\cdot}10^{-2}$	5.210^{-3}	1.99	1.141^{-5}	4.09	2.20^{-3}	2.11
	$5.00{\cdot}10^{-2}$	3.344^{-3}	1.99	4.641^{-6}	4.03	1.39^{-3}	2.05
2	$1.25{\cdot}10^{-1}$	2.190^{-4}	–	9.721^{-7}	–	4.42^{-3}	–
	$8.33{\cdot}10^{-2}$	4.049^{-5}	4.16	8.473^{-8}	6.02	2.09^{-3}	1.85
	$6.25{\cdot}10^{-2}$	1.243^{-5}	4.11	1.472^{-8}	6.08	1.18^{-3}	1.98
	$5.00{\cdot}10^{-2}$	5.004^{-6}	4.08	3.768^{-9}	6.11	7.52^{-4}	2.03

Table A-51: *2D DG Estimate 1 Global Results* – $p_{inc} = 1$

p	h	$\mathcal{E}_{\text{glob}}$	Rate	$\Delta\tilde{\mathcal{E}}_{\text{glob}}$	Rate	Θ_{glob}	Rate
1	$1.25{\cdot}10^{-1}$	2.066^{-2}	–	2.036^{-4}	–	9.95^{-3}	–
	$8.33{\cdot}10^{-2}$	9.228^{-3}	1.99	3.701^{-5}	4.21	4.03^{-3}	2.23
	$6.25{\cdot}10^{-2}$	5.210^{-3}	1.99	1.141^{-5}	4.09	2.20^{-3}	2.11
	$5.00{\cdot}10^{-2}$	3.344^{-3}	1.99	4.641^{-6}	4.03	1.39^{-3}	2.05
2	$1.25{\cdot}10^{-1}$	2.190^{-4}	–	9.721^{-7}	–	4.42^{-3}	–
	$8.33{\cdot}10^{-2}$	4.049^{-5}	4.16	8.473^{-8}	6.02	2.09^{-3}	1.85
	$6.25{\cdot}10^{-2}$	1.243^{-5}	4.11	1.472^{-8}	6.08	1.18^{-3}	1.98
	$5.00{\cdot}10^{-2}$	5.004^{-6}	4.08	3.768^{-9}	6.11	7.52^{-4}	2.03

Table A-52: *2D DG Estimate 2 Global Results* – $p_{inc} = 1$

p	h	$\mathcal{E}_{\text{glob}}$	Rate	$\Delta\tilde{\mathcal{E}}_{\text{glob}}$	Rate	Θ_{glob}	Rate
1	$1.25{\cdot}10^{-1}$	2.066^{-2}	–	2.190^{-4}	–	1.07^{-2}	–
	$8.33{\cdot}10^{-2}$	9.228^{-3}	1.99	4.049^{-5}	4.16	4.41^{-3}	2.19
	$6.25{\cdot}10^{-2}$	5.210^{-3}	1.99	1.243^{-5}	4.11	2.39^{-3}	2.13
	$5.00{\cdot}10^{-2}$	3.344^{-3}	1.99	5.004^{-6}	4.08	1.50^{-3}	2.09
2	$1.25{\cdot}10^{-1}$	2.190^{-4}	–	6.019^{-7}	–	2.74^{-3}	–
	$8.33{\cdot}10^{-2}$	4.049^{-5}	4.16	5.163^{-8}	6.06	1.27^{-3}	1.89
	$6.25{\cdot}10^{-2}$	1.243^{-5}	4.11	9.009^{-9}	6.07	7.24^{-4}	1.96
	$5.00{\cdot}10^{-2}$	5.004^{-6}	4.08	2.328^{-9}	6.07	4.65^{-4}	1.99

Table A-53: *2D DG with Lifting Operator Error Local Results* – $p_{inc} = 1$

p	h	$\frac{\mathcal{E}_{\text{agg}}}{N}$	Rate	$\frac{\Delta\tilde{\mathcal{E}}_{\text{agg}}}{N}$	Rate	Θ_{agg}	Rate
1	$1.25{\cdot}10^{-1}$	1.801^{-4}	–	5.791^{-6}	–	3.22^{-2}	–
	$8.33{\cdot}10^{-2}$	3.514^{-5}	4.03	5.641^{-7}	5.74	1.61^{-2}	1.71
	$6.25{\cdot}10^{-2}$	1.129^{-5}	3.95	1.195^{-7}	5.4	1.06^{-2}	1.45
	$5.00{\cdot}10^{-2}$	4.642^{-6}	3.98	3.677^{-8}	5.28	7.92^{-3}	1.3
2	$1.25{\cdot}10^{-1}$	2.018^{-6}	–	9.547^{-9}	–	4.73^{-3}	–
	$8.33{\cdot}10^{-2}$	1.707^{-7}	6.09	4.256^{-10}	7.67	2.49^{-3}	1.58
	$6.25{\cdot}10^{-2}$	2.980^{-8}	6.07	4.931^{-11}	7.49	1.65^{-3}	1.43
	$5.00{\cdot}10^{-2}$	7.719^{-9}	6.05	9.508^{-12}	7.38	1.23^{-3}	1.32

Table A-54: *2D DG without Lifting Operator Error Local Results* – $p_{inc} = 1$

p	h	$\frac{\mathcal{E}_{\text{agg}}}{N}$	Rate	$\frac{\Delta\tilde{\mathcal{E}}_{\text{agg}}}{N}$	Rate	Θ_{agg}	Rate
1	$1.25{\cdot}10^{-1}$	1.801^{-4}	–	5.654^{-6}	–	3.14^{-2}	–
	$8.33{\cdot}10^{-2}$	3.514^{-5}	4.03	5.548^{-7}	5.73	1.58^{-2}	1.7
	$6.25{\cdot}10^{-2}$	1.129^{-5}	3.95	1.171^{-7}	5.41	1.04^{-2}	1.46
	$5.00{\cdot}10^{-2}$	4.642^{-6}	3.98	3.617^{-8}	5.27	7.79^{-3}	1.28
2	$1.25{\cdot}10^{-1}$	2.018^{-6}	–	1.143^{-8}	–	5.66^{-3}	–
	$8.33{\cdot}10^{-2}$	1.707^{-7}	6.09	4.703^{-10}	7.87	2.76^{-3}	1.78
	$6.25{\cdot}10^{-2}$	2.980^{-8}	6.07	5.267^{-11}	7.61	1.77^{-3}	1.54
	$5.00{\cdot}10^{-2}$	7.719^{-9}	6.05	1.022^{-11}	7.35	1.32^{-3}	1.29

Table A-55: *2D DG Estimate 1 Local Results – $p_{inc} = 1$*

p	h	$\frac{\mathcal{E}_{agg}}{N}$	Rate	$\frac{\Delta\tilde{\mathcal{E}}_{agg}}{N}$	Rate	Θ_{agg}	Rate
1	$1.25\cdot10^{-1}$	1.801^{-4}	–	5.654^{-6}	–	3.14^{-2}	–
	$8.33\cdot10^{-2}$	3.514^{-5}	4.03	5.548^{-7}	5.73	1.58^{-2}	1.7
	$6.25\cdot10^{-2}$	1.129^{-5}	3.95	1.171^{-7}	5.41	1.04^{-2}	1.46
	$5.00\cdot10^{-2}$	4.642^{-6}	3.98	3.617^{-8}	5.27	7.79^{-3}	1.28
2	$1.25\cdot10^{-1}$	2.018^{-6}	–	1.143^{-8}	–	5.66^{-3}	–
	$8.33\cdot10^{-2}$	1.707^{-7}	6.09	4.703^{-10}	7.87	2.76^{-3}	1.78
	$6.25\cdot10^{-2}$	2.980^{-8}	6.07	5.267^{-11}	7.61	1.77^{-3}	1.54
	$5.00\cdot10^{-2}$	7.719^{-9}	6.05	1.022^{-11}	7.35	1.32^{-3}	1.29

Table A-56: *2D DG Estimate 2 Local Results – $p_{inc} = 1$*

p	h	$\frac{\mathcal{E}_{agg}}{N}$	Rate	$\frac{\Delta\tilde{\mathcal{E}}_{agg}}{N}$	Rate	Θ_{agg}	Rate
1	$1.25\cdot10^{-1}$	1.801^{-4}	–	1.931^{-3}	–	1.07^{1}	–
	$8.33\cdot10^{-2}$	3.514^{-5}	4.03	5.648^{-4}	3.03	1.61^{1}	−1
	$6.25\cdot10^{-2}$	1.129^{-5}	3.95	2.390^{-4}	2.99	2.12^{1}	−0.96
	$5.00\cdot10^{-2}$	4.642^{-6}	3.98	1.230^{-4}	2.98	2.65^{1}	−1.01
2	$1.25\cdot10^{-1}$	2.018^{-6}	–	3.023^{-4}	–	1.50^{2}	–
	$8.33\cdot10^{-2}$	1.707^{-7}	6.09	8.856^{-5}	3.03	5.19^{2}	−3.06
	$6.25\cdot10^{-2}$	2.980^{-8}	6.07	3.754^{-5}	2.98	1.26^{3}	−3.08
	$5.00\cdot10^{-2}$	7.719^{-9}	6.05	1.933^{-5}	2.98	2.50^{3}	−3.08

Table A-57: *2D DG with Lifting Operator Error Global Results – $p_{inc} = 2$*

p	h	$\mathcal{E}_{glob}$	Rate	$\Delta\tilde{\mathcal{E}}_{glob}$	Rate	Θ_{glob}	Rate
1	$1.25\cdot10^{-1}$	2.066^{-2}	–	6.019^{-7}	–	2.91^{-5}	–
	$8.33\cdot10^{-2}$	9.228^{-3}	1.99	5.163^{-8}	6.06	5.60^{-6}	4.07
	$6.25\cdot10^{-2}$	5.210^{-3}	1.99	9.009^{-9}	6.07	1.73^{-6}	4.08
	$5.00\cdot10^{-2}$	3.344^{-3}	1.99	2.328^{-9}	6.07	6.96^{-7}	4.08
2	$1.25\cdot10^{-1}$	2.190^{-4}	–	2.462^{-9}	–	1.12^{-5}	–
	$8.33\cdot10^{-2}$	4.049^{-5}	4.16	9.066^{-11}	8.14	2.24^{-6}	3.98
	$6.25\cdot10^{-2}$	1.243^{-5}	4.11	8.846^{-12}	8.09	7.12^{-7}	3.98
	$5.00\cdot10^{-2}$	5.004^{-6}	4.08	1.464^{-12}	8.06	2.93^{-7}	3.98

Table A-58: *2D DG without Lifting Operator Error Global Results – $p_{inc} = 2$*

p	h	$\mathcal{E}_{glob}$	Rate	$\Delta\tilde{\mathcal{E}}_{glob}$	Rate	Θ_{glob}	Rate
1	$1.25\cdot10^{-1}$	2.066^{-2}	–	4.527^{-6}	–	2.19^{-4}	–
	$8.33\cdot10^{-2}$	9.228^{-3}	1.99	6.660^{-7}	4.73	7.22^{-5}	2.74
	$6.25\cdot10^{-2}$	5.210^{-3}	1.99	1.942^{-7}	4.28	3.73^{-5}	2.3
	$5.00\cdot10^{-2}$	3.344^{-3}	1.99	7.831^{-8}	4.07	2.34^{-5}	2.08
2	$1.25\cdot10^{-1}$	2.190^{-4}	–	3.838^{-7}	–	1.75^{-3}	–
	$8.33\cdot10^{-2}$	4.049^{-5}	4.16	3.560^{-8}	5.86	8.79^{-4}	1.7
	$6.25\cdot10^{-2}$	1.243^{-5}	4.11	6.340^{-9}	6	5.10^{-4}	1.89
	$5.00\cdot10^{-2}$	5.004^{-6}	4.08	1.642^{-9}	6.05	3.28^{-4}	1.98

Table A-59: *2D DG Estimate 1 Global Results* – $p_{inc} = 2$

p	h	$\mathcal{E}_{\text{glob}}$	Rate	$\Delta\tilde{\mathcal{E}}_{\text{glob}}$	Rate	Θ_{glob}	Rate
1	$1.25{\cdot}10^{-1}$	2.066^{-2}	–	4.527^{-6}	–	2.19^{-4}	–
	$8.33{\cdot}10^{-2}$	9.228^{-3}	1.99	6.660^{-7}	4.73	7.22^{-5}	2.74
	$6.25{\cdot}10^{-2}$	5.210^{-3}	1.99	1.942^{-7}	4.28	3.73^{-5}	2.3
	$5.00{\cdot}10^{-2}$	3.344^{-3}	1.99	7.831^{-8}	4.07	2.34^{-5}	2.08
2	$1.25{\cdot}10^{-1}$	2.190^{-4}	–	3.838^{-7}	–	1.75^{-3}	–
	$8.33{\cdot}10^{-2}$	4.049^{-5}	4.16	3.560^{-8}	5.86	8.79^{-4}	1.7
	$6.25{\cdot}10^{-2}$	1.243^{-5}	4.11	6.340^{-9}	6	5.10^{-4}	1.89
	$5.00{\cdot}10^{-2}$	5.004^{-6}	4.08	1.642^{-9}	6.05	3.28^{-4}	1.98

Table A-60: *2D DG Estimate 2 Global Results* – $p_{inc} = 2$

p	h	$\mathcal{E}_{\text{glob}}$	Rate	$\Delta\tilde{\mathcal{E}}_{\text{glob}}$	Rate	Θ_{glob}	Rate
1	$1.25{\cdot}10^{-1}$	2.066^{-2}	–	6.019^{-7}	–	2.91^{-5}	–
	$8.33{\cdot}10^{-2}$	9.228^{-3}	1.99	5.163^{-8}	6.06	5.60^{-6}	4.07
	$6.25{\cdot}10^{-2}$	5.210^{-3}	1.99	9.009^{-9}	6.07	1.73^{-6}	4.08
	$5.00{\cdot}10^{-2}$	3.344^{-3}	1.99	2.328^{-9}	6.07	6.96^{-7}	4.08
2	$1.25{\cdot}10^{-1}$	2.190^{-4}	–	2.462^{-9}	–	1.12^{-5}	–
	$8.33{\cdot}10^{-2}$	4.049^{-5}	4.16	9.066^{-11}	8.14	2.24^{-6}	3.98
	$6.25{\cdot}10^{-2}$	1.243^{-5}	4.11	8.846^{-12}	8.09	7.12^{-7}	3.98
	$5.00{\cdot}10^{-2}$	5.004^{-6}	4.08	1.464^{-12}	8.06	2.93^{-7}	3.98

Table A-61: *2D DG with Lifting Operator Error Local Results* – $p_{inc} = 2$

p	h	$\frac{\mathcal{E}_{\text{agg}}}{N}$	Rate	$\frac{\Delta\tilde{\mathcal{E}}_{\text{agg}}}{N}$	Rate	Θ_{agg}	Rate
1	$1.25{\cdot}10^{-1}$	1.801^{-4}	–	9.365^{-8}	–	5.20^{-4}	–
	$8.33{\cdot}10^{-2}$	3.514^{-5}	4.03	6.222^{-9}	6.69	1.77^{-4}	2.66
	$6.25{\cdot}10^{-2}$	1.129^{-5}	3.95	8.605^{-10}	6.88	7.62^{-5}	2.93
	$5.00{\cdot}10^{-2}$	4.642^{-6}	3.98	1.850^{-10}	6.89	3.99^{-5}	2.9
2	$1.25{\cdot}10^{-1}$	2.018^{-6}	–	5.423^{-10}	–	2.69^{-4}	–
	$8.33{\cdot}10^{-2}$	1.707^{-7}	6.09	1.347^{-11}	9.11	7.89^{-5}	3.02
	$6.25{\cdot}10^{-2}$	2.980^{-8}	6.07	9.945^{-13}	9.06	3.34^{-5}	2.99
	$5.00{\cdot}10^{-2}$	7.719^{-9}	6.05	1.317^{-13}	9.06	1.71^{-5}	3

Table A-62: *2D DG without Lifting Operator Error Local Results* – $p_{inc} = 2$

p	h	$\frac{\mathcal{E}_{\text{agg}}}{N}$	Rate	$\frac{\Delta\tilde{\mathcal{E}}_{\text{agg}}}{N}$	Rate	Θ_{agg}	Rate
1	$1.25{\cdot}10^{-1}$	1.801^{-4}	–	1.651^{-6}	–	9.17^{-3}	–
	$8.33{\cdot}10^{-2}$	3.514^{-5}	4.03	1.864^{-7}	5.38	5.30^{-3}	1.35
	$6.25{\cdot}10^{-2}$	1.129^{-5}	3.95	4.065^{-8}	5.29	3.60^{-3}	1.35
	$5.00{\cdot}10^{-2}$	4.642^{-6}	3.98	1.270^{-8}	5.21	2.74^{-3}	1.23
2	$1.25{\cdot}10^{-1}$	2.018^{-6}	–	4.770^{-9}	–	2.36^{-3}	–
	$8.33{\cdot}10^{-2}$	1.707^{-7}	6.09	2.345^{-10}	7.43	1.37^{-3}	1.34
	$6.25{\cdot}10^{-2}$	2.980^{-8}	6.07	2.786^{-11}	7.41	9.35^{-4}	1.34
	$5.00{\cdot}10^{-2}$	7.719^{-9}	6.05	5.370^{-12}	7.38	6.96^{-4}	1.32

Table A-63: *2D DG Estimate 1 Local Results – $p_{inc} = 2$*

p	h	$\frac{\mathcal{E}_{agg}}{N}$	Rate	$\frac{\Delta\tilde{\mathcal{E}}_{agg}}{N}$	Rate	Θ_{agg}	Rate
1	$1.25{\cdot}10^{-1}$	1.801^{-4}	–	1.651^{-6}	–	9.17^{-3}	–
	$8.33{\cdot}10^{-2}$	3.514^{-5}	4.03	1.864^{-7}	5.38	5.30^{-3}	1.35
	$6.25{\cdot}10^{-2}$	1.129^{-5}	3.95	4.065^{-8}	5.29	3.60^{-3}	1.35
	$5.00{\cdot}10^{-2}$	4.642^{-6}	3.98	1.270^{-8}	5.21	2.74^{-3}	1.23
2	$1.25{\cdot}10^{-1}$	2.018^{-6}	–	4.770^{-9}	–	2.36^{-3}	–
	$8.33{\cdot}10^{-2}$	1.707^{-7}	6.09	2.345^{-10}	7.43	1.37^{-3}	1.34
	$6.25{\cdot}10^{-2}$	2.980^{-8}	6.07	2.786^{-11}	7.41	9.35^{-4}	1.34
	$5.00{\cdot}10^{-2}$	7.719^{-9}	6.05	5.370^{-12}	7.38	6.96^{-4}	1.32

Table A-64: *2D DG Estimate 2 Local Results – $p_{inc} = 2$*

p	h	$\frac{\mathcal{E}_{agg}}{N}$	Rate	$\frac{\Delta\tilde{\mathcal{E}}_{agg}}{N}$	Rate	Θ_{agg}	Rate
1	$1.25{\cdot}10^{-1}$	1.801^{-4}	–	4.525^{-3}	–	2.51^{1}	–
	$8.33{\cdot}10^{-2}$	3.514^{-5}	4.03	1.320^{-3}	3.04	3.76^{1}	−0.99
	$6.25{\cdot}10^{-2}$	1.129^{-5}	3.95	5.581^{-4}	2.99	4.94^{1}	−0.95
	$5.00{\cdot}10^{-2}$	4.642^{-6}	3.98	2.871^{-4}	2.98	6.18^{1}	−1
2	$1.25{\cdot}10^{-1}$	2.018^{-6}	–	6.803^{-4}	–	3.37^{2}	–
	$8.33{\cdot}10^{-2}$	1.707^{-7}	6.09	1.993^{-4}	3.03	1.17^{3}	−3.06
	$6.25{\cdot}10^{-2}$	2.980^{-8}	6.07	8.446^{-5}	2.98	2.83^{3}	−3.08
	$5.00{\cdot}10^{-2}$	7.719^{-9}	6.05	4.348^{-5}	2.98	5.63^{3}	−3.08

BIBLIOGRAPHY

[1] Mark Ainsworth and J. Tinsley Oden. A posteriori error estimation in finite element analysis. *Comput. Methods Appl. Mech. Engrg.*, 142:1–88, 1997.

[2] Douglas N. Arnold, Franco Brezzi, Bernardo Cockburn, and L. Donatella Marini. Unified analysis of discontinuous Galerkin methods for elliptical problems. *SIAM J. Numer. Anal.*, 39(5):1749–1779, 2002.

[3] I. Babuska and A. Miller. The post-processing approach in the finite element method- part 1: Calculation of displacements, stesses and other higher derivatives of the displacements. *Internat. J. Numer. Methods Engrg.*, 20:1085–1109, 1984.

[4] I. Babuska and A. Miller. The post-processing approach in the finite element method- part 2: The calculation of stess intensity factors. *Internat. J. Numer. Methods Engrg.*, 20:1111–1129, 1984.

[5] I. Babuska and A. Miller. The post-processing approach in the finite element method- part 3: A posteriori error estimates and adaptive mesh selection. *Internat. J. Numer. Methods Engrg.*, 20:2311–2324, 1984.

[6] I. Babuška and W. C. Reinboldt. Error esimate for adpative finte element computations. *SIAM J. Numer. Anal.*, 15(4):736–754, 1978.

[7] I. Babuška and W. C. Reinboldt. *A-posteriori* error estimates for the finite element method. *Internat. J. Numer. Methods Engrg.*, 12:1597–1615, 1978.

[8] I. Babuška and W. C. Reinboldt. *A-posteriori* error analysis of finite element solutions for one-dimensional problems. *SIAM J. Numer. Anal.*, 18:565–589, 1981.

[9] R. E. Bank and A. Weiser. Some a posteriori error estimators for elliptic partial differential equations. *Math. Comp.*, 44(170):283–301, 1985.

[10] John W. Barrett and Charles M. Elliott. Total flux estimates for a finite-element approximation of elliptic equations. *IMA J. Numer. Anal.*, 7(2):129–148, 1987.

[11] F. Bassi and S. Rebay. GMRES discontinuous Galerkin solution of the compressible Navier-Stokes equations. In Karniadakis Cockburn and Shu, editors, *Discontinuous Galerkin Methods: Theory, Computation and Applications*, pages 197–208. Springer, Berlin, 2000.

[12] R. Becker and R. Rannacher. A feed-back approach to error control in finite element methods: Basic analysis and examples. *East-West J. Numer. Math.*, 4:237–264, 1996.

[13] R. Becker and R. Rannacher. An optimal control approach to a posteriori error estimation in finite element methods. In A. Iserles, editor, *Acta Numerica.* Cambridge University Press, 2001.

[14] Malte Braack and Alexandre Ern. A posteriori control of modeling errors and discretization errors. *Multiscale Modeling & Simulation*, 1(2):221–238, 2003.

[15] Susanne C. Brenner and L. Ridgway Scott. *The Mathematical Thoery of Finite Element Methods, Third Edition.* Springer, New York, 2008.

[16] F. Brezzi, M. Manzini, D. Marini, P. Pietra, and A. Russo. Discontinuous finite elements for diffusion problems. In *Francesco Brioschi (1824-1897) convegno di studi matematici, October 22-23, 1997*, Ist. Lomb. Acc. Sc. Lett., Incontro di studio N. 16, pages 197–217, 1999.

[17] Bernardo Cockburn, Jayadeep Gopalakrishnan, and Raytcho Lazarov. Unified hybridization of discontinuous Galerkin, mixed, and continuous Galerkin methods for second order elliptic problems. *SIAM J. Numer. Anal.*, 47(2):1319–1365, 2009.

[18] Bernardo Cockburn, Jayadeep Gopalakrishnan, and Francisco-Javier Sayas. A projection-based error analysis of hdg methods. *Math. Comp.*, 79:1351–1367, 2010.

[19] Krzysztof Fidkowski and David Darmofal. Review of output-based error estimation and mesh adaptation in computational fluid dynamics. *AIAA Journal*, 49(4):673–694, 2011.

[20] M. Giles and N. Pierce. Adjoint error correction for integral outputs. In T.J. Barth, M. Griebel, D. E. Keyes, R. M. Nieminen, D. Roose, and T. Schlick, editors, *Lecture Notes in Computational Science and Engineering: Error Estimation and Adaptive Discretization Methods in Computational Fluid Dynamics*, volume 25. Springer, Berlin, 2002.

[21] M. B. Giles and E. Süli. Adjoint methods for PDEs: a posteriori error analysis and postprocessing by duality. In *Acta Numerica*, volume 11, pages 145–236, 2002.

[22] M.B. Giles, N.A. Pierce, and E. Suli. Progress in adjoint error correction for integral functionals. *Computing and Visualisation in Science*, 6(2-3):113–121, 2004.

[23] Ralf Hartmann and Paul Houston. Error estimation and adaptive mesh refinement for aerodynamic flows. In H. Deconinck, editor, *VKI LS 2010-01: 36^{th} CFD/ADIGMA course on hp-adaptive and hp-multigrid methods, Oct. 26-30, 2009.* Von Karman Institute for Fluid Dynamics, Rhode Saint Genèse, Belgium, 2009.

[24] N.C. Nguyen, J. Peraire, and B. Cockburn. An implicit high-order hybridizable discontinuous Galerkin method for linear convection-diffusion equations. *J. Comput. Phys.*, 228:3232–3254, 2009.

[25] Niles A. Pierce and Michael B. Giles. Adjoint recovery of superconvergent functionals from PDE approximations. *SIAM Rev.*, 42(2):247–264, 2000.

[26] Thomas Richter and Thomas Wick. Variational localizations of the dual weighted residual estimator. *J. Computational Applied Mathematics*, 279:192–208, 2015.

[27] Rüdiger Verfürth. A posteriori error estimation and adaptive mesh-refinement techniques. *J. Comput. Appl. Math.*, 50(1–3):67–83, 1994.

[28] Pin Tong. Exact solution of certain problems by finite- element method. *AIAA Journal*, 7:178–180, January 1969.

[29] Masayuki Yano. *An Optimization Framework for Adaptive Higher-Order Discretizations of Partial Differential Equations on Anisotropic Simplex Meshes.* PhD thesis, Massachusetts Institute of Technology, Department of Aeronautics and Astronautics, June 2012.

[30] Masayuki Yano and David Darmofal. An optimization framework for anisotropic simplex mesh adaptation: Application to aerodynamic flows. AIAA 2012–0079, January 2012.